The Maximum Scatter TSP on a Regular Grid – How to Avoid Heat Peaks in Additive Manufacturing

Von der Universität Bayreuth
zur Erlangung des Grades eines
Doktors der Naturwissenschaften (Dr. rer. nat.)
genehmigte Abhandlung

von

Isabella Stock, geb. Hoffmann

aus Aschaffenburg

1. Gutachter: Prof. Dr. Jörg Rambau
2. Gutachter: Prof. Dr. Sven O. Krumke

Tag der Einreichung: 24.08.2016
Tag des Kolloquiums: 21.11.2016

Mit Unterstützung der

(03.2012-02.2015)

und durch ein

Promotionsstipendium nach dem „Programm zur Realisierung der Chancengleichheit für Frauen in Forschung und Lehre“ aus Mitteln des Bayerischen Staatshaushalts
(12.2015-02.2016)

in Zusammenarbeit mit

Betreuer: Prof. Dr. Jörg Rambau

Zusammenfassung

Die vorliegende Arbeit besteht aus den erweiterten Ergebnissen eines Teils des Projekts CHAMP – Control of Heat in Automatic Model Production. Das Projekt ist eine von der Oberfrankenstiftung geförderte Kooperation der Lehrstühle für Wirtschafts- und Ingenieurmathematik der Universität Bayreuth sowie der Concept Laser GmbH in Lichtenfels. Es befasst sich mit den Auswirkungen der Lasersteuerung auf die Verzüge in Bauteilen, die mit dem patentierten LaserCUSING® Verfahren hergestellt werden. LaserCUSING® ist eine Technologie zur additiven Fertigung, bei der einkomponentiges Metallpulver vollständig aufgeschmolzen wird. Dies geschieht schichtweise, wobei die einzelnen Schichten in sogenannte „Islands“ unterteilt sind. Das Aufschmelzen erfolgt Islandweise.

In dieser Arbeit werden die Auswirkungen unterschiedlicher Island-Strategien, das heißt unterschiedlicher Island-Reihenfolgen, auf die Verzüge im Bauteil untersucht, um dadurch die am besten geeignete Strategie zu finden. Dabei wird das folgende Resultat erzielt: Bei unseren Testbauteilen aus einem nichtrostenden, austenitischen Stahl gibt es keine signifikanten Unterschiede bezüglich der Verzüge bei sehr unterschiedlichen Island-Strategien. Folglich können kurze Distanzen zwischen aufeinanderfolgenden Islands die Verfahrwege des Lasers verringern und die Produktionszeit verkürzen ohne dass man einen Verlust der Bauteilqualität hinnehmen muss. Bei empfindlichen Bauteilen kann die Menge von erlaubten Nachfolge-Islands eingeschränkt werden.

Bei der Untersuchung, ob verschiedene Optimierungsprobleme zur Modellierung der Problemstellung geeignet sind, werden einige neue Erkenntnisse zum Maximum Scatter Traveling Salesman Problem (MSTSP) gewonnen. Beim MSTSP wird eine Tour durch eine Punktemenge gesucht, in der die kürzeste vorkommende Kante so lang wie möglich ist. Dieses Optimierungsproblem ist im allgemeinen NP-vollständig. Für die Einschränkung auf den zweidimensionalen Fall mit euklidischen Distanzen ist die Frage der NP-Vollständigkeit noch ungeklärt.

Ausgehend von einem Verfahren, das mit linearem Zeitaufwand eine optimale Lösung für das MSTSP für Punkte auf einer Linie ausgibt, entwickeln wir ein Verfahren für Punkte auf einem zweidimensionalen $(m \times n)$-Gitter mit euklidischen Distanzen. Dieses wird mit $\textsc{Weave}(m, n)$ bezeichnet. In Kombination mit zusätzlichen kombinatorischen Lösungen des MSTSP ($\textsc{Boeven}(m, n)$ und $\textsc{Bobodd}(m, n)$) für spezielle Arten von Gittern können wir so das MSTSP für die meisten Gittergrößen optimal lösen; für die übrigen Fälle können wir zumindest asymptotische Optimalität zeigen. Bei fast allen Gittergrößen bis auf vier Ausnahmen beträgt die kürzeste Kante aus unseren Verfahren mindestens 80% der Länge der maximalen kürzesten Kante. Auch im dreidimensionalen Gitter können die neuen Verfahren

unter Anpassungen an die neue Dimension angewandt werden. Für mehr als die Hälfte aller möglichen Gittergrößen erhält man optimale Lösungen. Für die übrigen Gittergrößen lassen sich Approximationen herleiten.

Gleichzeitig ist unsere neue Lösung des MSTSP eine asymptotisch optimale Lösung für das „TSP on grids with forbidden neighborhoods“ (TSPN), wenn eine bestimmte minimale Kantenlänge gewählt wird. Bei diesem Optimierungsproblem wird eine kürzeste Tour durch eine gegebene Knotenmenge gesucht, wobei die Mindestkantenlänge zwischen aufeinanderfolgenden Knoten fest vorgegeben ist. $\textsc{Weave}(m, n)$, $\textsc{Bobeven}(m, n)$ und $\textsc{Bobodd}(m, n)$ sind asymptotisch optimal für das TSPN mit einer Mindestkantenlänge, die der Länge der kürzesten Kante des kombinatorischen Algorithmus entspricht.

Des Weiteren wird eine allgemeinere Heuristik LS_MSTSP zur Approximation des Maximum Scatter TSP entwickelt. Diese basiert auf der Idee von local search-Heuristiken und der Lin-Kernighan Heuristik. LS_MSTSP hat eine Laufzeitkomplexität von $\mathcal{O}(n^3)$. Diese Heuristik findet für über 80% der berechneten Beispielinstanzen eine Lösung mit einer kürzesten Kante von mindestens 80% der Länge der maximalen kürzesten Kante.

Ein verwandtes Problem zum MSTSP ist das Max-Min 2-Neighbor TSP. Bei diesem wird neben der kürzesten Kante einer Tour gleichzeitig auch die kürzeste Kante zwischen dem Vorgänger und dem Nachfolger eines Knotens maximiert. Die Berechnung einer Lösung ist mindestens genauso schwer wie beim MSTSP. LS_MSTSP wird für dieses Problem angepasst (LS_MM2NTSP) mit gleichbleibender Komplexität. Bei mehr als 30% der getesteten Instanzen liefert LS_MM2NTSP eine Tour mit einer Mindestkantenlänge, die das 0,5-fache der optimalen Mindestkantenlänge beträgt. Für allgemeinere Instanzen als Gitter kann mit LS_MSTSP und LS_MM2NTSP in Polynomialzeit eine Lösung approximiert werden.

Bisher finden die entwickelten Algorithmen noch keine direkte Anwendung im Laserschmelzprozess, allerdings erscheinen sie gerade für eine Verkürzung der Laserwege mit einer Mindestsprungweite des Lasers weiterhin relevant.

Abstract

The thesis at hand consists of the extended results of a part of the project CHAMP – Control of Heat in Automatic Model Production. The project was carried out in cooperation between the chairs of business mathematics and mathematics for engineering sciences at the University of Bayreuth as well as Concept Laser GmbH in Lichtenfels and supported by the Oberfrankenstiftung. It deals with the control of a laser and its impact on the deflections in workpieces which are produced with the patented LaserCUSING® technology. LaserCUSING® is a technology for additive manufacturing which means that one-component metal powder is completely melted. This process is completed layer by layer. The single layers are divided into so-called "islands". The laser – and therefore the melting – proceeds from one island to another.

In this work, different island strategies are examined with regard to the deflections of the workpiece. The results are used to find the most appropriate strategy. Thereby the following result is obtained: Despite very different island strategies, our test samples made of austenitic stainless steel showed no significant differences in the deflections. Consequently, short distances between consecutive islands can reduce the length of the laser's route and thus decrease the production time without reducing the quality of the workpiece. If a workpiece is made of a very sensitive material or has a very complex geometry, the amount of possible consecutive islands can be restricted.

Testing the adequacy of the different optimization problems for modeling the LaserCUSING® process yields several new findings. The Maximum Scatter Traveling Salesman Problem (MSTSP) aims to find a tour through a set of nodes such that the shortest appearing edge is as long as possible. In general, this optimization problem is NP-complete. Regarding the restriction to two-dimensional instances with Euclidean distances, it still remains open whether it is NP hard or not.

Starting from a linear-time procedure which computes an optimal solution of the MSTSP for nodes in one line, we develop an algorithm for nodes on a two-dimensional $(m \times n)$-grid with Euclidean distances. It is called $\textsc{Weave}(m, n)$. In combination with further combinatorial solutions of the MSTSP for particular kinds of grid sizes ($\textsc{Boboven}(m, n)$ and $\textsc{Bobodd}(m, n)$), we can produce an optimal solution of the MSTSP for most grid sizes; for the remaining cases, we can prove at least an asymptotical optimality of $\textsc{Weave}(m, n)$. For all but four grid sizes, the length of the shortest edge received from our algorithms is at least 80% of the optimal shortest edge. $\textsc{Weave}(m, n)$, $\textsc{Boboven}(m, n)$ and $\textsc{Bobodd}(m, n)$ can be extended to a three-dimensional grid. For more than half of all possible grid sizes, these extensions yield an optimal solution. For the remaining grid sizes,

approximation algorithms can be deduced.

At the same time, the new solution of the MSTSP is an asymptotically optimal solution for the "TSP with forbidden neighborhoods" (TSPN) if a particular minimum edge length is chosen. In this optimization problem, the shortest tour through a given set of nodes is required such that the used edges are longer than a minimum length. WEAVE(m, n), BOBEVEN(m, n) and BOBODD(m, n) are asymptotically optimal for the TSPN with a specific minimum edge length which equals the length of the shortest edge of the combinatorial algorithm.

Furthermore, a more general heuristic LS_MSTSP is developed for the approximation of the MSTSP. It is based on the idea of local search heuristics and the heuristic of Lin and Kernighan. The complexity of LS_MSTSP is $\mathcal{O}(n^3)$. For more than 80% of the tested instances, this heuristic computes a solution whose shortest edge has a length of at least 80% of the longest possible shortest edge.

A related problem to the MSTSP is the Max-Min 2-Neighbor TSP (MM2NTSP). In this optimization problem two kinds of edges are maximized at the same time: the shortest edge in the tour and the shortest edge between the predecessor and the successor of a node. The computation of a solution is at least as hard as for the MSTSP. LS_MSTSP is adapted to that problem (LS_MM2NTSP) with remaining complexity $\mathcal{O}(n^3)$. For more than 30% of the tested instances, LS_MM2NTSP produces a tour whose shortest edge has a length of at least half the length of the longest possible shortest edge. For more general instances than grids, solutions of the MSTSP can be approximated in polynomial time by LS_MSTSP and LS_MM2NTSP.

So far, the developed algorithms are not yet applied in the laser melting process, but continue to appear relevant for a reduction of the laser's route with certain minimum distances.

Acknowledgments

I want to say thank you to all who supported me during the last years and all my life.

To my supervisor Prof. Dr. Jörg Rambau who was almost always available for my questions and for discussions. He encouraged me to find my own way even if it did not coincide with his own opinion and he supported my special wish to work from Berlin, even though this meant a more difficult communication and many e-mails.

To my colleagues who always gave me advice whenever I was having problems and who corrected the preprint of this work.

To Simon who worked with me on CHAMP. We had long discussions and prepared reports and presentations together. He helped me to better understand the laser melting process and suggested models which I could include in my studies.

To Concept Laser GmbH for the cooperation and the support especially in the writing period. It was an impressive experience to see the computed order applied on real workpieces.

To my friend Florian, who answered all my English questions and polished several phrases.

To my parents who always care for me, who have encouraged me to do this work and supported me with nice postcards and a lot of advise in complicated situations.

To my best sister who gave me advise and always takes her time to support me in final corrections.

To my fiancé Florian who supported me in various ways. We spent evenings discussing my ideas or proofs, he helped me organize my thoughts and he encouraged me and calmed me down when I got desperate or in panic.

Contents

1. Introduction

Concept Laser GmbH in Lichtenfels is one of the key drivers of powder-bed-based laser melting with metals. They developed the patented LaserCUSING® which is also referred to as 3D metal printing [27]. Their technology is used in various fields of application which require functional parts with sophisticated geometries. This is the case for the aviation, aerospace and the automotive industry. Further to that, dental products such as crowns and caps or medical instruments and implants as well as individual items of jewelry can be produced with the help of LaserCUSING® [27].

LaserCUSING® is a type of layered manufacturing method. Different types of layered manufacturing methods are described in Nickel [64], such as stereolithography, selective laser sintering and fused deposition modeling. The idea of layered manufacturing is that a workpiece is designed as a computer solid model which is dissected into several layers and eventually built layer by layer. LaserCUSING® is based on this concept, but differs from the previously mentioned types of methods. It is a complete melting process with powder consisting of one single component. The base material is steel powder or powder of various metal alloys or even gold. By melting the powder in layers which are divided into several segments called islands by a grid, the workpiece is produced step by step.

In laser melting processes like LaserCUSING® deflections arise because of thermal gradients in the material [53]. As the deflections usually come with porosity and deformation of the workpiece, much effort is taken to reduce them. From private communication with employees of Concept Laser we know that the process is currently being improved by a good positioning of the workpiece in the working space such that there are only little and steep overhangs. That way, the surface which is connected to the base plate by solid material is as large as possible. Support structures – thin solid shapes of the same material as the workpiece – form additional connections to the base plate. They stabilize the workpiece and simultaneously conduct heat to the base plate. By heat treatment after cooling and further post processing steps several deflections can be reduced. Not always used but possible on certain machines is the heating of the base plate which allows less laser power to cause a melting process and therefore diminishes heat peaks in certain parts of the workpiece. The current exposure strategy is randomized such that it is not predictable whether consecutive islands lie close on the grid.

In this work, we will examine the relation between the scanning order in a layer and the resulting deflection in the workpiece. In order to find a good scanning strategy, we will consider variations of traveling salesman problems (TSP) with different objective functions which could describe the situation best. Thus, we will attempt to find an optimal order by solving the optimization problem. We will

complete the spectrum of strategies by considering some basic orders like a random order or serial strategy and a slower strategy which leaves more time for cooling in between heating.

For one of the optimization problems, namely the maximum scatter TSP (MSTSP) introduced in Arkin et al. [7] we have developed linear-time procedures for nodes on a regular grid. The MSTSP maximizes the shortest edge in a Hamiltonian tour. Our procedures solve the problem in many cases or otherwise approximate a solution such that the difference between the optimal value and the approximated value is less than the distance between two columns which is 1 in our computations. We will introduce these procedures and deduce their properties concerning the optimality or approximation ratio. Furthermore, we will consider an extension to a three-dimensional grid and the applicability of the procedures on a different yet very similar kind of optimization problem which turned out to be a good model for the production process.

In regards to preliminary work, it has to be said that many studies have been done on various parameters in the production process. Pohl et al. [70] have tested the influence of several scan patterns on the residual stresses of the densified structure in direct laser sintering. They also considered further process conditions and material aspects like the hatch distance, the number of layers and the kind of material. Their scan patterns include a typical raster pattern, a spiral pattern, stripes – a combination of long and short raster patterns – and squares which resemble an island grid. For their workpiece which comprised several layers of a rectangle, the stripes and squares came proved to be the best strategies which also confirms the use of an island grid in LaserCUSING®. Even though their test was done for laser sintering, the influence of the residual stresses is similar for LaserCUSING® albeit less intense. Kruth et al. [53] also tested long scanning vectors and two different sizes of islands with serial heating and a distributed strategy which should lead to the least heat influence between the scanned sectors. They also found that the islands led to less deformation and that the island size did not have a significant impact on the curvature, except that the energy input could be reduced for smaller islands. They prefer the serial heating method, but as their figures mainly illustrate the deformations in one direction and Concept Laser chose the randomized strategy by experience, we did not exclude any strategy in advance.

Kruth et al. [55] compare different selective laser melting and selective laser sintering machines in regards to their lasers, powder depositions and optics. They focused on the best possible setting of the following parameters: the layer thickness, the laser power and the scanning strategy which only affects the path of the laser beam and not the island strategy in this work. Vandenbroucke and Kruth [78] developed improved parameter settings of the laser power, the layer thickness, the scan speed and the hatch spacing. In the specimens, mechanical properties such as hardness, strength, stiffness and ductility were measured. Campanelli et al. [22] worked out a good adjustment for scanning speed and laser power. Branner [20] and Zaeh and Branner [82] developed a general method which numerically describes the

influence of the process on the workpiece. However, there has not been any explicit study regarding the influence of the island order on the deflections or an explicit statement about a possible relation.

Considering the TSP and the MSTSP in particular, we refer to Gutin and Punnen [44] who deal with many problems related to the classic TSP. We refer to Papadimitriou [66], Papadimitriou et al. [67] and Arora et al. [9] for the background on complexity theory. The following basic definition will be frequently used to express the complexity of a procedure.

Definition 1. *Let $f(n)$, $g(n)$ be functions from the positive integers to the positive reals. We write $f(n) = \mathcal{O}(g(n))$ if there exists a constant $c > 0$ such that, for large enough n, $f(n) \leq cg(n)$.*

The MSTSP was introduced in Arkin et al. [7] who did a lot of basic and advanced research on this problem like complexity results, approximation algorithms, and many extensions to further problems. They proved that the MSTSP is NP-complete in general, but it is not known whether this problem is NP-hard for nodes in the plane with Euclidean distances. Particularly their procedures for an exact solution for nodes on a line play an important role in the development of the new algorithm $\textsc{Weave}(m, n)$ for nodes on a regular grid in chapter 4 and is the basis of all further considerations in that chapter.

This overview over the relevant literature is followed by the actual research done in this dissertation. The contribution of this work is the following: According to our tests, there is no significant influence of the island order on the deflections for an austenitic stainless steel, a result which has not been proved or published before. In the tests, the workpieces are randomly positioned, the variety of strategies representing nearly the whole spectrum of strategies spanning from a successive to a randomized order to an order with a short break between the scanning of two islands and without too close consecutive nodes. This surprising result allows us to put our focus regarding the island order on productivity. As all of our test workpieces consist of the same material and various powders, even more sensitive ones, can be used for LaserCUSING®, the new objective may be a shortest tour for which we want to forbid shorter edges in the case of very complicated and delicate geometries or very sensitive materials. Thus, we propose a solution of a TSP while restricting the set of allowed edges. The solution could be computed for example with Concorde [6]. These shorter tours reduce the production time of a sample. For our test samples, about $3 - 5\%$ of the melting and moving time of the laser scan time could be reduced and also 80% of the move length of the laser between the islands. Furthermore, also the abrasion of the LaserCUSING® machine can be diminished by shorter moves of the laser between the islands.

When considering different models and optimization problems, we put our focus on the MSTSP and especially on regular grids. In our case, the specification "grid" describes only the arrangement of the nodes. The distances are the Euclidean distances unless otherwise stated. For regular two-dimensional grids we

succeed in constructing a linear-time procedure WEAVE(m, n) and further procedures BOBEVEN(m, n) and BOBODD(m, n) for special cases. These procedures are asymptotically optimal and yield in many cases an optimal solution to the MSTSP. Except for four small grid sizes, the yielded objective value is always greater than 0.8 times the optimal value. For more than three quarters of the possible $(m \times n)$-grids, an optimal solution of the MSTSP can be computed in linear time. The regular grid is motivated by the island grid. For most workpieces the island grid is not complete, there are missing nodes within the grid or single nodes which are added at the edge of the grid. Some are even split into several components in several layers, but connected in the other ones.

The start of our consideration, however, is the complete $(m \times n)$-grid for which we have gained new results concerning the solution of the MSTSP. Even though we do not know whether this problem is NP-hard, we can solve it on the grid in most cases in polynomial time. Building upon these new algorithms, this work generates further progress. Not considering Euclidean distances but the Manhattan metric, the number of cases for which WEAVE(m, n) yields an optimal solution increases. Taking all procedures together, the cases for which there is an optimal solution are the same as for the Euclidean distances. However, for the ∞-norm, we can yield an optimal solution for any $(m \times n)$-grid either with WEAVE(m, n), BOBEVEN(m, n) or BOBODD(m, n). Another consideration is the extension of WEAVE(m, n), BOBEVEN(m, n) and BOBODD(m, n) on a three-dimensional grid. For certain cases dependent on the number of layers, rows and columns of the grid, this extension yields an optimal solution.

We want to point out a particular result concerning another kind of TSP, namely that the tours created by WEAVE(m, n), BOBEVEN(m, n) and BOBODD(m, n) also yield an asymptotically optimal solution to the TSP with forbidden edges if we set the minimum edge length to the length of the shortest edge in the tour of the respective algorithm (WEAVE(m, n), BOBEVEN(m, n), BOBODD(m, n)). When trying to find combinatorial solutions to that problem one usually starts at small minimum edges. Fischer and Hungerländer [38] are currently dealing with this topic as we know from private communication. Our approximation, however, yields a solution to a TSP with large minimum edges, the longest possible or nearly the longest possible minimum edges. This can be stated because our procedures yield (approximate) solutions to the MSTSP, whose shortest edges are the longest minimum ones such that there still exists a Hamiltonian tour. For longer minimum edges there is no Hamiltonian cycle. Computations for a fixed set of grids yield approximations with a tour length of less than 1.33 times the optimal value.

Furthermore, we develop an approximation procedure for the MSTSP and extend this procedure to the Max-Min 2-Neighbor TSP (MM2NTSP). The MM2NTSP maximizes the shortest edge between consecutive nodes in a tour and at the same time the shortest edge between the predecessor and the successor of a node. For both problems we develop a draft of an approximation strategy according to the heuristic of Lin and Kernighan [57] and apply it to some samples like a number

of grids and to some instances of the TSPLIB [72], a library of TSP instances. We chose the grids as we know (close to) optimal solutions of the MSTSP for these graphs. In order to better determine the quality of the heuristics of the MM2NTSP, we deduce some closer new upper bounds for the regular two-dimensional grids. For the tested samples both heuristics yield suitable results, especially the results for the MSTSP, but also for many samples of the MM2NTSP. However, the current results are a draft which could be enhanced by including more of the achievements of the Lin-Kernighan heuristic.

During the writing of this thesis some obstacles had to be overcome. In the project work, transmitting the order to the LaserCUSING® machine proved rather challenging. There is a common layer interface (CLI) [21], which can be read by the software and then be transmitted to the machine, but as the current version of the interface asks for the list of all scan vectors where the laser has to melt the powder, each single scan vector has to be computed. Computing the scan vectors was not the scope of this work, but it had to be done in order to be able to transmit different island orders to the LaserCUSING® machine. This had a great impact on the choice of the test samples which could not be too complicated such that the CLI-file could be created in reasonable time. But at the same time, the samples had to fulfill certain criteria. For example, they should contain an acute angle and be deposited on a small base and support structures which could fortunately be added by Concept Laser. This resulted in the choice of mainly two kinds of samples with a rectangular and a triangular contour and some special code which computes all scan vectors in shifted islands where the scanning direction varies from layer to layer. Some of the samples were cut faultily. Hence, it was not possible to measure the deflection for them. In order to use them anyway, we invented computations of the angle which made comparison possible. All in all, the cooperation worked quite well and we successfully coped with the restricting points.

In the part of this work which deals with the models and algorithms, we were frequently faced with case analyses. It was a challenge to keep an overview on all cases done and to not forget any special case, be it during the development of the procedures for the two- and three-dimensional grids or when decreasing the upper bound for the MM2NTSP on a regular grid. When constructing the first procedure, combining horizontal and vertical moves such that the total move was long enough required dexterity. Another obstacle consisted in formalizing the idea for a linear-time algorithm on a regular grid to a mapping that can be easily applied. Furthermore, one should be able to prove with this formulation more or less intuitively that the order from the mapping results in a Hamiltonian cycle and it should be possible to determine the shortest edge of that tour in a reasonable way.

The work at hand is composed in the following way. In chapter 2, we will consider the project CHAMP, which initiated this dissertation and frames it. We will have a look at the technical context and the problems we dealt with. In the third chapter, we will introduce the models which we considered in the project and delve into

the literature we consulted regarding these. All of the models are variants of the traveling salesman problem (TSP). One of them, the MSTSP, is examined in this work in more detail in the fourth, fifth and sixth chapter. The fourth chapter which contains the main part of this work is about a new combinatorial solution of the MSTSP on a regular two-dimensional grid. For most kinds of grids, we can get an optimal solution, for the remaining kinds of grids we obtain approximations. The approximations are asymptotically optimal. Furthermore, we will also mention the path version of the MSTSP.

This is followed by further considerations, like different metrics and the extension of the procedure on a 3D-grid. We finally use our solution of the MSTSP on the grid to approximate a TSP with the (nearly) longest possible minimum edge. This tour is an asymptotically optimal approximation to another problem, namely a TSP with a minimum edge length. After the combinatorial solution, we will also consider the approach of Lin and Kernighan and start to adapt this procedure to the MSTSP. We will do first computations with the first draft of this procedure. The adaptation is expanded to the MM2NTSP, a problem related to the first one, which considers one more predecessor than the MSTSP. The MM2NTSP is also an important model which was applied in CHAMP. We will finish our considerations by describing the tests of strategies that we did in CHAMP and presenting our practical results in chapter 7.

2. CHAMP – Control of Heat in Automatic Model Production

The ideas and concepts that we describe and explain in this thesis were originally motivated by a project about generative production. The project CHAMP took place from March 2012 to March 2015. It was carried out in cooperation between the University of Bayreuth – represented by the Chair of Business Mathematics and the Chair of Mathematics for Engineering Sciences – and Concept Laser GmbH in Lichtenfels. The project was supported by the Oberfrankenstiftung. The objective of the project was to diminish deflections in the LaserCUSING® process by regulating the order of islands and controlling the laser intensity.

The preliminaries of this project are described as well in my master thesis [47], and its progress in the reports about the project [15, 14, 11, 12, 13]. Before explaining the tests and results of the project in more detail in chapter 7, I will first give an overview over the state of the art in Selective Laser Melting, particularly the LaserCUSING® technology from Concept Laser GmbH, then describe the objective of the project and the models as well as the process parameters that we worked with.

2.1. Generative Production and LaserCUSING®

The variety of techniques of additive manufacturing is large. Nickel [64] gives an overview over various techniques of layered manufacturing, such as stereolithography, selective laser sintering, fused deposition modeling and shape deposition manufacturing. Since then, the technologies have become more advanced and the variety has increased. A current overview of methods and the used variety of materials is given in Gibson et al. [41].

In CHAMP, we cooperated with Concept Laser GmbH [27] who developed the LaserCUSING® technology which is a laser melting process. At this stage, it can be applied to different metals, for example stainless steel, cobalt-chromium alloys, precious metals and also reactive powder materials. That is why, in this work, we focus on selective laser melting with metals and particularly on stainless steel in our tests.

The following definition and description is based on the web page of Concept Laser GmbH [27], the articles of Kruth et al. [55], Sinirlioglu [77], and Campanelli [22]. LaserCUSING® is a technology that fuses metallic powder by heating it with a laser beam. The components are generated layer by layer from 3D CAD

data [27, 77]. It belongs to the additive manufacturing processes where material is added to the workpiece, more precisely to the Selective Laser Melting processes. "Selective Laser Sintering (SLS) and Selective Laser Melting (SLM) are layer-wise material addition techniques that allow generating complex 3D parts by selectively consolidating successive layers of powder material on top of each other, using thermal energy supplied by a focused and computer controlled laser beam" (Kruth et al. [55], introduction). In Selective Laser Sintering components of a low melting point are melted. These components can be either synthetic materials or a polymer coating of metal powders and ceramics. The latter requires post-treatment with high energy in order to melt the metal component. That is why it is more common to label the melting of synthetic material as Selective Laser Sintering. For the Selective Laser Sintering, it is always either a binary component or two different grain sizes of the powder that are used and only the component with a low melting point is melted. Conversely, the Selective Laser Melting uses an integral powder metal without adding low melting point elements. Therefore, Selective Laser Melting requires a much higher energy density to completely melt the powder. The workpieces produced with a laser melting process are massively dense and have similar metallurgical characteristics to workpieces produced with conventional production processes (Campanelli et al. [22]). In the following, we describe the complete laser melting process in more detail with the help of figure 2.1 from Concept Laser about LaserCUSING®. It is explained in the same way as in my master thesis [47].

Number (1) and (2) point to the dosing chamber filled with metal powder whose base plate (3) can be moved upwards. (4) and (5) point to the coating system with its coating blades that spread the powder for the new layer from the dosing chamber evenly over the platform on which the workpiece is built (6). This platform can be moved down so that the height of the latest layer is always the same.

The laser above the working platform (as well as the coating system) is highlighted in orange. It can be moved to allow for the powder to be melted at any place on the platform. A mirror deflecting unit (scanner) directs the laser beam more precisely.

The procedure is the following: A thin layer of powder is distributed on a platform. After that, a high-energy fibre laser locally heats up the powder until it fuses. The information which positions have to be heated and molten by the laser is gathered from CAD-data that is divided into thin slices, each slice representing one layer of powder. After this process, the base platform is moved down by the height of one layer and a new layer of powder is spread. Thus the process restarts. This explanation corresponds to the information about the technology on the Concept Laser website [27].

This process offers some advantages compared to conventional procedures like milling, two of which will be explained in the following. First of all, there is freedom of geometry. Very complex components can be built without using any tools. Furthermore, almost all the powder can be used. As the powder that is not molten in the process can be reused for another workpiece, the laser melting process pro-

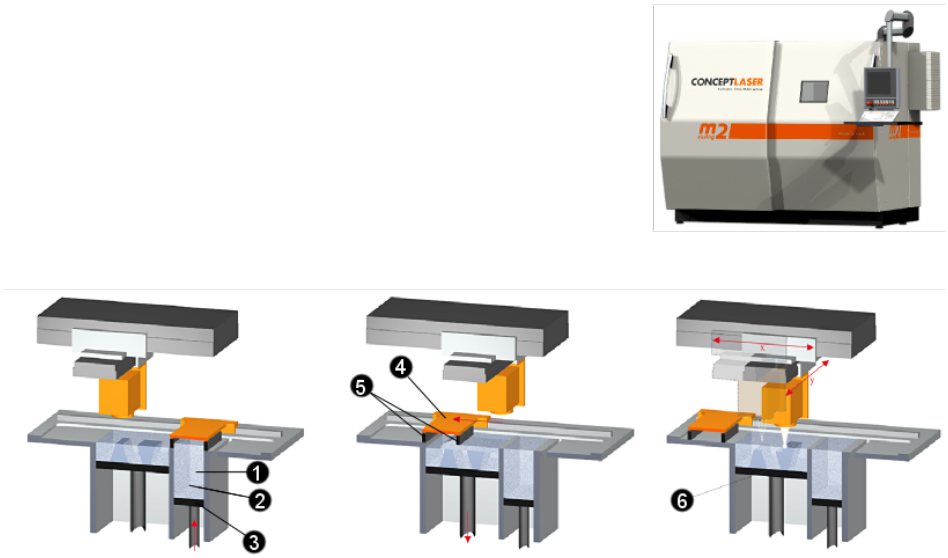

Figure 2.1.: LaserCUSING® process [Concept Laser]

duces hardly any waste. Further advantages and information about the process can be found on the website of Concept Laser [27] and in the dissertation of Branner [20] (section 2.4).

Within a layer, there are many possibilities of directing the laser beam on the surface. One frequently used strategy is the island principle. During a visit at Concept Laser in April 2012, I received the following information from the development manager Dr. Florian Bechmann. The surface of one layer is divided into equally spaced small squares (of $0.25\,\mathrm{mm}^2$ at Concept Laser) called islands. The grid of islands is shifted in each layer about 1mm in length and width, so the boundaries of two different close layers do not coincide, therefore the quality of the connection between two layers is improved and there is more stability in the production. As described above, the CAD-data provides the information, in which islands the laser beam has to melt powder, for each layer. The laser is then working through those islands in a certain order, one after another. Within each island a separate strategy describing the trajectory of the laser is applied. The orientation of the scan vectors of two neighboring islands with one edge in common is perpendicular and is changing from layer to layer. More information about the lengths of scan vectors and the position of the island grid within a workpiece can be found in section 2.3.

In the beginning, additive manufacturing was mainly used to get prototypes of different tools or more complex parts of machines. As the quality of the samples improved considerably, it is nowadays well-known for Rapid Manufacturing or Rapid Tooling, see Kruth et al. [54]. Due to the complete melting of the metal powder, laser melting processes have the great advantage that the density of the material

is almost full and the workpieces yield similar mechanical properties as samples produced with traditional technologies, see Campanelli et al. [22]. However, the high energy of the laser beam causes residual stresses and therefore deformations in the workpieces which should be avoided (Kruth et al. [53]).

Several studies on the optimization of the production process by laser melting or sintering have been conducted with different approaches. Residual stresses cause deformation in the workpieces after cooling and partly already during the production process. There are many parameters which can be varied to diminish the distortions. Campanelli et al. [22], for instance, vary the scanning speed and the laser power for several samples to find a good adjustment for the melting process. Kruth et al. [55] carry out several tests on different Selective Laser Melting and Selective Laser Sintering machines with different lasers, powder depositions and optics in order to point out the limitations and challenges of the different procedures. They consider the thickness of a layer as far as possible, the laser power and the scanning strategy which contains the path which the laser beam passes along. The criteria which are measured are surface roughness, density and bending tests. Vandenbroucke and Kruth [78] test different values of laser power, layer thickness, scan speed, and hatch spacing in the application of manufacturing of medical parts in order to determine a good parameter setting. The economical aspects such as production time and costs are considered, too. Abe [1] proposes a dual laser scanning system to avoid the deformations and cracking, whereas Branner [20] and Zaeh and Branner [82] develop a general method to numerically describe the influences of the process on the workpiece. The simulation is a finite element method which includes basics of heat transportation and simulates the temperature, distortions and residual stresses. The benchmark workpiece to verify the simulation is a T-cantilever.

Pohl et al. [70] test the influence of several scan patterns on the residual stresses of the densified structure in direct laser sintering, but also of other aspects like the hatch distance and the number of layers. Their favorite scan strategy is a special kind of island strategy consisting of typical raster patterns, spiral patterns, stripes and squares which resemble the islands. Kruth et al. [53] mention the effects that arise from a large energy input like balling, residual stresses and deformations. They examine the deformation and stresses and explain physical effects like the temperature gradient mechanism and the difference in process temperatures. The phenomena are verified by an experiment in which base plates are scanned with different scanning patterns and their deflection in height is measured and analyzed. In this paper a first study is included where the difference of deflection according to an island scanning strategy is examined. They also find that island strategies generally lead to better results.

Up to now Concept Laser has applied a stochastic exposure strategy which means that the order of the islands is not given before the process but just developed randomly. The patented process of Concept Laser that generates components in layers using 3D-CAD-data with a stochastic exposure strategy in line with the

island principle is called LaserCUSING®. The term "CUSING" is a combination of the words Concept (name of the company) and Fusing [27]. For large surfaces with many islands this strategy works well.

In CHAMP, we focused on a small number of islands for which consecutive fusion in neighboring islands happens more frequently. We examined different island strategies in order to find out which one leads to the least distortions in the workpieces. Even though Kruth et al. [53] conclude from their test that a successive order is preferable, which they have tested for a quadratic plate, experiences of Concept Laser and their current method lead to the question if a spread entry of heat within a layer could avoid distortions. Furthermore, there have been tests with different levels of laser power, but most times, it was one adjustment of the power per tests. So the question remains how a continuous control of the laser power should look. At this point we started the project. The concrete task in CHAMP is given in the following.

2.2. Objective of CHAMP

There are several parameters which could be adjusted to increase accuracy or to diminish deflections. Just to name some examples, there are parameters which are related to the process, like the single layer thickness, the scan velocity, the hatch spacing and the scan strategy. There are also parameters depending on the laser, like the laser power, the spot diameter and the wavelengths. Other parameters depend on the type of material and the used powder or on the geometry of the final component [22]. The original idea of the project CHAMP was to diminish deflections in the workpieces by means of an order planning of the islands and a control of laser intensity within an island. Figure 2.2 shows the original plan for the project. This thesis focuses solely on the order of islands. The examination of the control of the laser intensity will be part of Simon Bechmann's work.

2.3. Technical Environment

During the project, several workpieces were produced to test strategies. The following measures and process properties were provided by staff members of Concept Laser. The information was collected for the Technical Report [13]. The machine used for our tests is the M2 machine of Concept Laser which has a working space of $250 \times 250 \times 280 mm^3$. The base plate has an area of $220 \times 220 mm^2$. The material (powder) which our samples consist of is CL20 ES, an austenitic stainless steel. The machine has a radiation system which we did not use in our production processes. If no control for the power of the laser is given, the common value at Concept Laser is 180 W, the speed of the laser beam within an island during the melting process is 800 millimeters per second, and it is $1,600$ millimeters per second during contouring. The diameter of a powder particle lies between $15 \mu m$ to $45 \mu m$ and is

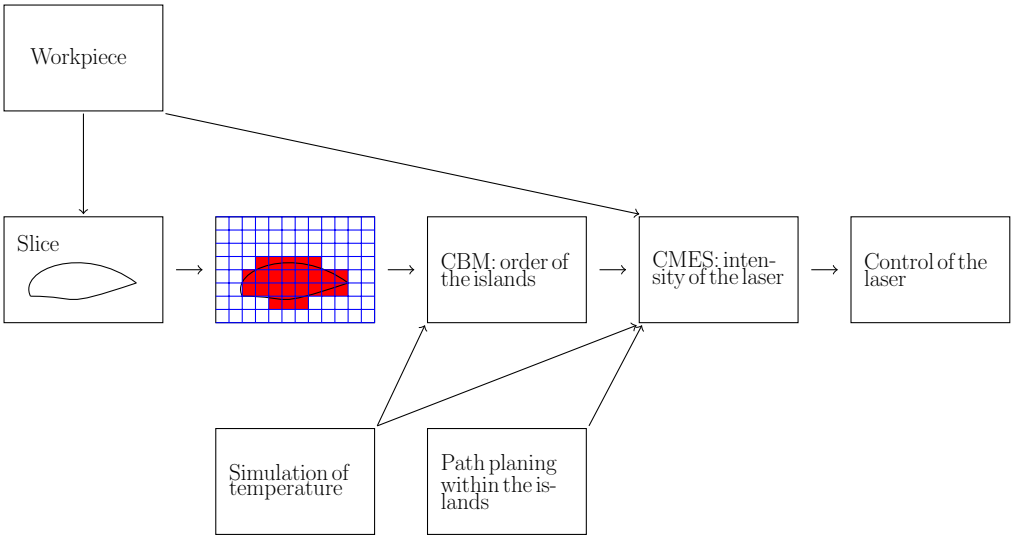

CBM := Chair of Business Mathematics

CMES := Chair of Mathematics for Engineering Sciences

Figure 2.2.: Original structure of the project

normally distributed. There is a laser on and off delay to synchronize the laser and the scanner card and to avoid local energy peaks.

After the completion of each layer, the island grid is turned about 90° and at the same time shifted about $1mm$ in horizontal and in vertical direction. Therefore, the number of islands can vary from layer to layer even if the geometry remains the same.

For our tests of strategies, we used the Common Layer Interface (CLI) [21] to transmit the information about the proposed order of the islands and power of the laser. The original version that we used was CLI 2.0, but there had to be some adaptations to our needs. It was extended to combine the scan vector with an individual value of the laser power and a value of the velocity. The creation of the CLI-file will be described in more detail in section 7.1. The files were transmitted to the server of Concept Laser and after downloading they could read it with the control software of the LaserCUSING® machine.

In order to compute the scan vectors, we have to know their exact positions. The grid in each layer is defined independently for each component that is built on the base plate. It starts $30\mu m$ within the contour of the workpiece. For the single islands, which have a size of $5 \times 5mm^2$ if they are complete, the partition of figure 2.3 holds. The distance of the first scan vector to the boundary of an island is $52.5\mu m$. The laser beam has a diameter of $50\mu m$. The width of the trace

where the powder is molten is about $150\mu m$. In order to get an overlapping of the heating, the overlapping of two consecutive traces has a width of $45\mu m$. There are also non-complete islands which depend on the geometry and result from the shift of grid. Even in those islands, the scan vectors start with the same distance to the boundary of the non-complete island.

Within one layer, a path through all nodes would be sufficient. Nevertheless, the tour is chosen to have a connection to the next layer such that, depending on the strategy, the starting point is either not too close to the last point in the previous layer or at a close position.

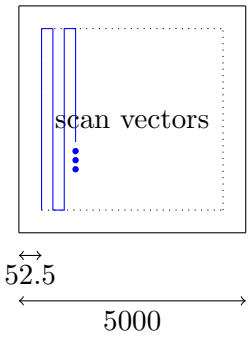

Figure 2.3.: Position of the scan vectors within a complete island (in μm)

The contour of the workpiece is scanned with the laser at a distance of half a track width ($75\mu m$) from the real contour when the scanning of islands of one layer is finished. The speed of the laser beam is two times the speed within the islands (800 and $1,600 mm/s$). An overview on the different parts near the contour of the workpiece is given in figure 2.4.

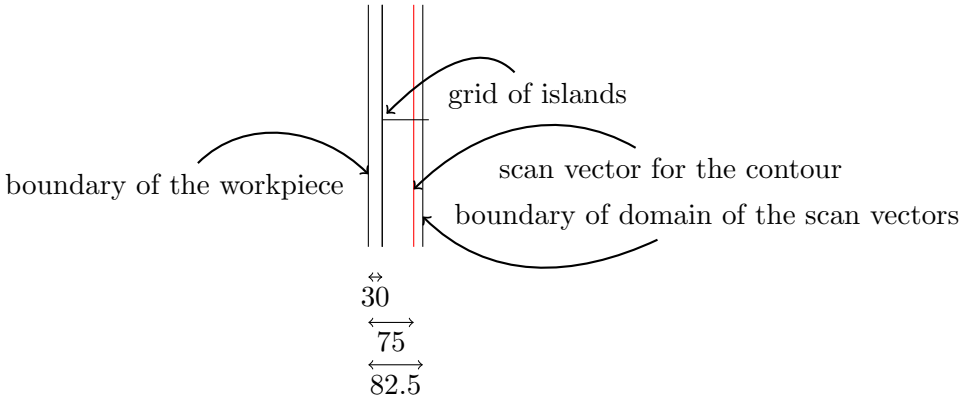

Figure 2.4.: Distribution at the contour of the workpiece (lengths in μm)

2.4. Models and Strategies

When we chose the models, we had in mind that according to Kruth et al. [53] steep temperature gradients usually cause deflections. Heating very close islands in succession leads to a high temperature in that place while the other parts are not heated.

Therefore, we chose strategies which avoid scanning close islands right after one another. We took existing optimization problems and modeled the problem in a suitable way. The optimization problems had in common that they asked for a tour through all nodes. When we reduced every island on its center and defined the Euclidean distances between the nodes as the edge lengths, the situation was adapted to the different kinds of TSP. With our tests, we wanted to ascertain the best fitting model for the real problem. In order to cover more than only this kind of orders and to get some reference samples, we also included serial and random orders.

The following models were applied to workpieces:

The Maximum Scatter TSP (MSTSP) is a special form of the traveling salesman problem (TSP). The MSTSP searches for a tour or a path through all vertices in a graph such that the shortest edge of the tour is as long as possible (see Arkin et al. [7]). In our considerations, we took the Euclidean distances. More details about this model and its solution in certain cases will be given in section 3.2 and sections 4-6.

The Max-Min-2-Neighbor TSP (MM2NTSP) maximizes the shortest edge of the set of edges appearing in the tour and the edges between those vertices which are connected with exactly one further vertex between them (see Arkin et al. [7] and Chiang [23]). This model will be also considered in sections 3.2 and 6.3.

The TSP with Squared Inverse Distances (TSPSID) minimizes the tour *length*, the *length* being defined as the sum of all squared inverted lengths of edges in the tour. The longer the Euclidean distance between two vertices, the less it increases the *length* of the tour.

The TSP with Forbidden Neighborhoods (TSPN) minimizes the length of a tour containing exclusively edges of at least length L. L is a constant that is chosen in advance. The TSPN will be considered in section 3.4.

A Random Order was included as well to have some reference pieces. The current strategy of Concept Laser was imitated. In this strategy, the order of islands in each layer is random.

A Serial Order is the order of islands in lines. For nearly all geometries there are distinctions between horizontal and vertical direction as well as meandering from row to row or always starting at the same side.

The theory of the models and some approaches are described in more detail in the following chapters.

3. Modeling and Theory

This chapter deals with different kinds of the TSP which were applied to model the islands in CHAMP and whose optimal tours were tested for the workpieces. Before the introduction of the special TSP with different distances or objective functions, we will give an overview over the necessary TSP background.

3.1. The Classic Traveling Salesman Problem

The traveling salesman problem (TSP) is a well-known and frequently studied discrete optimization problem. There is a huge number of publications dealing with this problem. *The traveling salesman problem – A computational study* by Applegate et al. [6], Cook's *In pursuit of the traveling salesman: mathematics at the limits of computation* [28], *The traveling salesman: computational solutions for TSP applications* by Reinelt [73] as well as *The traveling salesman problem and its variations* by Gutin and Punnen [44] are important books which cover a wide range of TSP studies.

> The traveling salesman problem (TSP) is to find a routing of a salesman who starts from a home location, visits a prescribed set of cities and returns to the original location in such a way that the total distance travelled is minimum and each city is visited exactly once ([44], chapter 1).

The TSP is relatively easy to understand but it is very challenging to solve it. There is no general algorithm that solves any instance of a TSP in reasonable time. This is one of the main reasons for the popularity of the problem [6]. We will deal with this problem as a mixed-integer program which goes along with the notation of one of the first well-known publications about the TSP by Dantzig, Fulkerson and Johnson [31]. Let $G = (V, A)$ be the graph of cities V with the connections A, let n be the number of given cities, let a_{ij} be the cost of the distance between city i and city j, and let x_{ij} be a binary variable of value 1 if the arc from city i to city j belongs to the tour and is otherwise 0. The optimization problem can be written

in the following way:

$$\min_{x\in\{0,1\}^{|A|}} \quad \sum_{i=1}^{n}\sum_{j=1}^{n} a_{ij}x_{ij} \tag{3.1}$$

$$\sum_{j=1}^{n} x_{ij} = 1 \ \forall i = 1,\ldots,n \tag{3.2}$$

$$\sum_{i=1}^{n} x_{ij} = 1 \ \forall j = 1,\ldots,n \tag{3.3}$$

$$\sum_{i\in S}\sum_{j\in S} x_{ij} \leq |S| - 1 \ \forall S : \emptyset \subset S \subset \{1,\ldots,n\}. \tag{3.4}$$

The constraints (3.2) to (3.4) guarantee that the solution is a tour. A tour is defined in the following as a set of arcs (i, j) which fulfills these three constraints. We will later have a look at optimization problems that also yield a tour, but have different objective functions. The formulation above is a general formulation of the asymmetric TSP. In the case of a symmetric TSP, i.e. the distances between two vertices are symmetric ($d_{ij} = d_{ji}$), we could also use a formulation with undirected edges. Many studies about the complexity of this problem have been done and a variety of approximations have been invented. According to Papadimitriou [65], the Euclidean TSP is NP-complete. In general, it is NP-hard (Karp [50]). The Euclidean TSP has a polynomial-time approximation scheme (PTAS) in any fixed number of d dimensions (Arora [8]), so there are several possibilities to approximate the solution of the Euclidean TSP. Applegate et al. [6] deal with procedures which are significantly influenced by TSP studies. We will build on the following literature. The mixed-integer programming formulation is created by Dantzig, Fulkerson and Johnson [31] and the results and general research on this topic can be found in Schrijver [75], Wolsey and Nemhauser [81] and Wolsey [80]. Grötschel et al. [42], [43] determine inequalities and facets of the TSP. Many aspects of the mixed-integer programming formulation are included in Concorde [6] which is a computer code for the symmetric TSP and for some related network optimization problems. Applegate et al. [6] explain the components of the solver which are LP bounds, cutting planes of different kinds and most of the techniques regarding the TSP. Also the two following techniques in this passage and a chained Lin Kernighan heuristic are incorporated in Concorde. A second procedure is the branch-and-bound method introduced by Little et al. [58], Bock [18], Croes [30], and Eastman [34]. The optimization problem is solved by splitting the feasible set of solutions into two or more subsets. Then, the optimal solution of each subset is computed and finally the best solution of all subsets is the optimal solution for the optimization problem.

The heuristic search algorithms are designed to yield a good solution within a small amount of time. This is a general approach, but also applies well to TSP tours. Just to name two examples of heuristic search algorithms, there are local search algorithms and the simulated annealing paradigm. Local search algorithms

originate in Morton and Land [63], Flood [39], Bock [18] and Croes [30]. We will consider their ideas of developing an optimal or nearly optimal tour by improving a given tour in section 6.1. Kirkpatrick et al. [51] introduced the simulated annealing paradigm. This procedure is a relaxed version of the local search algorithms; it modifies a given initial tour but can accept a worse tour than the previous one with a certain probability. The tours remain similar to the previous one which is reasonable if the previous solution is already quite good. Martin et al. [61], [60] extended this paradigm and developed the chained Lin Kernighan from it where the slow annealing which preserves properties of the previous solutions is replaced by faster steps.

In regards to approximation procedures, different results have been gained. Vygen [79] gives an overview over the current approximation procedures of TSP and the latest achievements for symmetric and asymmetric TSP as well as for graphic TSP. One easily comprehensible 1.5-approximation which runs in $\mathcal{O}(n^3)$ and had an enormous impact on the research on TSP is the Christofides algorithm [24] for metric TSP. It is still the best general approximation. For n nodes in $\mathbb{R}^2$ and every fixed $c > 1$, Arora found a randomized scheme which yields a $(1+\frac{1}{c})$-approximation to the optimum TSP tour [8]. This algorithm runs in $\mathcal{O}(n(\log n)^{\mathcal{O}(c)})$. This result was achieved for any fixed dimension $\mathbb{R}^d$ which means that the procedure needs $\mathcal{O}(n(\log n)^{(\mathcal{O}(\sqrt{d}c))^{d-1}})$. Arora et al. [10] proved that unless P$\neq$NP, the metric TSP does not have a polynomial approximation scheme. Mitchel [62] independently discovered a similar $n^{\mathcal{O}(\frac{1}{\epsilon})}$-time approximation scheme.

There are many particular TSP using certain kinds of distances like the graphic TSP which is described in Vygen [79] and the TSP with squared inverse distances (see section 3.3). Furthermore, there are several variations of the TSP with different objective functions. These variations are considered in Gutin and Punnen [44].

The basic problem of the TSP without any objective function is the Hamiltonian circuit problem which asks if a graph contains a circuit consisting of all nodes. In the plane, this problem is NP-complete [40]. The idea of preserving a Hamiltonian tour is included in most approximation algorithms for the TSP or any variation. In the following chapters, we will mainly deal with the maximum scatter TSP (MSTSP), but also with the max-min 2-neighbor TSP (MM2NTSP) which were both introduced by Arkin et al. [7]. As there are similar optimization problems whose approximation algorithms do not work for the MSTSP according to Arkin et al. [7], we refer to the bottleneck TSP and the maximum TSP which are both considered in Gutin and Punnen [44]. In the bottleneck TSP (BTSP), the longest edge in the tour must be minimized. There are exact branch-and-cut procedures as well as approximate procedures for this problem. Approximation results are also given in Parker et al. [68]. In Ramakrishnan et al. [71], an approximation procedure according to Lin and Kernighan is introduced. They transform the BTSP to a classic TSP and solve this transformed problem with the Lin Kernighan heuristic.

The maximum TSP (MAX TSP) is the optimization problem that asks for a longest tour through a given set of nodes. This problem is NP-hard in general,

particularly for nodes in $\mathbb{R}^d$ with $d \geq 3$ with distances in the Euclidean norm (Fekete [35]). For $d = 2$ it is not stated whether it is NP-hard. An ϵ-approximation in $\mathcal{O}(n^3)$ is achieved asymptotically for any fixed $\epsilon > 0$ (Serdyukov [76]).

In Arkin et al. [7], it is stated that neither the approximation results of BTSP nor of MAX TSP can be directly applied to the MSTSP. Hence, they considered this problem in more detail. We will deal with this in the following section and the following chapters.

3.2. The Max-Min 1 and 2-Neighbor TSP

This section deals with a TSP with a different objective function from the classic TSP. To better understand the model, we will provide our example interpretation of this model which fits the problem quite well. It was already introduced in my master thesis [47].

A vet has to examine all carnivores in a zoo. Each animal has a cage of its own. When the vet examines a carnivore, it gets aggressive. So do the carnivores in the surrounding cages. The longer the distance to the cage where the vet is, the less aggressive the animal gets. By and by, the carnivores calm down. The vet wants the animals to be as calm as possible when he examines them. The task is to find an order in which the vet should examine the carnivores.

The vet has to find a path or a tour through all nodes such that the shortest distance between two consecutive cages is as long as possible. We only consider the case when the examination is divided into two parts meaning that the vet has to do a second turn and therefore needs a closed tour through the nodes. This optimization problem is in line with the MSTSP which is described in equations (3.7) - (3.10). Depending on how fast the carnivores calm down, he can also try to keep a large distance to the predecessor cage of the last animal visited when choosing the next cage. This problem equals the Max-Min 2-Neighbor TSP. In this optimization problem, the set of edges of the tour and the set of edges between the predecessor and the successor of a node are considered.

The max-min 1 and 2-Neighbor TSP was mainly considered by Arkin et al. [7] and Chiang [23] who proved among other things that the maximum scatter TSP is NP-complete in general, only for the geometric MSTSP they hypothesize that it is still NP-hard.

Even though we usually use symmetric distances, we define the problem as an asymmetric problem in order to generalize it and to get a clear formulation. Let $G(V, A)$ be the complete graph with the vertex set V with $|V| = n$ and the set of directed edges A. Let d_{ij} be the Euclidean distance between vertex i and vertex j in V. Let $x \in \mathbb{B}^{n \times n}$ determine which edges belong to the tour

$$x_{ij} = \begin{cases} 1 & \text{if edge } (i,j) \text{ is part of the tour} \\ 0 & \text{else.} \end{cases} \tag{3.5}$$

The MSTSP can be formulated in the following way:

$$\max \min_{i \in V} \sum_{j=1}^{n} d_{ij} x_{ij} \tag{3.6}$$

$$s.t. \sum_{j=1}^{n} x_{ij} = 1 \ \forall i = 1, \ldots, n \tag{3.7}$$

$$\sum_{i=1}^{n} x_{ij} = 1 \ \forall j = 1, \ldots, n \tag{3.8}$$

$$\sum_{i \in S} \sum_{j \in S} x_{ij} \leq |S| - 1 \ \forall \emptyset \subset S \subset \{1, \ldots, n\} \tag{3.9}$$

$$x \in \mathbb{B}^{n \times n}. \tag{3.10}$$

The constraints of the problem are exactly the same as of the classical TSP as the MSTSP also requires a tour. The constraint $x_{ii} = 0$ is included in equation (3.9). The objective contains a maximization of the shortest edge in the tour.

The MM2NTSP can be formulated as

$$\max \min \{ \min_{j \in V} \sum_{i \in V \setminus \{j\}} d_{ij} x_{ij}, \quad \min_{j \in V} \sum_{i \in V \setminus \{j\}} \sum_{k \in V \setminus \{i,j\}} d_{ij} u_{ikj} \} \tag{3.11}$$

$$s.t. \sum_{j=1}^{n} x_{ij} = 1 \qquad \forall i \in V \tag{3.12}$$

$$\sum_{i=1}^{n} x_{ij} = 1 \qquad \forall j \in V \tag{3.13}$$

$$\sum_{i \in S} \sum_{j \in S} x_{ij} \leq |S| - 1 \qquad \forall S : \emptyset \subset S \subset V \tag{3.14}$$

$$u_{ikj} - x_{ik} \leq 0 \qquad \forall i, k, j \in V \text{ and pairwise distinct} \tag{3.15}$$

$$u_{ikj} - x_{kj} \leq 0 \qquad \forall i, k, j \in V \text{ and pairwise distinct} \tag{3.16}$$

$$-u_{ikj} + x_{ik} + x_{kj} \leq 1 \qquad \forall i, k, j \in V \text{ and pairwise distinct} \tag{3.17}$$

$$u_{ikj}, x_{ij} \in \mathbb{B} \qquad \forall i, k, j \in V \text{ and pairwise distinct.} \tag{3.18}$$

The definitions of V, E, x stay the same, but one further variable is introduced. $u_{ikj} = x_{ik} \cdot x_{kj}$ is a variable which linearizes the non-linear expressions in the 2-neighbor problem. Its value is then and only then 1 if i and j are 2-neighbors and k is the vertex between them. The constraints (3.12)-(3.14) are the same as for the MSTSP and the classical TSP. Constraints (3.15)-(3.17) define u_{ikj} without any non-linear expressions. The first two of them require that u_{ikj} may only be 1 if both arcs (i, k) and (k, j) belong to the tour. The third one guarantees that u_{ikj} has to be 1 as soon as both edges are part of the tour. For the tests in the

project CHAMP, we extended the objective function such that the edges between 2-neighbors do not count as much as the regular edges. There is a weight $c \geq 1$ for the 2-edges such that the edges between 2-neighbors do not have to have the same lengths as the direct edges. In our computations, we set $c = 1.5$. We chose this value because it is a weakening of the restrictions to a 2-edge, but at the same time the distances between 2-neighbors influence the optimization.

When solving the problem with a MIP-solver, we have to rewrite the objective function. We introduce a real variable z which we maximize. This variable has to be smaller than any edge appearing in the tour. This means that the objective function is reformulated in the following way and the following constraints are added:

$$\max z \tag{3.19}$$

$$z \leq \sum_{i \in V \setminus \{j\}} d_{ij} x_{ij} \qquad \forall j \in V; \tag{3.20}$$

$$(z \leq \min_{j \in V} \sum_{i \in V \setminus \{j\}} \sum_{k \in V \setminus \{i,j\}} d_{ij} u_{ikj} \qquad \forall j \in V) \text{ if MM2NTSP} \tag{3.21}$$

$$x_{ij}, u_{ikj} \in \mathbb{B} \ \forall i, k, j \in V \text{ and pairwise distinct} \tag{3.22}$$

$$z \in \mathbb{R}_0^+. \tag{3.23}$$

In Gutin and Punnen [44] it is stated that an optimal solution of the MSTSP with the weight matrix D is equivalent to an optimal solution of the BNTSP with weight matrix $C = -D$ and vice versa. However, most procedures for one of the problems benefit from a special structure of the weight matrix which can easily be violated by the transformation. So the procedure yields a much worse performance. Therefore, both problems are considered separately and have different approximation procedures.

Arkin et al. [7] proposed an $\frac{1}{2}$-optimal approximation in $\mathcal{O}(n^2)$ for the maximum scatter TSP. The procedure removes the shortest edges from a graph and stops just before one node has degree less than $\lceil \frac{n}{2} \rceil$. The shortest edge of any Hamiltonian tour in the remaining graph has a length of at least half the optimum value of the MSTSP. The condition that the degree of each node has to be greater than or equal to $\lceil \frac{n}{2} \rceil$ was established by Dirac [33]. Gutin and Punnen [44] proposed further sufficient conditions of Hamiltonian cycles and showed how the algorithm of Arkin et al. [7] can be adapted to one of these conditions. For special cases of node configurations, which are nodes on a line or a circle, Arkin et al. [7] even gave exact solutions. We will particularly refer to these results in chapter 4 where we extend the results for nodes on a line to an equidistant grid. Arkin et al. [7] also provided an upper bound for the MSTSP which was obtained in the following way: From each subset of $\lfloor \frac{n}{2} \rfloor$ nodes the longest edge between two nodes of the subset is taken to a set. From this set of longest edges the length of the shortest edge is an upper bound for the MSTSP.

Furthermore, they introduced an $\frac{1}{2}$-optimal polynomial-time approximation for the MM2NTSP. Chiang [23] pursued this topic and published an $O(n^{2.5})$-time approximation algorithm for the MM2NTSP with a factor of 18 for the cycle version with distances which fulfill the triangle inequality.

For general solutions of the MM2NTSP, we also refer to Fischer [36] and Fischer et al. [37] who dealt with cutting planes of the quadratic traveling salesman problem (QTSP) and the lifting of valid inequalities of the symmetric TSP to stronger inequalities for the symmetric QTSP. The MM2NTSP can be transformed to the QTSP quite well.

3.3. The TSP with Squared Inverse Distances

In addition to the MSTSP, we will also consider a model which has a similar objective but which is closer to the classical TSP. It was chosen for testing purposes to see if slight changes of the order deduced from the solution of the MSTSP already have an impact on the quality of the workpieces. If this were not the case and if the solution of the MSTSP was a good strategy for an island order, this would mean that it is possible to work with a less degenerate problem. Let $G(V, E)$ be the graph with $n = |V|$ vertices and the edge set E. The TSP with squared inverse distances is a classical TSP with the following distance function:

$$\begin{aligned} \tilde{d} :& V \times V \to \mathbb{R}_0^+ \\ & (i, j) \mapsto \frac{1}{d_{ij}^2} \end{aligned} \tag{3.24}$$

where d_{ij} is the Euclidean distance between vertex i and vertex j. Let $\mathcal{T}$ be the set of all tours through all nodes of V. The optimization problem can be written in the following way:

$$\min_{T \in \mathcal{T}} \sum_{(i,j) \in T} \frac{1}{d_{i,j}^2}.$$

The longer the Euclidean length of an edge, the shorter is the value of the new distance function and vice versa. This is caused by the inverse distance. By taking the square of the inverse Euclidean distance, the longer edges become even more preferable than the shorter ones.

As the TSP does not have a polynomial-time approximation scheme for arbitrary symmetric distances [16], many of the efficient approximation procedures lose their efficiency for problems which do not satisfy the triangle inequality. Several papers consider traveling salesman problems with inputs satisfying a relaxed triangle inequality, that means that $c(u, v) \leq \tau(c(u, w) + c(w, v))$ for nodes $u, v, w \in X$ and the cost function $c : X \to \mathcal{R}$. Andreae and Bandelt [4] and Andreae [3] introduced a heuristic called T^3-algorithm and refine it to a $(\tau^2 + \tau)$-approximation. Böckenhauer et al. [19] introduced a Christofides-based $(\frac{3\tau^2}{2})$-approximation and de Berg et al. [32] found a 5-approximation algorithm for the TSP with squared

distances. The approximations of Andreae [3] and Bandelt and Andreae [3] are 6-approximations just like the approximation of Böckenhauer et al. [19]. Bender and Checkuri introduced a 4τ-approximation, that means an 8-approximation for the squared distance, which is based on finding a minimum weight 2-connected subgraph and a Hamiltonian tour in the square of this subgraph.

Unfortunately, these approximations can not be applied to the TSP with squared inverse distances as the relaxed triangle inequality is not fulfilled. The following proposition is proved in appendix B.

Proposition 1. *There is no $\tau \in \mathbb{R}^+$ such that for all a, b, c the following holds:*

$$\tilde{d}(a,c) \leq \tau \left(\tilde{d}(a,b) + \tilde{d}(b,c) \right) \tag{3.25}$$

with $\tilde{d}$ defined in equation (3.24).

Thus, for the TSP with squared inverse distances, the algorithms for the TSP with a distance fulfilling a relaxed triangular inequality cannot be applied.

For the samples that we produced at Concept Laser, we computed the order of the islands of the single layers with Concorde [6], a computer code for the symmetric traveling salesman problem. The components of that code are described precisely in Applegate et al. [6]. The format of the input files is according to the documentation about the TSPLIB [74]. The distances are written in a lower triangular matrix with a large enough value on the diagonal and scaled distances in order to get sufficiently large and different integer lengths. As Concorde requires integer values for the distances and the inverse distances are all smaller 1, we multiply the distances with 10,000 for smaller samples and with 1,000,000 for the greater samples where the values of $\tilde{d}$ get quite small. For the samples in the tests at Concept Laser, we set $\tilde{d}_{ii} = 2$ which means 20,000 or 2,000,000 in the input file. In regards to our workpieces, we were able to compute the solution by Concorde as one layer of the samples was not too big and we did not have to include the computation of the optimal order into the production process.

The samples are described in more detail in section 7.2. For testing this strategy, we chose the value 2, but for general considerations this value should be chosen more carefully.

3.4. TSP with Forbidden Neighborhoods

This section treats the TSP with forbidden neighborhoods (TSPN), a variation of the TSP where the set of edges is restricted. Fischer and Hungerländer [38] work on this optimization problem called TSPFN in their article.

Let $G = (V, E)$ be a complete graph with the distance function $d : E \to \mathbb{R}_0^+$ and with a minimum distance $d_{\min}$ between two nodes. V is the set of vertices and E the set of edges between the vertices. Let $E^* = \{(i,j) \in E : d(i,j) \geq d_{\min}\}$ be the restricted set of edges. The objective is to find a tour through all nodes which only

contains edges in E^*. The complexity of the TSPN on regular grids is not known at the moment [38] and will not be considered in this work. Fischer and Hungerländer approach this problem from small $d_{\min}$ as I know from private communication. They create combinatorial solutions for regular grids as far as possible. In CHAMP, we decided for this model in order to get a short tour through the islands while keeping a minimum distance between consecutive islands. This is a compromise between the optimization of the production time and at the same time an attempt to avoid heat peaks at certain positions. For the test samples in the project, we computed the order resulting from this problem by Concorde [6] by setting all smaller distances to a large value such that they did not get chosen. In Concorde, the distances need to be rounded to integer values.

One further step we did was to combine this problem with the MSTSP, setting $d_{\min}$ to the objective value of the MSTSP. In doing so, we get the shortest tour with the longest possible minimum edge. The approximation of this result will be considered in section 5.3.

4. Maximum Scatter TSP on an Equidistant Grid

In this chapter, we will introduce a linear-time algorithm WEAVE(m, n) for the maximum scatter TSP on a regular grid which is optimal for several cases and at least asymptotically optimal in the remaining cases. We create WEAVE(m, n) by extending the idea of an algorithm for points on a line from Arkin et al. [7] to a regular grid. After an examination of upper and lower bounds, some further exact procedures will be given for the cases where the tour returned from WEAVE(m, n) is not optimal. This chapter includes a preprint [48] which is accepted for the proceedings of the OR 2015.

4.1. Preliminaries

A regular rectangular grid is defined as the complete graph $G(m, n)$ on the vertex set $V(m, n) = \{\binom{x}{y} \in \mathbb{Z}^2 : 0 \leq x \leq n-1, 0 \leq y \leq m-1\}$ where m is the number of rows and n the number of columns. On this graph with Euclidean distances between the nodes, we will solve or at least approximate the geometric MSTSP in the plane. Our procedure is called WEAVE(m, n).

The idea of our new algorithm WEAVE(m, n) comes from a solution presented in Arkin et al. [7] (section 6). As the resulting order of the points on a line coincides with the order of columns in the regular grid, we will consider their solution in more detail before extending it.

In Arkin et al. [7], the nodes need not be equidistant, but this has an impact on the starting node for the pattern of the solution. In the case of equidistant nodes, the pattern can always be started at the first node. There are two subroutines in the algorithm, one for an odd number of points and one for an even number of points. For an odd number of points $n = 2k + 1 \geq 3$, the distances between subsequent points in the order are either k or $k + 1$, the order is $0, k + 1, 1, k + 2, 2, ..., 2k - 1, k - 1, 2k, k$. The tour is completed by returning to the first point. The pattern is illustrated for two examples in figure 4.1(a). For an even number of points $n = 2k \geq 4$ the distances are alternately $k - 1$ and $k + 1$ except when either one of the endpoints or one of the points in the middle (nodes $k - 1$ and k) is reached. In these cases, a single distance of k is inserted into the pattern. One could also say that the end points have incident edges of length k and $k+1$ and the two points around the center are incident to edges of length $k-1$ and k. The order is $0, k+1, 2, k+3, \ldots, n-2, k-1, n-1, k-2, n-3, k-4, \ldots, 1, k$ if k is odd and

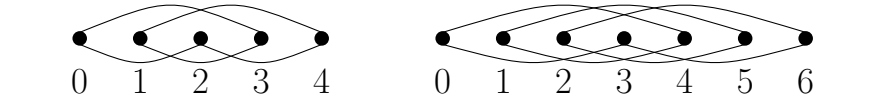

(a) LineOdd(n)

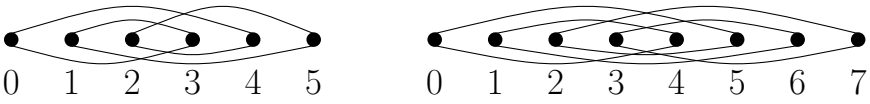

(b) LineEven(n)

Figure 4.1.: Order of LineOdd(n) and LineEven(n) for $n = 5, 6, 7, 8$

$0, k+1, 2, k+3, \ldots, k-2, n-1, k-1, n-2, \ldots, k+1$ if k is even. This is visualized in figure 4.1(b). In the following, we will call these procedures LineOdd(n) and LineEven(n). For the small illustrated examples, not all of the listed nodes appear in the order: for example for $n = 6$, node $k+1$ is $n-2$ and node $k-2$ is 1, so the part in between each of those two can be skipped. The procedure is completely defined in function $j(p)$ in the definition of Weave(m, n), see equations (4.2) and (4.5).

From Arkin et al. [7] (section 6.1 and 6.2) it follows that the tours generated by LineOdd(n) and LineEven(n) are optimal tours for the MSTSP for points on a line. Thus, Weave($1, n$) is set to LineOdd(n) or LineEven(n), respectively.

4.2. The Algorithm Weave(m, n) to find a Hamiltonian Cycle

In the following, we will present Weave(m, n) for $m \geq 2$. We will use the following notation for the nodes.

Definition 2. *A node in the regular $(m \times n)$-grid is defined by an ordered pair (i, j) of its row index i and its column index j.*

W.l.o.g. we will consider grids with a distance of 1 between the columns and rows and with $m \leq n$. For any scaled grid, Weave(m, n) can also be applied. If a grid has more rows than columns, we apply Weave(m, n) to the grid rotated by 90°.

4.2.1. Procedure

Weave(m, n) uses the distances of LineOdd(n) and LineEven(n) in horizontal direction. At the same time it takes vertical distances in order to get longer edges than $(0, k-1)$-edges. The order of columns is the same as in LineOdd(n) or

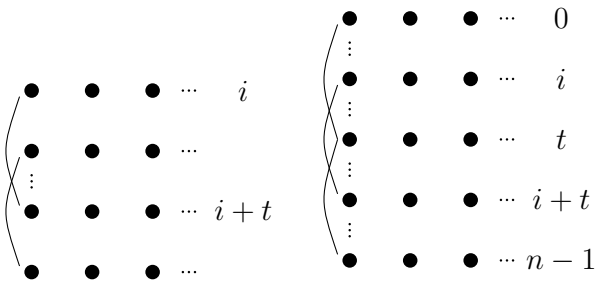

(a) Even number of rows (b) Odd number of rows

Figure 4.2.: Pairs and triples of rows

LineEven(n) but the initial node is node $k+1$. If we took the same pattern for the rows as for the columns, we could not yield a closed tour and some of the distances still would not be long enough, so we have to take a new pattern for the rows.

The rows are partitioned in $\frac{m}{2}$ pairs of rows if m is even and in $\frac{m-1}{2} - 1$ pairs and one triple of rows if m is odd. The pairs are chosen such that the distance between the two rows is $t = \left\lfloor \frac{m}{2} \right\rfloor$ which is also true for the triple, see figure 4.2. The idea is to jump back and forth inside a pair (triple) of rows where the order of columns is given by Weave$(1, n)$. For an odd number of columns, the pattern is done twice in a pair and three times in a triple, so all nodes get visited. For n even, applying Weave$(1, n)$ twice to a pair would definitely yield a subtour visiting half of the nodes in the pair twice. That is why the pattern is only applied to a pair once for n even, then Weave(m, n) switches to the subsequent pair. When the pattern has been applied to every pair once, Weave(m, n) returns to the second row of the first pair for the second turn. When returning to a pair for the second time, Weave(m, n) starts in the other row, respectively, to ensure that the second half of the nodes is visited. If there is a triple of rows, the pattern is applied to it three times in the beginning and afterwards the pairs are visited.

As switching to another pair can yield a short vertical distance of $t-1$ or $t-2$, we compensate it with the longest possible horizontal distance from Weave$(1, n)$, i.e. we always combine it with a horizontal length of $k+1$. In order to guarantee this, we start with column $k+1$ in any pair, so we always finish one pair in column 0 and have a horizontal distance of $k+1$ to the next node.

If m was odd and n was a multiple of 3, LineOdd(n) or LineEven(n) would start three times in the same row when visiting the triple of rows. This has to be avoided. Therefore, in this case Weave(m, n) skips one row of the triple when restarting the order of LineOdd(n) or LineEven(n).

The complete definition of the algorithm is given in the following. In all definitions of algorithms in this work, we usually make use of the residue class ring $\mathbb{Z}/n\mathbb{Z}$ with the canonical representatives $0, \ldots, n-1$.

Definition 3 (WEAVE(m,n))**.** *We define* WEAVE(m,n) *as a mapping w from a set $\mathcal{P} = \{0,\dots,m\cdot n-1\}$ of positions to a node (i,j) in the two-dimensional grid.*

Let $M = \{0,\dots,m-1\}$ be the index set of rows and $N = \{0,\dots,n-1\}$ the index set of columns. WEAVE(m,n) *is described by*

$$\begin{aligned} w : \mathcal{P} &\to M \times N \\ p &\mapsto (i(p), j(p)) \end{aligned} \tag{4.1}$$

with $i(p)$ and $j(p)$ defined in the following way: If n is even,

$$j(p) = \begin{cases} (1-(p \bmod 2))\cdot\left((p \bmod n)+\frac{n}{2}+1\right) & \\ +(p \bmod 2)\cdot((p \bmod n)+1) & \text{if } p \bmod n < \frac{n}{2}-1 \\ (1-(p \bmod 2))\cdot\left(\frac{3}{2}n-2-(p \bmod n)\right) & \\ +(p \bmod 2)\cdot(n-2-(p \bmod n)) & \text{if } \frac{n}{2}-1 \le p \bmod n < n-1 \\ 0 & \text{if } p \bmod n = n-1. \end{cases} \tag{4.2}$$

For m odd or even and n even, $i(p)$ differs. If m even,

$$i(p) = \begin{cases} q+(p \bmod 2)\cdot\frac{m}{2} & \text{if } qn \le p < (q+1)n \\ & q \in \{0,1,\dots,\frac{m}{2}-1\} \\ q-(p \bmod 2)\cdot\frac{m}{2} & \text{if } qn \le p < (q+1)n \\ & q \in \{\frac{m}{2},\dots,m-1\} \end{cases} \tag{4.3}$$

and if m odd,

$$i(p) = \begin{cases} (p \bmod 3)\cdot\frac{m-1}{2} & \text{if } p < 3n \text{ and } n \bmod 3 \neq 0 \\ (p \bmod 3)\cdot\frac{m-1}{2} & \text{if } 0 \le p < n \text{ and } n \bmod 3 = 0 \\ ((p+1) \bmod 3)\cdot\frac{m-1}{2} & \text{if } n \le p < 2n \text{ and } n \bmod 3 = 0 \\ ((p+2) \bmod 3)\cdot\frac{m-1}{2} & \text{if } 2n \le p < 3n \text{ and } n \bmod 3 = 0 \\ q+(p \bmod 2)\cdot\frac{m-1}{2} & \text{if } (3+q-1)n \le p < (3+q)n \\ & q \in \{1,2,\dots,\frac{m-1}{2}-1\} \\ q+1-(p \bmod 2)\cdot\frac{m-1}{2} & \text{if } (3+q-1)n \le p < (3+q)n \\ & q \in \{\frac{m-1}{2},\dots,m-3\}. \end{cases} \tag{4.4}$$

If n is odd,

$$\begin{aligned} j(p) = (((p+1) \bmod n) \bmod 2)\cdot\left(\frac{((p+1) \bmod n)-1}{2}+\frac{n+1}{2}\right) \\ +(1-(((p+1) \bmod n) \bmod 2))\cdot\frac{((p+1) \bmod n)}{2}. \end{aligned} \tag{4.5}$$

If m is even and n is odd,

$$\begin{aligned} i(p) = \frac{q}{2}+[p \bmod 2]\cdot\frac{m}{2} \quad & \text{if } qn \le p < (q+2)n \\ & \text{and } q \in \{0,2,4,\dots,2(\frac{m}{2}-1)\}. \end{aligned} \tag{4.6}$$

n o, m e	n e, m e
(t,k)	(t,k)
$(t,k+1)$	$(t,k+1)$
$(t-1,k+1)$	$(t-1,k+1)$
$(m-1,k+1)$	$(t,k-1)$
	$(t+1,k+1)$

Table 4.1.: Edge lengths for m even in WEAVE(m,n) (o=odd, e=even)

If m and n are odd,

$$i(p) = \begin{cases} (p \bmod 3) \cdot \frac{m-1}{2} & \text{if } 0 \le p < 3n \text{ and } n \bmod 3 \neq 0 \\ (p \bmod 3) \cdot \frac{m-1}{2} & \text{if } 0 \le p < n \text{ and } n \bmod 3 = 0 \\ ((p+1) \bmod 3) \cdot \frac{m-1}{2} & \text{if } n \le p < 2n \text{ and } n \bmod 3 = 0 \\ ((p+2) \bmod 3) \cdot \frac{m-1}{2} & \text{if } 2n \le p < 3n \text{ and } n \bmod 3 = 0 \\ \frac{q}{2} + ((p+1) \bmod 2) \cdot \frac{m-1}{2} & \text{if } (q+1)n \le p < (q+3)n \\ & \text{and } q \in \{2,4,\ldots,2(\frac{m-1}{2}-1)\}. \end{cases} \tag{4.7}$$

If $m = 3$, then WEAVE(m,n) *terminates when the triple of rows is finished with a largest position of $p = 3n-1$. If $m = 2$, the pattern of* LINEODD(n) *or* LINEEVEN(n) *is applied twice while the row changes after each node. If n even, there is a $(0,k+1)$-move between the first and the second turn.*

We state the following lemma.

Lemma 1. WEAVE(m,n) *yields a tour through all nodes.*

We will prove in section 5.2 that w is a bijection. Thus, WEAVE(m,n) returns a tour. In the following we will focus on the shortest edges which appear in WEAVE(m,n).

4.2.2. Bounds

In the following descriptions, the first component t of a (t,k)-edge refers to the vertical direction and the second one k to the horizontal direction. When we search for a lower bound for the MSTSP(m,n), it is expedient to take a look at the shortest edges appearing in WEAVE(m,n). Therefore, we have created a table of all lengths appearing in WEAVE(m,n) (see tables 4.1 and 4.2).

We get these types of edges by computing the horizontal and vertical distance between two subsequent nodes. We consider the definitions of $i(p)$ and $j(p)$ and write down the different lengths in each direction. Therefore, we have to compute several distances. Firstly, we need to compute the difference between the function

n o, m o	$n \bmod 3 \neq 0$ e, m o	$n \bmod 3 = 0$ e, m o
(t,k)	(t,k)	(t,k)
$(t,k+1)$	$(t,k+1)$	$(t,k+1)$
	$(t,k-1)$	$(t,k-1)$
$(t-1,k+1)$	$(t-1,k+1)$	$(t-1,k+1)$
$(m-1,k)$	$(m-1,k)$	$(m-1,k)$
$(m-1,k+1)$	$(m-1,k+1)$	$(m-1,k+1)$
	$(m-1,k-1)$	$(m-1,k-1)$
$(m-2,k+1)$	$(m-2,k+1)$	
	$(t-2,k+1)$	$(t-2,k+1)$
	$(t+1,k+1)$	$(t+1,k+1)$

Table 4.2.: Edge lengths for m odd in WEAVE(m,n) (o=odd, e=even)

values of consecutive positions within one interval. Afterwards, also the differences between the function values of the last position in an interval and the first position in the following interval are taken into account. And finally, the difference between the function values of the last position of the last interval and the first position of the first interval is computed. These differences are combined for each direction.

For example, we consider a grid with m even and n odd. We get the horizontal distances from $j(p)$ (equation (4.5)). Considering the first part of the first summand, we obtain $((p+2) \bmod n) \bmod 2 \neq ((p+1) \bmod n) \bmod 2$ for $(p+1) \bmod n \neq n-1$. In this case $((p+1) \bmod n) \bmod 2$ always changes between 0 and 1. If $p+1$ is a multiple of n, it is 0 for two consecutive positions. The distance is

$$\begin{aligned} |j(p+1) - j(p)| &= \left| \left(\frac{((p+1+1) \bmod n) - 1}{2} + \frac{n+1}{2} \right) - \frac{((p+1) \bmod n)}{2} \right| \\ &= \frac{n+1}{2} = k+1 \end{aligned} \tag{4.8}$$

for $(p+1) \bmod n < n-1$ even and

$$\begin{aligned} |j(p+1) - j(p)| &= \left| \frac{((p+1+1) \bmod n)}{2} - \left(\frac{((p+1) \bmod n) - 1}{2} + \frac{n+1}{2} \right) \right| \\ &= \frac{n-1}{2} = k \end{aligned} \tag{4.9}$$

for $(p+1) \bmod n < n-1$ odd and

$$|j(n-1) - j(n-2)| = \left| \frac{((n-1+1) \bmod n)}{2} - \frac{((n-1) \bmod n)}{2} \right| = \frac{n-1}{2} = k \tag{4.10}$$

for $(p+1) \bmod n = n-1$. In vertical direction we consider $i(p)$. Within one interval the distance is always

$$|i(p+1) - i(p)| = \left|\frac{q}{2} + \frac{m}{2} - \frac{q}{2}\right| = \frac{m}{2} = t. \tag{4.11}$$

When changing from one interval to the next one, the position p of the last node of the interval is odd. Thus, the distance is

$$|i(p+1) - i(p)| = \left|\frac{q+2}{2} - \frac{q}{2} - \frac{m}{2}\right| = \frac{m}{2} - 1 = t - 1. \tag{4.12}$$

This vertical distance only appears for $p = (q+2)n-1$ odd. For such a p we always have $p \bmod n = n-1$ even and

$$\begin{aligned} |j(p+1) - j(p)| &= |j(n) - j(n-1)| \\ &= \left|\left(\frac{((n+1) \bmod n) - 1}{2} + \frac{n+1}{2}\right) - \frac{n \bmod n}{2}\right| \\ &= \frac{n+1}{2} = k+1. \end{aligned} \tag{4.13}$$

The last vertex is connected to the first vertex. In horizontal direction we get the same distance as at any end of an interval, but in vertical direction, we compute

$$|i(0) - i(mn-1)| = \left|-\left(\frac{m}{2} - 1\right) - \frac{m}{2}\right| = m - 1. \tag{4.14}$$

Thus, WEAVE(m,n) takes $(t-1, k+1)$-edges, $(m-1, k+1)$-edges, (t,k)-edges and $(t, k+1)$-edges for m even and n odd. For all other cases we can compute the distances analogously.

Because of the extending structure it is usually possible to consider first the different moves in columns while the moves in rows are constantly the same within one interval. The change of the row interval always goes along with the last move in the column turn. The quantity of an edge can be computed or counted in the mapping by counting the number of intervals in which an edge appears and the number of times this edge appears per interval. A list of the edges and their frequency can be found in the tables 5.3 and 5.4.

For many edges it is obvious that they are longer than others in the list. Hence, the candidates for the shortest edge are (t,k) and $(t-1, k+1)$ if n is odd and $(t-2, k+1)$ only if m is odd and $m \geq 5$, $(t, k-1)$ and $(t-1, k+1)$ if n is even. In the following, we compare the lengths of these edges:

$$\sqrt{t^2+k^2} \leq \sqrt{t^2 + k^2 + 2\underbrace{(k-t)}_{\geq 0} + 2} = \sqrt{(t-1)^2 + (k+1)^2} \tag{4.15}$$

$$\begin{aligned} &\sqrt{(t-1)^2 + (k+1)^2} \geq \sqrt{(t-2)^2 + (k+1)^2} \\ =&\sqrt{t^2 + \underbrace{5}_{\geq 1} + k^2 + \underbrace{2k - 4t}_{\geq -2k}} \geq \sqrt{t^2 + (k-1)^2}. \end{aligned} \tag{4.16}$$

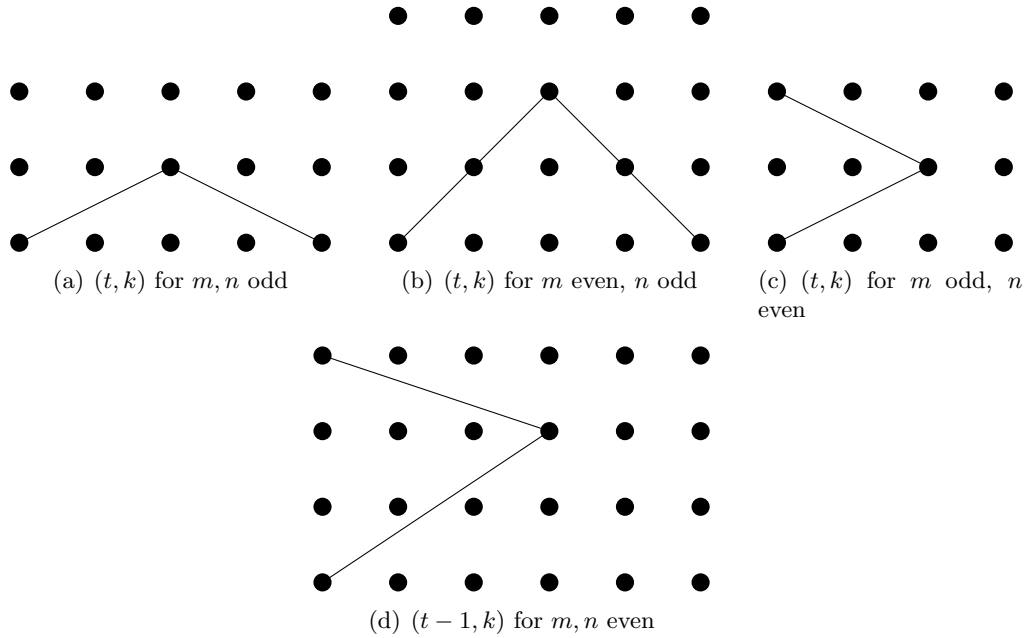

Figure 4.3.: Upper bounds for all kinds of grids

The straightforward calculations show that the shortest edge is a (t, k)-edge if n is odd and a $(t, k-1)$-edge if n is even.

We can get upper bounds for the MSTSP(m, n) by choosing one of the central nodes and determining the second-longest edge incident to that node (see figure 4.3). This choice is motivated by the two facts that any node has to be connected twice in a tour and that the longest incident edges to the central nodes are shorter than those of the other nodes.

For all grids the (t, k)-edge is an upper bound for the longest of the shortest edges, whereas for the grid with an even number of rows and columns, we can refine this bound to a $(t-1, k)$-edge. When we compare the upper and lower bounds, we ascertain the following:

Proposition 2. WEAVE(m, n) *produces an optimal solution of the MSTSP for grids with n odd and for quadratic grids.*

This proposition covers more than half of all possible grids. For grids with an even number of columns, more detailed examinations have to be done. However, it is evident that for a quadratic grid ($m = n$ even) the upper bound equals the lower bound since $t = k$. There is one further case in which the tour computed by WEAVE(m, n) is optimal.

If $m = 2$, a tour using only edges of at least length $\sqrt{(t-1)^2 + k^2}$ would always

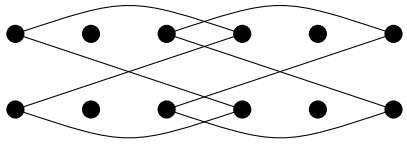

Figure 4.4.: Subtour for a $(2 \times n)$-grid

include subtours. This is due to the fact that the nodes in the center columns could only be connected to the corners (see figure 4.4). Therefore, we can conclude:

Corollary 1. *For any grid with $m = 2$,* WEAVE(m, n) *produces an optimal solution of the MSTSP.*

In all other cases, there is a gap which we will consider in the following subsections.

However, before we examine the gap, we will consider the upper bound in more detail.

We state the following:

Proposition 3. *Let n be even. If $k > \frac{1}{2}(3t^2-2t+1)$ for m even and $k > \frac{1}{2}(3t^2+1)$ for m odd, the objective value of the MSTSP is at most $\sqrt{(m-1)^2+(k-1)^2}$.*

Proof. Consider a grid with an odd number of rows ($m = 2t + 1$) and an even number of columns ($n = 2k$) where the number of columns is greater than $3t^2 + 1$. We transform the inequality in the following way:

$$\begin{aligned} & k > \frac{1}{2}(3t^2+1) \\ \Leftrightarrow\ & 0 > 3t^2 + 1 - 2k = 4t^2 + 4t + 1 - 2k - t^2 - 4t - 2 + 2 + k^2 - k^2 \\ \Leftrightarrow\ & t^2 + k^2 > (2t+1)^2 - 2(2t+1) + 1 + k^2 - 2k + 1 \\ \Leftrightarrow\ & t^2 + k^2 > m^2 - 2m + 1 + (k-1)^2 \\ \Leftrightarrow\ & t^2 + k^2 > (m-1)^2 + (k-1)^2 > 0 \\ \Leftrightarrow\ & \sqrt{t^2+k^2} > \sqrt{(m-1)^2+(k-1)^2}. \end{aligned} \tag{4.17}$$

For an even number of rows and columns ($m = 2t$ and $n = 2k$) with $k > \frac{1}{2}(3t^2 - 2t + 1)$ we deduce

$$\begin{aligned} & k > \frac{1}{2}(3t^2-2t+1) \\ \Leftrightarrow\ & 0 > 3t^2 - 2t + 1 - 2k = 4t^2 - 4t + 1 + k^2 - 2k + 1 - 1 - k^2 - t^2 + 2t \\ \Leftrightarrow\ & t^2 - 2t + 1 + k^2 > m^2 - 2m + 1 + (k-1)^2 \\ \Leftrightarrow\ & (t-1)^2 + k^2 > (m-1)^2 + (k-1)^2 > 0 \\ \Leftrightarrow\ & \sqrt{(t-1)^2+k^2} > \sqrt{(m-1)^2+(k-1)^2}. \end{aligned} \tag{4.18}$$

It is not possible to get a tour without any edge of the horizontal length $k-1$ as this would lead to subtours (see figure 4.5). Since an $(m-1, k-1)$-edge is the longest possible edge with a horizontal distance of $k-1$, we receive a new upper bound of $\sqrt{(m-1)^2+(k-1)^2}$ for k greater than the given bounds. □

We can do the same calculation for $k \leq \frac{1}{2}(3t^2+1)$ and $k \leq \frac{1}{2}(3t^2-2t+1)$ and find that there is at least one kind of edge with a horizontal distance of $k-1$ that is longer than the current upper bound, so for these cases the value of the upper bound does not change. Of course, it is not clear at that point if the upper bounds and the optimal value coincide. An overview of the current upper bounds is given in table 4.5.

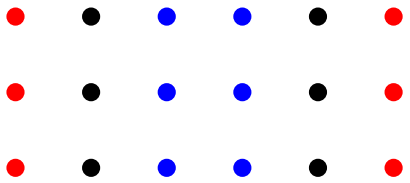

Figure 4.5.: Candidates (red) for consecutive nodes for the nodes of the middle columns (blue) with a horizontal distance of at least k

4.2.3. Approximation Ratio for an Even Number of Columns

From the bounds that we computed in the previous subsection we can now compute the gap between the upper and lower bounds to derive the gap between Weave(m, n) and an optimal solution for the different cases of the algorithm. In table 4.3, the absolute values of the gaps and the gaps relative to the upper bounds are listed. Figures 4.3 and 4.7 show the relative gaps from table 4.3 for some even numbers of columns. In figures 4.6(a) and 4.6(b) smaller grids are illustrated while figures 4.7(a) and 4.7(b) give an impression of the gap for larger grids. According to the graphs, the following holds: For m odd the gap is monotonically decreasing for an increasing number of columns, for m even it is decreasing for large values of n.

For the quadratic grids (first point of each curve) with an even number of rows and columns, the gap is monotonically decreasing for an increasing size of the grid. The same holds for near-quadratic grids ($m = n-1$) with m odd and n even. For any fixed m, the relative gap converges to 0 for an increasing n.

We will prove most of these observations in the following.

For the absolute gap the following lemma, which we have also presented in [48], holds.

Lemma 2. *For any regular grid with n even, the gap between the solution of* Weave(m, n) *and the upper bound of the MSTSP deduced from the distances between corner and central points is always smaller than one.*

Grid	abs. value	rel. value
m even, $k < a$	$\sqrt{(t-1)^2+k^2} - \sqrt{t^2+(k-1)^2}$	$1 - \sqrt{1 - \frac{2(k-t)}{(t-1)^2+k^2}}$
m even, $k \geq a$	$\sqrt{(m-1)^2+(k-1)^2} - \sqrt{t^2+(k-1)^2}$	$1 - \sqrt{1 - \frac{3t^2-2t+1}{(m-1)^2+(k-1)^2}}$
m odd, $k < b$	$\sqrt{t^2+k^2} - \sqrt{t^2+(k-1)^2}$	$1 - \sqrt{1 - \frac{2k-1}{t^2+k^2}}$
m odd, $k \geq b$	$\sqrt{(m-1)^2+(k-1)^2} - \sqrt{t^2+(k-1)^2}$	$1 - \sqrt{1 - \frac{3t^2}{(m-1)^2+(k-1)^2}}$

Table 4.3.: Gaps between lower and upper bound for n even – absolute value and value relative to the upper bound with $a = \frac{1}{2}(3t^2 - 2t + 1)$ and $b = \frac{1}{2}(3t^2 + 1)$

Proof. As the upper bound for even m is smaller than the upper bound for odd m (recall that $\sqrt{(t-1)^2+k^2} < \sqrt{t^2+k^2}$), it suffices to prove

$$\sqrt{t^2+k^2} < \sqrt{t^2+(k-1)^2} + 1. \tag{4.19}$$

We can square both sides of the inequality, because all values are greater zero:

$$\begin{aligned} & t^2 + k^2 < t^2 + (k-1)^2 + 2\sqrt{t^2+(k-1)^2} + 1 \\ \Leftrightarrow\ & 0 < -2k + 2 + 2\sqrt{t^2+(k-1)^2} \\ \Leftrightarrow\ & k - 1 < \sqrt{t^2+(k-1)^2}. \end{aligned} \tag{4.20}$$

By observing that $t^2 > 0$ for $m > 1$ on the right hand side, the strict inequality is true. Therefore, the value of the gap between the lower and the upper bound is always strictly smaller than one. □

We can even prove that the convergence of $\textsc{Weave}(m,n)$ to the optimum is asymptotic.

Proposition 4. *For n even and m odd we have*

$$\textsc{Weave}(m,n) \geq \underbrace{\sqrt{1 - \frac{2k-1}{t^2+k^2}}}_{\alpha_{t,k}} \cdot OPT(m,n).$$

For even m, n we have

$$\textsc{Weave}(m,n) \geq \underbrace{\sqrt{1 - \frac{2(k-t)}{(k-t)^2+2t(k-1)+1}}}_{\beta_{t,k}} \cdot OPT(m,n).$$

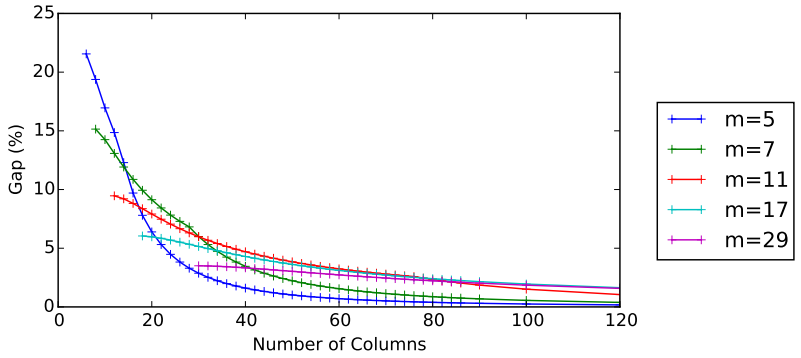

(a) Relative gap for an odd number of rows

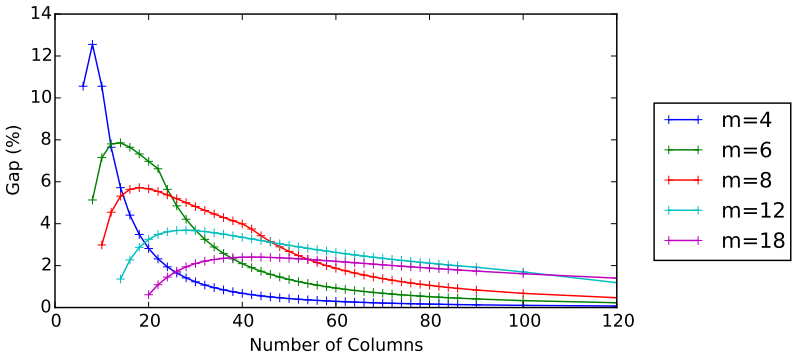

(b) Relative gap for an even number of rows

Figure 4.6.: Gaps for an even number of columns and a small number of rows

Proof. The proof works by straightforward calculations: It is obvious that

$$OPT(m,n) \leq \text{Upper Bound}(m,n).$$

Therefore,

$$\textsc{Weave}(m,n) = \alpha_{t,k} \cdot \text{Upper Bound}(m,n) \geq \alpha_{t,k} \cdot OPT(m,n) \tag{4.21}$$
$$\textsc{Weave}(m,n) = \beta_{t,k} \cdot \text{Upper Bound}(m,n) \geq \beta_{t,k} \cdot OPT(m,n) \tag{4.22}$$

with

$$\alpha_{t,k} = \frac{\textsc{Weave}(m,n)}{\text{Upper Bound}(m,n)} = \frac{\sqrt{t^2+(k-1)^2}}{\sqrt{t^2+k^2}} = \sqrt{1-\frac{2k-1}{t^2+k^2}} \tag{4.23}$$

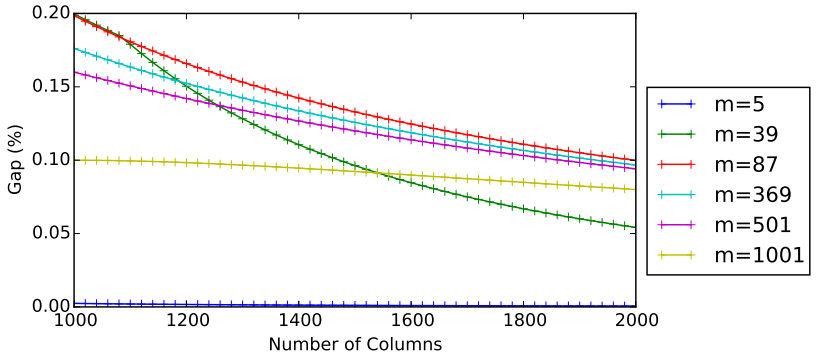

(a) Relative gap for an odd number of rows

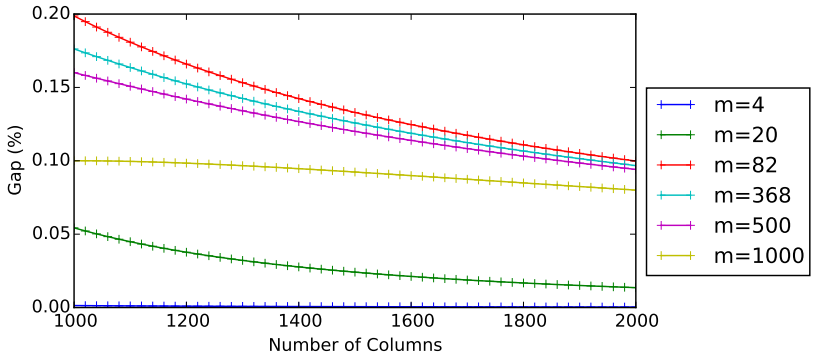

(b) Relative gap for an even number of rows

Figure 4.7.: Gaps for an even number of columns and a large number of rows

if m odd and n even;

$$\beta_{t,k} = \frac{\textsc{Weave}(m,n)}{\text{Upper Bound}(m,n)} = \frac{\sqrt{t^2+(k-1)^2}}{\sqrt{(t-1)^2+k^2}} = \sqrt{1-\frac{2(k-t)}{(k-t)^2+2t(k-1)+1}} \tag{4.24}$$

if m even and n even. □

Since the approximation guarantee converges to one for increasing m and n, we conclude the following:

Corollary 2. *For all but 4 small sizes of grids* $\alpha, \beta \geq 0.8$. *Moreover, for all* $t \geq 1$ $\lim_{k\to\infty} \alpha_{t,k} = 1$ *and* $\lim_{t\to\infty,k\to\infty} \alpha_{t,k} = 1$. *The same convergence holds for* $\beta_{t,k}$. *In this sense,* $\textsc{Weave}(m,n)$ *is asymptotically optimal.*

Proof. Obviously, for any t and k with $0 < t \leq k$

$$\alpha_{tk} = \sqrt{\frac{t^2 + (k-1)^2}{t^2 + k^2}} < \sqrt{\frac{t^2 + (k-1)^2}{(t-1)^2 + k^2}} = \beta_{tk} \leq 1. \tag{4.25}$$

After a transformation, we obtain

$$\alpha_{tk} = \sqrt{1 - \frac{2k-1}{t^2 + k^2}}. \tag{4.26}$$

As $\lim_{t,k\to\infty} \frac{2k-1}{t^2+k^2} = 0$, α converges to 1 and thus, with equation (4.25) β also converges to 1.

Now, we prove that α_{tk} is monotonically increasing. Thus, we restrict to grids with an odd number of rows m and an even number of columns n. As in this case $t = \frac{m-1}{2}$ and $k = \frac{n}{2}$ and $m \leq n$, we need not consider the case of $t = k$ for those grids, but only $t \leq k - 1$. As the square root is monotonically increasing, it suffices to show for m odd that the subtrahend under the square root from equation (4.26) is monotonically decreasing. The partial derivatives are

$$\frac{\partial}{\partial t}\left(\frac{2k-1}{t^2 + k^2}\right) = -\frac{(2k-1) \cdot 2t}{(t^2 + k^2)^2} < 0 \tag{4.27}$$

$$\frac{\partial}{\partial k}\left(\frac{2k-1}{t^2 + k^2}\right) = \frac{2(t^2 - k^2 + k)}{(t^2 + k^2)^2}. \tag{4.28}$$

The derivative in equation (4.28) is negative if $t \leq \sqrt{k(k-1)}$. As $\sqrt{k(k-1)} > \sqrt{(k-1)^2} = k - 1$, the derivative is negative for all considered grids. Thus, α_{tk} is monotonically increasing. We compute a list of α_{tk} starting from a 3×4-grid (α_{12}) and increasing k until $\alpha_{tk} \geq 0.8$ for one grid. Then we continue with α_{56} and so on. We see that $\alpha_{tk} \geq 0.8$ for a 3×10-grid, a 5×8-grid and a 7×8-grid. For all larger grids $\alpha_{tk} \geq 0.8$. There are only 4 grid sizes, namely the 3×4-grid, 3×6-grid, 3×8-grid, and the 5×6-grid, for which $\alpha_{tk} < 0.8$.

For each grid with m and n even and $m < n$, there is a grid with m odd and n even such that they have the same t and k and equation (4.25) holds. For quadratic grids and for grids with two rows we have already proved that Weave(m, n) yields an optimal solution. Therefore, we only check if $\beta_{23} \geq 0.8$, which is true. □

Since Weave(m, n) is a bijective mapping of the nodes to positions on the grid, it is a linear-time algorithm in the number of nodes.

The following definition of the asymptotic performance ratio is taken from Korte et al. [52] (S.361):

Definition 4. *Let $\mathcal{P}$ be an optimization problem with nonnegative weights and $k \geq 1$. A **k-factor approximation algorithm** for $\mathcal{P}$ is a polynomial-time algorithm A for $\mathcal{P}$ for which there exists a constant c such that*

$$\frac{1}{k} OPT(I) \leq A(I) \leq k \; OPT(I) \tag{4.29}$$

*for all instances I of $\mathcal{P}$. We also say that A has **performance ratio** k.*

Let us set $k = \frac{1}{\alpha} \geq 1$, respectively $k = \frac{1}{\beta} \geq 1$. We proved that $\frac{1}{k}\text{OPT}(m,n) \leq \textsc{Weave}(m,n)$ and $\textsc{Weave}(m,n) \leq k\text{OPT}(m,n)$ is obvious. So $\textsc{Weave}(m,n)$ has an asymptotic performance ratio of $\sqrt{\frac{t^2+k^2}{t^2+(k-1)^2}}$ if m odd and n even and of $\sqrt{\frac{(t-1)^2+k^2}{t^2+(k-1)^2}}$ if m and n even. For all other cases it is 1. For the following algorithms for the MSTSP, we will mostly only mention α or β as these values describe how close the approximation is to the optimum. The ratio could, however, easily be computed.

4.3. Improvements for Special Cases

In addition to the summarized ideas of $\textsc{Weave}(m,n)$ which were presented in our preprint [48], we continue our considerations on procedures on grids for the MSTSP. For some special cases where $\textsc{Weave}(m,n)$ does not yield an optimal solution, we have found other procedures to determine an optimal solution of the MSTSP. The optimality of the procedures is derived from the current upper bound which can be reached.

A list of the edges used in those further procedures is given in table 4.4. We will deduce the algorithms and the related edges in the following.

$\textsc{Boeven}(m,n)$		$\textsc{Bobodd}(m,n)$		
$m=4$	$m \geq 6$	$m=3$	$m=n-1$	$5 \leq m < n-1$
	(t,k)	(t,k)	(t,k)	(t,k)
$(t-1,k)$	$(t-1,k)$		$(t+1,k-1)$	$(t-1,k)$
			$(t+1,k)$	$(t+1,k)$
$(m-1,k-1)$	$(m-1,k-1)$	$(m-1,k-1)$	$(t+1,k+1)$	$(m-1,k-1)$
$(m-1,k+1)$	$(m-1,k+1)$	$(m-1,k+1)$		$(m-2,k)$
		$(m-1,n-1)$	$(t+1,n-1)$	$(m-3,k+1)$

Table 4.4.: Edges of the special procedures (for $m=5$ the second edge in the list does not appear)

For the description of the algorithms we will use the following notation:

Notation 1. *If a formula does continue in the following line, it is marked with a* $\hookleftarrow$.

4.3.1. Exact Algorithm for 4 and 6 Rows and an Even Number of Columns

If the number of columns is even, $\textsc{Weave}(m,n)$ does not yield an optimal solution. We will deduce an optimal solution in a different way for grids with an even number

of rows and columns. In this subsection we consider an optimal procedure for $m = 4$ and $m = 6$, which we will extend to an optimal procedure for grids with m and n even in the next subsection. The general definition of the function b describing the algorithm can be found in equation (4.31). In order to get a better understanding of the construction of our second method, we will first consider the smaller cases.

For $m = 4$ the procedure starts at the node in the left upper corner and builds a path through all rows by moves of $(1, k)$, then returns to the second node in the first row and goes on like this until it finishes by connecting the kth node of the fourth row to the first node in the first row:

$$(0,0),(1,k),(2,0),(3,k),(0,1),(1,k+1),\ldots,(0,n-1),(1,k-1),(2,n-1),(3,k-1).$$

An example of a (4×6)-grid is illustrated in figure 4.8(a). The edges that appear are $(1, k)$-edges, $(3, k-1)$-edges and $(3, k+1)$-edges. Thus the shortest of them is either the $(2, k)$-edge if $k = 4$ or the $(3, k-1)$-edge for greater k. This yields the upper bound from table 4.5. As we will also extend this procedure to a 3-dimensional grid later on, the tour in a two-dimensional grid should be finished by the longest edge of the algorithm which is a $(3, k+1)$-edge in this case. Therefore, a new starting point $(0, k+1)$ is chosen. As the solution is a tour, it is easy to start at another node without changing the order. For $m = 6$, the method works similarly, particularly for the columns, but with paths through every second row instead of every row. When a node in the second to last row is reached the method gets on in the second row and finishes in the last row. The order of a (6×8)-grid is illustrated in figure 4.8(b) and we can write the order in the following way:

$$\begin{aligned}&(0,0),(2,k),(4,0),(1,k),(3,0),(5,k),(0,1),(2,k+1),\ldots,\\&(0,n-1),(2,k-1),(4,n-1),(1,k-1),(3,n-1),(5,k-1).\end{aligned} \tag{4.30}$$

The edges which appear here are similar to those for $m = 4$: $(t-1, k)$-edges, $(m-1, k-1)$-edges, $(m-1, k+1)$-edges and additionally (t, k)-edges, which are neither the shortest nor the longest edges. The shortest appearing edge is analogous to $m = 4$ and also yields the upper bound from table 4.5. In this procedure we will also start in general at node $(0, k+1)$ in order to terminate with a long edge.

4.3.2. General Algorithm for $m > 6$ Even

The previously mentioned optimal procedures for grids with 4 or 6 rows can be extended to grids with an even number of rows and columns for $m \geq 8$. We will call it BOBEVEN(m, n) (definition 5) in the following. We have two triples of rows consisting of the rows 0, $t-1$, $m-2$ and rows 1, t, $m-1$ and the remaining rows are matched to pairs of the distance $t-1$. All columns of the distance k are matched in pairs as well. Within one pair of columns, the following order which is visualized in figure 4.9 is worked through: While continuously swaying between the columns, the row number increases by $t-1$ until it is no longer possible. This is two times in a triple and once in a pair. Then a decrease of t guides to another

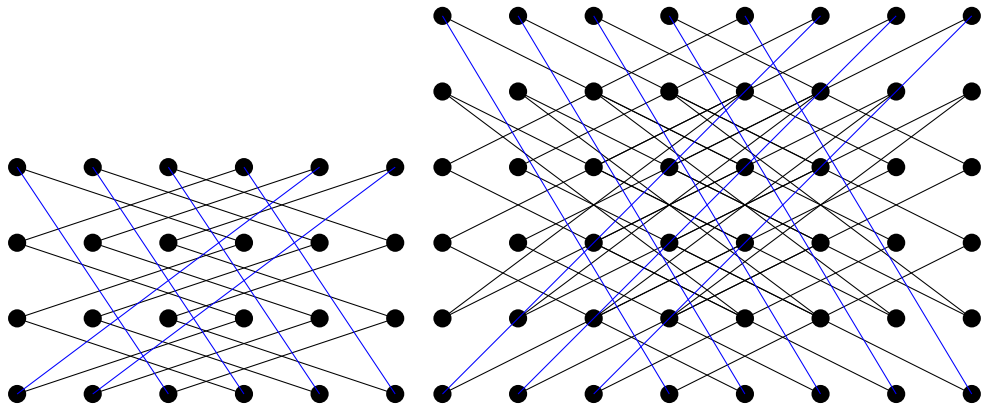

(a) 4 rows (b) 6 rows

Figure 4.8.: Optimal procedure for 4 and 6 rows

pair. This is repeated until the second triple reaches the last row. The next pair of columns is connected by an $(m-1, k-1)$-move backwards for the first half of pairs and an $(m-1, k+1)$-move forward in the second half. The tour is closed by an $(m-1, k-1)$-move. In the following, we will shift the procedure such that the starting node is $(0, k+1)$ in order to have a long distance when closing the tour.

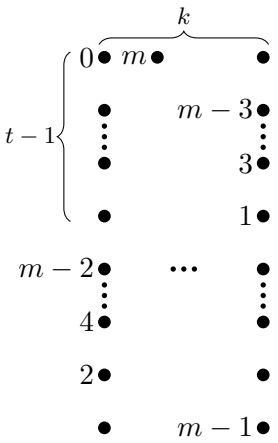

Figure 4.9.: Order of rows for m, n even

BOBEVEN(m, n) is defined as a mapping b from a set $\mathcal{P}$ of positions to a node in the two-dimensional grid.

Definition 5 (BOBEVEN(m, n))**.** *Let* $M = \{0, \ldots, m-1\}$ *be the index set of rows and* $N = \{0, \ldots, n-1\}$ *the index set of columns. Then* BOBEVEN(m, n) *is described*

by

$$\begin{aligned} b : \mathcal{P} &\to M \times N \\ p &\mapsto (i(p), j(p)) \end{aligned} \tag{4.31}$$

with $i(p)$ and $j(p)$ defined in the following way:

$$i(p) = \begin{cases} 0 & \text{if } p \bmod m = 0 \\ m-1 & \text{if } p \bmod m = m-1 \\ t-1-(p \bmod 2) \cdot \left(\left\lfloor \frac{p \bmod m}{2} \right\rfloor \right) \hookleftarrow & \\ \quad + (1-(p \bmod 2)) \cdot (t - \left\lfloor \frac{p \bmod m}{2} \right\rfloor) & \text{if } p \bmod m \in \{1, \ldots, m-2\} \end{cases} \tag{4.32}$$

$$j(p) = \begin{cases} (k+1) + q - (p \bmod 2) \cdot k & \text{if } q \cdot m \leq p < (q+1) \cdot m, \\ & q \in \{0, \ldots, k-2\} \\ q - (k-1) + (p \bmod 2) \cdot k & \text{if } q \cdot m \leq p < (q+1) \cdot m, \\ & q \in \{k-1, \ldots, n-2\} \\ k - (p \bmod 2) \cdot k & \text{if } p = m(n-1). \end{cases} \tag{4.33}$$

The mapping b yields a tour through all nodes. The proof that b is a bijection works analogously to the proof for g in section 5.2 starting with the order of rows $i(p)$ instead of the order of columns $j(p)$. Furthermore, the following proposition holds.

Proposition 5. *Let m, n be even. Then* Bobeven(m, n) *produces an optimal tour for MSTSP(m, n).*

Proof. We compute the appearing edge lengths in Bobeven(m, n) as described in section 4.2.2. Edges which occur in the tour are $(t-1, k)$-edges, (t, k)-edges, $(m-1, k-1)$-edges and $(m-1, k+1)$-edges. It is obvious that a (t, k)-edge is longer than a $(t-1, k)$-edge, therefore the shortest edges are either $(t-1, k)$-edges or $(m-1, k-1)$-edges. The upper bounds of proposition 3 coincide with the solution of Bobeven(m, n). □

4.3.3. Optimal Procedure for a Grid with Three Rows and an Even Number of Columns

We will create a separate procedure for grids with an odd number of rows and an even number of columns which is a better approximation than Weave(m, n) and in several cases yields an optimal solution, namely for $m = 3$, $m = 5$ or $k \geq \frac{1}{2}t(3t+2)$. In order to make the construction understandable and also to stress the optimal cases, we will treat these particular cases separately. We will consider the case of $m = 3$ in this subsection, and the case of $m = 5$ and $k \geq \frac{1}{2}t(3t+2)$ in the next subsection after the general definition.

For grids with 3 rows and an even number of columns, we have found a procedure which only uses edges with a length of at least $\sqrt{t^2 + k^2}$ for the (3×4)-grid and of $\sqrt{(m-1)^2 + (k-1)^2}$ for $n \geq 6$. These values coincide with the upper bounds of table 4.5. The tour of some example grids are visualized in figure 4.10.

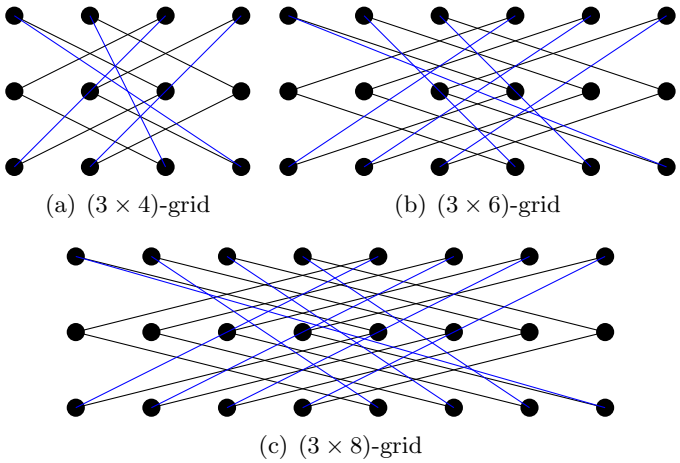

(a) (3×4)-grid (b) (3×6)-grid

(c) (3×8)-grid

Figure 4.10.: Tour in a $(3 \times n)$-grid

The procedure uses (t, k)-edges, that is $(1, k)$-edges, to connect the first to the second row and the second to the third row. Every node of the second row is thus connected to two edges. Furthermore, $(2, k-1)$-edges and $(2, k)$-edges – $\frac{n}{2}$ of each – are needed to connect the triples of nodes to a tour without producing subtours. The node in the last row and in the first column is connected to the first node in the kth column, the last node of the second column to the first node in the $(k+1)$st column, and so on until the connection of the last node in the $(k-1)$th column to the first node in the $(n-1)$th column. The last nodes of the following columns $j = k, \ldots, n-2$ are connected to the first node in column $j - k + 1$. Finally, the last node in the last column is connected to the first node in the first column.

The extended procedure is given in the following subsection and it can be proved that it results in a tour. Regarding the principle, we can deduce the used edges. They could also be obtained from definition 6. The procedure includes (t, k)-edges, $(m-1, k-1)$-edges, $(m-1, k)$-edges and one $(m-1, n-1)$-edge. The shortest of them are obviously (t, k) and $(m-1, k-1)$ which coincide with the table of the upper bounds table 4.5 and therefore the new algorithm is an optimal procedure.

4.3.4. Approximation Algorithm for an Odd Number of Rows and an Even Number of Columns

For all grids with an odd number of rows and an even number of columns, the following procedure yields an approximation for the MSTSP that is closer to the

optimum than WEAVE(m, n) and is optimal for large grids with a considerably greater number of columns than rows. We will call this procedure BOBODD(m, n). The exact sizes of grids are deduced in the following. The patterns that are applied are illustrated in figure 4.13. The pattern from figure 4.11(a) is applied to all pairs of columns starting with 0 in the first column. The last turn starts in column $k-1$ and ends in the last row in column $n-1$. For this pair, the algorithm starts with the second pattern directly after finishing the first pattern and returns step by step backwards to the first pair.

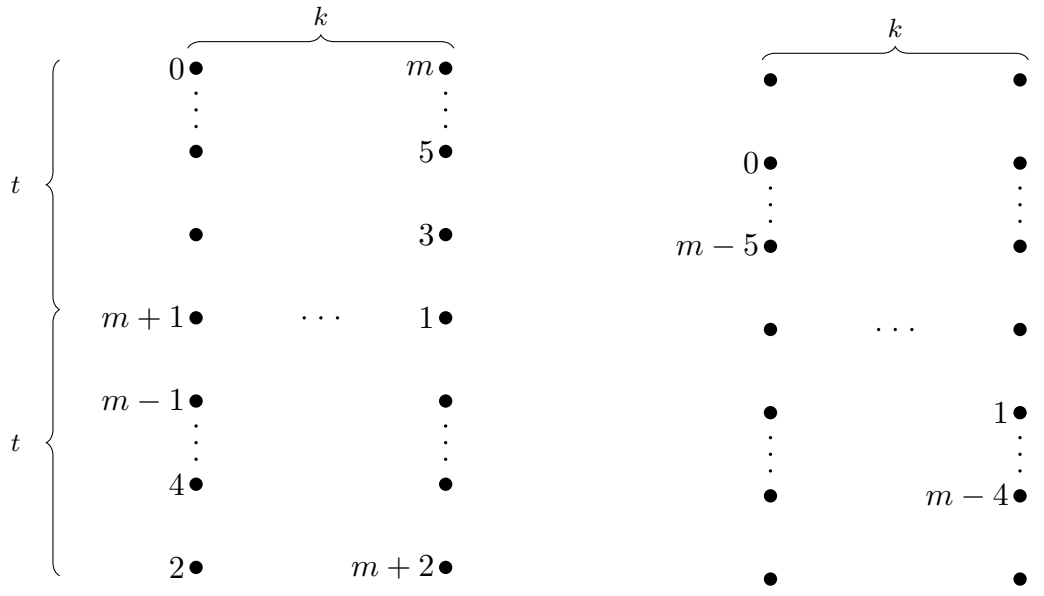

(a) Pattern within a pair of columns in the first run

(b) Pattern in the second run

Figure 4.11.: Pattern for m odd and n even ($m > 5$)

Formally, this procedure is defined in definition 6.

Definition 6 (BOBODD(m, n))**.** *Let $M = \{0, \ldots, m-1\}$ be the index set of rows and $N = \{0, \ldots, n-1\}$ the index set of columns. Then* BOBODD(m, n) *is described by*

$$\begin{aligned} o : \mathcal{P} &\to M \times N \\ p &\mapsto (i(p), j(p)) \end{aligned} \tag{4.34}$$

with $i(p)$ and $j(p)$ defined in the following way:

$$i(p) = \begin{cases} 0 & \text{if } p \bmod (m+3) = 0 \\ & \text{and } p < \frac{1}{2}n(m+3) \\ m-1-(p \bmod 2)\cdot\frac{m-1}{2} \hookleftarrow & \text{if } p \bmod (m+3) > 0 \\ -\left\lfloor \frac{(p \bmod (m+3))-1}{2} \right\rfloor & \text{and } p < \frac{1}{2}n(m+3) \\ m-1 & \text{if } p \bmod (m+3) = m+2 \\ & \text{and } p < \frac{1}{2}n(m+3) \\ 1+\left(\left(p-\frac{n(m+3)}{2}\right) \bmod 2\right)\cdot\frac{m-1}{2} \hookleftarrow & \\ +\left\lfloor p-\frac{\frac{1}{2}n(m+3)}{2} \right\rfloor \bmod (\frac{m-3}{2}) & \text{if } p \geq \frac{1}{2}n(m+3) \end{cases} \tag{4.35}$$

$$j(p) = q(p) + ((p \bmod (m+3)) \bmod 2)\cdot\frac{n}{2} \tag{4.36}$$

$$\text{with } q(p) = \begin{cases} \left\lfloor \frac{p \bmod (mn)}{m+3} \right\rfloor & \text{if } p < (m+3)\cdot\frac{n}{2} \\ \frac{n}{2}-1-\left\lfloor \frac{(p \bmod (mn))-(m+3)\cdot\frac{n}{2})}{m-3} \right\rfloor & \text{else.} \end{cases} \tag{4.37}$$

It can be proved similar to the proof in section 5.2 that o is a bijection and therefore, o yields a tour. The computed edges that appear in BOBODD(m,n) are for the first pattern

$$(t,k) \tag{4.38}$$
$$(t+1,k) \tag{4.39}$$
$$(m-1,k-1). \tag{4.40}$$

For the change between the patterns and the second pattern this set is extended with

$$(m-2,k) \tag{4.41}$$
$$(t-1,k) \tag{4.42}$$
$$(m-3,k+1). \tag{4.43}$$

The shortest edge is the $(t-1,k)$-edge if $k < \frac{1}{2}t(3t+2)$ whose length is not equal to the upper bound for grids of this kind. For $k \geq \frac{1}{2}t(3t+2)$, $(m-1,k-1)$ is shorter than $(t-1,k)$ and is therefore the shortest edge. This edge yields the upper bound which is then $\sqrt{(m-1)^2+(k-1)^2}$, so BOBODD(m,n) is optimal for those grids. Analogous to the calculation of α_{tk}, we derive

$$\text{BOBODD}(m,n) \leq \sqrt{1-\frac{2t-1}{t^2+k^2}}\cdot OPT(m,n). \tag{4.44}$$

We compute the inverse approximation ratio α_{tk} from section 4.2.3. Comparing BOBODD(m,n) to the current upper bounds of the MSTSP, we see that

$$\begin{aligned}\alpha_{tk} &\geq \sqrt{1-\tfrac{2t-1}{t^2+k^2}} && \text{for } k < \frac{1}{2}(3t^2+1) \text{ and}\\ \alpha_{tk} &\geq \sqrt{1-\tfrac{3t^2+2t-2k}{4t^2+(k-1)^2}} && \text{for } \frac{1}{2}(3t^2+1) \leq k < \frac{1}{2}t(3t+2).\end{aligned}$$

For greater k we receive an optimal solution.

For $m = 5$, BOBODD(m,n) yields an optimal solution. As only one pair of nodes is missing after the first pattern, we only do the (t,k)-move and then get on in the next pair of columns, so the $(t-1,k)$-move never appears. We can prove this by considering the last case of equation (4.35). If $m = 5$, we compute the rounded down summand modulo 1 and so it remains 0, i.e. $i(p)$ changes between two values in the last part of the algorithm. Also in the second case of equation (4.36) the pair of columns is changed after every second node.

The current results are summarized in proposition 6.

Proposition 6. *Let m odd, n even.* BOBODD(m,n) *produces a tour which is asymptotically optimal for MSTSP(m,n) and whose shortest edge is longer than α_{tk} times the optimal value with*

$$\alpha_{tk} \geq \sqrt{1-\tfrac{2t-1}{t^2+k^2}} \quad \textit{for } k < \frac{1}{2}(3t^2+1) \textit{ and} \tag{4.45}$$

$$\alpha_{tk} \geq \sqrt{1-\tfrac{3t^2+2t-2k}{4t^2+(k-1)^2}} \quad \textit{for } \frac{1}{2}(3t^2+1) \leq k < \frac{1}{2}t(3t+2). \tag{4.46}$$

If $m = 3$ or $m = 5$ or $k \geq \frac{1}{2}t(3t+2)$ the tour is optimal.

4.3.5. Special Case of $m = n - 1$

For grids with an even number of columns and $m = n-1$ which results in m odd, we will compute an optimal solution for MSTSP. As $t = k-1$, the length of a (t,k)-edge is the same as of a $(t+1,k-1)$-edge ($t^2+k^2 = (k-1)^2+k^2 = (k-1)^2+(t+1)^2$). Therefore, both of them are the shortest edges which may be used to construct an optimal tour.

The procedure which is applied in an example in figure 4.12 for $m = 5$ and $n = 6$ is presented below. All nodes in the middle row t get connected twice by (t,k)-edges to a node in row 0 and one in row $m-1$. All nodes in the other rows are connected to one further node by a (t,k)-edge. Furthermore, all nodes, except those of row 0 and of row $t+1$ are incident to a $(t+1,k)$-edge. Now, there are only paths between two columns at a time. Each path has its endpoints in row 0 and in row $t+1$. In these two rows, the edges have to be chosen such that no subtours appear. The first $k+1$ nodes in row 0 are each connected to the node in row $t+1$ with the horizontal distance $k-1$. The next $k-2$ nodes in row 0 are connected to the node in row $t+1$ with the horizontal distance k. The last node of the first row is connected to

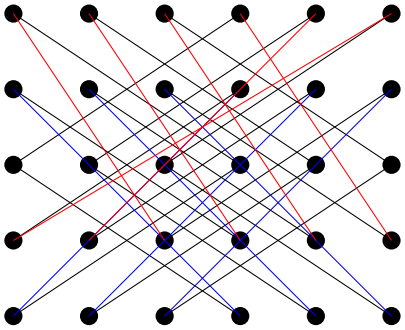

Figure 4.12.: Optimal tour for the MSTSP for a (5×6)-grid

the first one in row $t+1$. Figure 4.13(b) illustrates the order of nodes by dividing the procedure into patterns.

As the last node in the pattern is in the same column as the first one, it is obvious how to combine the order in figure 4.13(b) with the pattern. The horizontal distance between consecutive columns is either $k-1$ or k, and in the very last step which completes the tour, it is $n-1$. Thus, the shortest movement in this pattern is a $(t+1, k-1)$-move, that is a (t,k)-move, which yields the upper bound. Therefore, the procedure is optimal. This special procedure is defined as a mapping nq (nearly quadratic) from a set $\mathcal{P}$ of positions to a node in the two-dimensional grid in definition 7.

Definition 7 (NEAR_QUADRATIC(m,n))**.** *Let $M = \{0,\dots,m-1\}$ be the index set of rows and $N = \{0,\dots,n-1\}$ the index set of columns.* NEAR_QUADRATIC(m,n) *is defined by*

$$\begin{aligned} nq : \mathcal{P} &\to M \times N \\ p &\mapsto (i(p), j(p)) \end{aligned} \tag{4.47}$$

with $i(p)$ and $j(p)$ defined in the following way:

$$i(p) = \begin{cases} 0 & \text{if } p \bmod m = m-1 \\ ((p+1) \bmod m) \bmod 2 \cdot \frac{m-1}{2} + 1 + \left\lfloor \frac{p \bmod m}{2} \right\rfloor & \text{if } p \bmod m \neq m-1 \end{cases} \tag{4.48}$$

$$\begin{aligned} j(p) &= \frac{q(p)}{2} + (p \bmod 2) \cdot \frac{n}{2} \\ \text{with } q(p) &= \left(1 - \left(\left\lfloor \frac{p}{m} \right\rfloor \bmod 2\right)\right) \cdot \left\lfloor \frac{p}{m} \right\rfloor + \left(\left\lfloor \frac{p}{m} \right\rfloor \bmod 2\right) * \left(\left\lfloor \frac{p}{m} \right\rfloor - 1\right). \end{aligned} \tag{4.49}$$

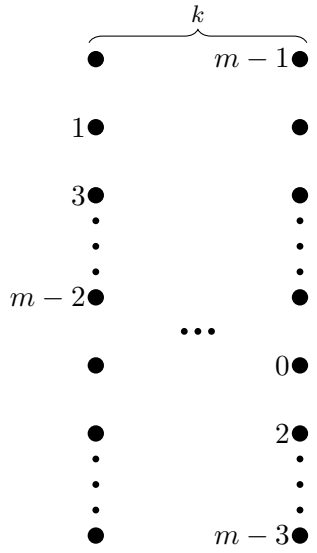

(a) Pattern within a pair of columns

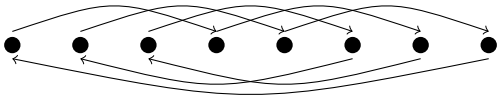

(b) Column of node 0 when one pattern is finished

Figure 4.13.: Pattern and order of the columns for n even and $m = n - 1$

This mapping is a bijection (proof analogous to the proof in section 5.2) and the shortest edge is a (t, k)-edge if $k \leq \frac{1}{2}(3t^2 + 2)$ or else an $(m - 1, k - 1)$-edge.

Proposition 7. NEAR_QUADRATIC(m, n) *defined for regular* $(m \times n)$*-grids with* $m = n - 1$ *creates an optimal solution to the MSTSP with Euclidean distances.*

4.4. A Variant to find a Hamiltonian Path

So far, the results do not change if the objective is to find a path instead of a tour. We may leave out only one single edge in case of a path compared to a tour, but the shortest edge appears several times in a tour. In the following we will have a more detailed look at the upper bounds that we got by considering the nodes in the middle. Either the nodes in the middle have two edges with the length of the upper bound (when n is odd or m is odd) or there are 4 nodes in the middle and at most two of them may be connected only once. So in those cases where we get optimal solutions, the solution is still optimal for the path version of the problem. Also for cases with an upper bound of $\sqrt{(m-1)^2 + (k-1)^2}$, the optimality is preserved. If the solution is not optimal for the cycle problem, it is not optimal for the path version either. The gap, however, is the same as for the tour, because the upper and lower bounds are the same.

For $m > 5$ odd and n even with $k \leq \frac{1}{2}t(3t + 2)$, we have not yet succeeded in the construction of an optimal tour, but for the path, we can get a solution with the

algorithm PATH_ALGORITHM(m, n) which yields an optimal solution. Figure 4.14 illustrates the order of rows within a pair of columns.

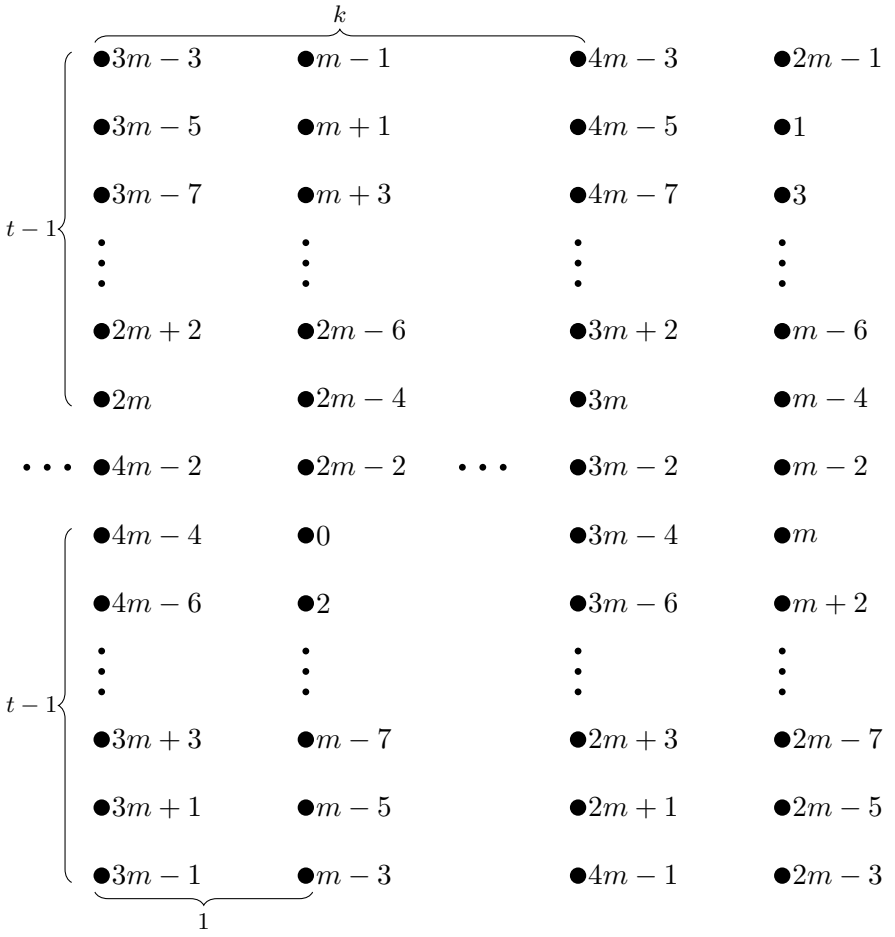

Figure 4.14.: Scheme of an optimal path for odd m and even n

Proposition 8. *The path version of the MSTSP on a regular $(m \times n)$-grid can be solved with the same procedures as the tour version. Any solution of the MSTSP cycle version is an optimal solution for the path version. For m odd and n even,* PATH_ALGORITHM(m, n) *produces an optimal solution to the path version, which is not an optimal solution to the cycle version.*

PATH_ALGORITHM(m, n) starts in the $t + 2$nd row in the kth column and only changes between nodes of this column and nodes of the last column. The vertical distance between consecutive nodes is either t or $t + 1$. When all nodes of the two columns have been visited, the next pair gets visited which consists of the column left to the kth one and the column left to the last column. The algorithm starts

for this pair in row t, so the pattern is now axisymmetrical to the first pattern where the axis is the $t+1$st row. When we proceed to a following pair, we therefore have a distance of $\sqrt{(t-1)^2+(k+1)^2}$ which is always longer than $\sqrt{t^2+k^2}$ as we observe by transformations of the inequality:

$$(t-1)^2+(k+1)^2 > t^2+k^2 \Leftrightarrow 2(k-t+1) \geq 2 > 0.$$

The path terminates at node $(m, k+1)$. We see that an edge closing the tour would be too short, therefore the algorithm is only optimal for the path version. The reflection on the $t+1$st row would not have been necessary to only receive an optimal path, but it decreases the length of the path which is also in our interest (see section 5.3). The order is defined by the following mapping.

Definition 8 (PATH_ALGORITHM(m,n))**.** *Let $m \leq n$ with m odd and n even. $\mathcal{P}$, M, and N are defined as before. Let $\eta(p) = p \bmod (4m)$.* PATH_ALGORITHM(m,n) *is defined by the mapping $g_{path} : \mathcal{P} \to M \times N$, $p \mapsto (i(p), j(p))$:*

$$i(p) = \begin{cases} \frac{m-1}{2} + 1 - (p \bmod 2) \cdot \frac{m-1}{2} \hookleftarrow & \\ + \left\lfloor \frac{p \bmod m}{2} \right\rfloor & \text{if } \eta(p) < m-1 \\ (p \bmod 2) \cdot (\frac{m-1}{2}+1) \hookleftarrow & \\ + \left\lfloor \frac{(p+1) \bmod m}{2} \right\rfloor & \text{if } m-1 \leq \eta(p) < 2m-1 \\ 0 & \text{if } \eta(p) = 2m-1 \\ \frac{m-1}{2} - 1 + (p \bmod 2) \cdot \frac{m-1}{2} \hookleftarrow & \\ - \left\lfloor \frac{p \bmod m}{2} \right\rfloor & \text{if } 2m \leq \eta(p) < 3m-1 \\ m-1-(p \bmod 2) \cdot (\frac{m-1}{2}+1) - \hookleftarrow & \\ \left\lfloor \frac{(p+1) \bmod m}{2} \right\rfloor & \text{if } 3m-1 \leq \eta(p) < 4m-1 \\ m-1 & \text{if } \eta(p) = 4m-1 \end{cases} \tag{4.50}$$

$$j(p) = \frac{n}{2} - 1 - q + (p \bmod 2) \cdot \frac{n}{2} \quad \text{if } 2qm \leq p < 2(q+1)m \text{ with } q = 0, 1, \ldots, \frac{n}{2}. \tag{4.51}$$

We state the following lemma:

Lemma 3. *The mapping g_{path} is a bijection and* PATH_ALGORITHM(m,n) *returns an optimal solution to the MSTSP.*

Analogously to the proof of theorem 3, it can be proved that g_{path} is a bijection and by listing all appearing edges the optimality of the solution can be ensured.

4.5. Main Theorem about the MSTSP on a Regular Grid with Euclidean Distances

We summarize the new insights of this chapter in Theorem 1 part of which was presented in our preprint [48].

Theorem 1. *Let* $m \leq n \in \mathbb{N}$, *and let* $k = \left\lfloor \frac{n}{2} \right\rfloor$ *and* $t = \left\lfloor \frac{m}{2} \right\rfloor$. *Then there is a linear-time algorithm* Weave(m, n) *that specifies a feasible tour for* MSTSP(m, n) *that is*

(i) optimal whenever n *is odd,* $m = n$, *or* $m = 2$;

(ii) a $\left(\sqrt{\frac{(t-1)^2+k^2}{t^2+(k-1)^2}}\right)$*-approximation whenever* m *and* n *are even;*

(iii) a $\left(\sqrt{\frac{t^2+k^2}{t^2+(k-1)^2}}\right)$*-approximation whenever* n *is even and* m *is odd.*

For $m = 3$ *or* $m = 5$ *or* $m = n - 1$ *or* $k \geq \frac{1}{2}t(3t + 2)$ *as well as for* m *and* n *even,* Bobodd(m, n), Near_Quadratic(m, n) *and* Bobeven(m, n) *are linear-time procedures which specify optimal tours for* MSTSP(m, n). *For* $m > 5$ *odd and* $k \leq \frac{1}{2}t(3t + 2)$, Bobodd$(m, n)$ *is a* $\left(\sqrt{\frac{t^2+k^2}{(t-1)^2+k^2}}\right)$*-approximation and* Path_Algorithm(m, n) *returns an optimal path. All of these approximation procedures create asymptotically optimal solutions. The upper bounds of table 4.5 are the best known ones. The best procedure for the general problem the best current procedure is a combination of all procedures:*

- Weave(m, n) *if* n *odd;*
- Bobeven(m, n) *if* m, n *even;*
- Near_Quadratic(m, n) *if* n *even and* $m = n - 1$;
- Bobodd(m, n) *if* m *odd,* n *even and* $m < n - 1$;
- Path_Algorithm(m, n) *if* m *odd,* n *even,* $m < n - 1$ *and path problem.*

Case	Bound	optimal?
Odd columns	$\sqrt{t^2+k^2}$	y
Quad. grid even	$\sqrt{(t-1)^2+k^2}$	y
2 rows even col. $n \leq 4$	$\sqrt{(t-1)^2+k^2}$	y
2 rows even col.	$\sqrt{t^2+(k-1)^2}$	y
3 rows even col. $k \leq \frac{1}{2}(3t^2+1)$	$\sqrt{t^2+k^2}$	y
3 rows even col. $k > \frac{1}{2}(3t^2+1)$	$\sqrt{(m-1)^2+(k-1)^2}$	y
4 rows even col. $k \leq \frac{1}{2}(3t^2-2t+1)$	$\sqrt{(t-1)^2+k^2}$	y
4 rows even col. $k > \frac{1}{2}(3t^2-2t+1)$	$\sqrt{(m-1)^2+(k-1)^2}$	y
5 rows even col. $k \leq \frac{1}{2}(3t^2+1)$	$\sqrt{t^2+k^2}$	y
5 rows even col. $k > \frac{1}{2}(3t^2+1)$	$\sqrt{(m-1)^2+(k-1)^2}$	y
odd rows even col. $k = t+1$	$\sqrt{t^2+k^2}$	y
odd rows even col. $k \leq \frac{1}{2}(3t^2+1)$	$\sqrt{t^2+k^2}$	?
odd rows even col. $k > \frac{1}{2}(3t^2+1)$	$\sqrt{(m-1)^2+(k-1)^2}$	p
even rows even col. $k \leq \frac{1}{2}(3t^2-2t+1)$	$\sqrt{(t-1)^2+k^2}$	y
even rows even col. $k > \frac{1}{2}(3t^2-2t+1)$	$\sqrt{(m-1)^2+(k-1)^2}$	y

Table 4.5.: List of current upper bounds for the Euclidean norm (y = yes, p=partly)

5. Excursions

This chapter examines three excursions starting from the combinatorial algorithms of the previous chapter. First we will determine the cases of optimality for two further metrics. After that, we develop algorithms which approximate the MSTSP on a three-dimensional grid. They consist of extensions of WEAVE(m, n), BOBEVEN(m, n) and BOBODD(m, n). Finally, we turn our attention to another kind of optimization problem, the TSPN – a classical TSP where only edges with a certain minimum length are allowed. We approximate a solution of this problem for particular minimum lengths with WEAVE(m, n), BOBEVEN(m, n) and BOBODD(m, n) in the two-dimensional case and also with WEAVE_3$D(l, m, n)$, BOBEVEN_3$D(l, m, n)$ and BOBODD_3$D(l, m, n)$.

5.1. Further Metrics

For different applications, other metrics than the Euclidean norm can be more suited. In this work, we will consider the 1-norm and the ∞-norm. The 1-norm is defined as $\|x\|_1 = \sum_{i=1}^{m} |x_i|$ and the ∞-norm as $\|x\|_\infty = \max_{i=1,\dots,m}(|x_i|)$. We repeat some of the studies of the case with the Euclidean norm for those two norms as there are differences in upper bounds, gaps and lengths. Referring to WEAVE(m, n), to BOBEVEN(m, n) and to BOBODD(m, n) we list all edges which are used there with their different norms in table 5.1.

Considering only the edges which appear in WEAVE(m, n) we see that for every mentioned norm, the shortest edges are the (t, k)-edges if n is odd and the $(t, k-1)$-edges if n is even. For BOBEVEN(m, n) and BOBODD(m, n) the shortest edges depend on the grid size. In the following, we present results about optimality and gaps for these norms. We can deduce upper bounds by considering the nodes in the middle of the grid and by finding out if there are lengths of shortest edges which would certainly lead to subtours.

5.1.1. The 1-Norm

Considering the nodes in the middle of a grid, the upper bounds for the longest shortest edge in $\|x\|_1$ can be received in the same way as for the Euclidean norm. One upper bound is the length of the second shortest incident edge, which is an (t, k)-edge of length $t + k$ if m or n is odd and an $(t - 1, k)$-edge of length $t + k - 1$ if m and n are even. In the norm $\|\cdot\|_1$ this valid upper bound cannot be decreased

Edge	$\|\|\cdot\|\|_2$	$\|\|\cdot\|\|_1$	$\|\|\cdot\|\|_\infty$
WEAVE(m,n), BOBEVEN(m,n), BOBODD(m,n), NEAR_QUADRATIC(m,n):			
(t,k)	$\sqrt{t^2+k^2}$	$t+k$	k
$(t,k+1)$	$\sqrt{t^2+(k+1)^2}$	$t+k+1$	$k+1$
$(t-1,k+1)$	$\sqrt{(t-1)^2+(k+1)^2}$	$t+k$	$k+1$
$(m-1,k)$	$\sqrt{(m-1)^2+k^2}$	$m+k-1$	$\max(k,m-1)$
$(m-1,k+1)$	$\sqrt{(m-1)^2+(k+1)^2}$	$m+k$	$\max(k+1,m-1)$
$(m-2,k+1)$	$\sqrt{(m-2)^2+(k+1)^2}$	$m+k-1$	$\max(k+1,m-2)$
only when n is even:			
$(t,k-1)$	$\sqrt{t^2+(k-1)^2}$	$t+k-1$	$\max(k-1,t)$
$(t+1,k+1)$	$\sqrt{(t+1)^2+(k+1)^2}$	$t+k+2$	$k+1$
$(t-2,k+1)$	$\sqrt{(t-2)^2+(k+1)^2}$	$t+k-1$	$k+1$
$(m-1,k-1)$	$\sqrt{(m-1)^2+(k-1)^2}$	$m+k-2$	$\max(k-1,t)$
used only in BOBEVEN(m,n), BOBODD(m,n), NEAR_QUADRATIC(m,n):			
$(t-1,k)$	$\sqrt{(t-1)^2+k}$	$t+k-1$	k
$(m-1,n-1)$	$\sqrt{(m-1)^2+(n-1)^2}$	$m+n-2$	$n-1$
$(t+1,k-1)$	$\sqrt{(t+1)^2+(k-1)^2}$	$t+k$	$\max(k-1,t+1)$
$(t+1,k)$	$\sqrt{(t+1)^2+k^2}$	$t+k+1$	$\max(k,t)$
$(t+1,n-1)$	$\sqrt{(t+1)^2+(n-1)^2}$	$t+n$	$n-1$
$(m-2,k)$	$\sqrt{(m-2)^2+k^2}$	$m+k-2$	$\max(k,m-2)$
$(m-3,k+1)$	$\sqrt{(m-3)^2+(k+1)^2}$	$m+k-2$	$\max(k+1,m-3)$

Table 5.1.: Edge lengths for different metrics

in the same way as for the Euclidean norm because

$$\|(m-1,k-1)\|_1 = (m-1)+(k-1) \geq t-1+k = \|(t-1,k)\|_1 \tag{5.1}$$

always holds and $\|(m-1,k-1)\|_1 < \|(t,k)\|_1$ only holds for $t=1$ which is negligible for a general reduction of the upper bound. Lower bounds are received from the combinatorial algorithms, they are $t+k$ if n is odd and $t+k-1$ if n is even. Thus, for the case of an odd number of columns and the case of an even number of rows and columns, the upper and lower bound (u, and l respectively) coincide and WEAVE(m,n) produces an optimal solution. Only in the case of an odd number of rows and an even number of columns there is a gap between the computed solution and the optimal solution of absolute value at most $1(=t+k-(t+k-1))$, which is the distance between the closest nodes in the scaled grid. The relative value (estimated by $\frac{u-l}{u}$) therefore diminishes when increasing the number of rows and columns. So we have an $\frac{1}{\alpha_{tk}}$-approximation with $\alpha_{tk} = \frac{t+k-1}{t+k} = 1-\frac{1}{t^2+k^2}$. With the list of used edges in table 4.4 we consider the shortest edges of BOBEVEN(m,n) and BOBODD(m,n) and NEAR_QUADRATIC(m,n). For BOBEVEN(m,n) the shortest edge in BOBEVEN(m,n) is a $(t-1,k)$-edge. Thus, the solution of BOBEVEN(m,n) is optimal. The shortest edge of NEAR_QUADRATIC(m,n) with $m=n-1$ and of BOBODD(m,n) with $m=3$ is a (t,k)-edge. So in these cases the solutions are optimal similar to the Euclidean norm. In all other cases BOBODD(m,n) uses $(t-1,k)$-edges with length $t+k-1$, so there is a gap between the lower and upper bound of 1 and we have a $\frac{t^2+k^2}{t^2+k^2-1}$-approximation like for WEAVE(m,n). Proposition 9 summarizes all important results about the 1-norm.

Proposition 9. *Let $m \leq n \in \mathbb{N}$ for the* MSTSP(m,n) *with the distances induced by $\|\cdot\|_1$. The following holds:*

i) WEAVE(m,n) *yields an optimal solution if n is odd or m and n are even. Also the tours for m,n even created by* BOBEVEN(m,n) *and the tours for $m=3$ or $m=5$ created by* BOBODD(m,n) *as well as the tours of* NEAR_QUADRATIC(m,n) *for $m=n-1$ are optimal solutions.*

ii) If m is odd and n is even, the absolute gap between our current upper bound and WEAVE(m,n) *or* BOBODD(m,n) *is at most* 1 *and the two algorithms yield an approximation of at least $(1-\frac{1}{\frac{m-1}{2}+\frac{n}{2}})$ times the optimal value.*

5.1.2. The ∞-Norm

For $\|x\|_\infty$, the upper bound for an $(m \times n)$-grid is k which is the length of a (t,k)-edge. We get this bound by considering the central nodes of the grid. For grids with $k > m-1$, the upper bound can be decreased at least to $k-1$. We get the lower bounds by taking the shortest edge of a procedure according to the length from table 5.1. We see that WEAVE(m,n) yields k as minimum length for m,n

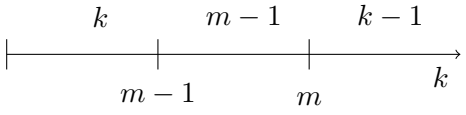

Figure 5.1.: Shortest edges ($\|\cdot\|_\infty$) dependent on k for BOBEVEN(m,n) and BOBODD(m,n)

odd and $k \leq m-1$. If $k > m-1$, the shortest length is $k-1$. These bounds are identical to the upper bounds so the solution of WEAVE(m,n) is optimal for m,n odd. If m and n are even, the shortest edge has length $t(=k)$ for the quadratic grid and length $k-1$ for all other sizes, so WEAVE(m,n) yields in this case an optimal solution for the quadratic grid and grids with $k > m-1$. If m is odd and n is even, the shortest edges always have length $k-1$, so the tours are optimal for grids with $k > m-1$.

For BOBEVEN(m,n) and BOBODD(m,n), the lower bounds are illustrated dependent on k in figure 5.1. For $k \leq m-1$ and for $k > m-1$, which covers the whole variety of grids, BOBEVEN(m,n) (for m,n even) and BOBODD(m,n) (for m odd, n even) yield optimal solutions. So we yield an optimal solution for any kind of grid. When having a look at the shortest edges in the special procedures for $m=3$ and $m=n-1$ we realize that they also yield optimal solutions.

In proposition 10 all results are summarized.

Proposition 10. *Let $m \leq n \in \mathbb{N}$ for the* MSTSP(m,n) *with the distances induced by $\|\cdot\|_\infty$. The following is true: For any grid size, at least one of the linear-time procedures yields an optimal solution.* WEAVE(m,n) *yields an optimal solution in the case of n odd,* BOBEVEN(m,n) *in the case of m,n even and* BOBODD(m,n) *in the case of m odd and n even.*

5.2. Extension to a 3D-Grid

Having started from an algorithm for the MSTSP for nodes on a line and extending it to an algorithm for a 2-dimensional grid, we will now extend some procedures for an optimal solution to the 3-dimensional grid. We will consider this new algorithm in more detail later on, but before that we will estimate upper bounds of the shortest edge of a tour in a 3-dimensional regular grid with Euclidean distances.

Let MSTSP(l,m,n) stand for the MSTSP on a regular 3-dimensional grid with l layers, each consisting of m rows and n columns with distance 1 between each two sequential layers, rows and columns. Let $r = \left\lfloor \frac{l}{2} \right\rfloor, t = \left\lfloor \frac{m}{2} \right\rfloor$ and $k = \left\lfloor \frac{n}{2} \right\rfloor$ (see figure 5.2). If l,m,n are odd, we have one central node which has the distance $\sqrt{r^2+t^2+k^2}$ to all 8 corners (see figure 5.3(a)). If two of the three components are odd, there are four corners for each of the two central nodes with the distance $\sqrt{t^2+k^2+r^2}$ and for one odd component there are still two corners (figure 5.3(b)

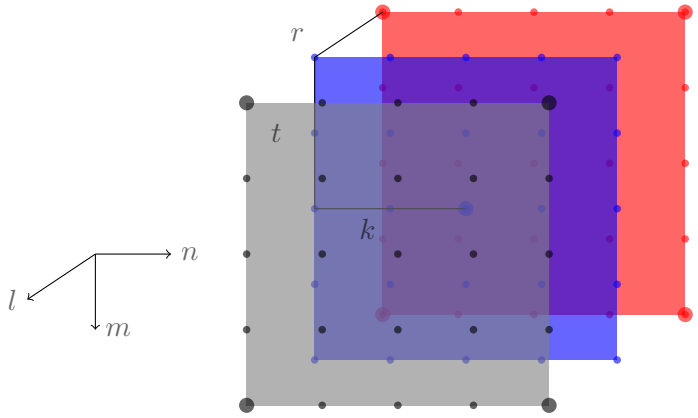

Figure 5.2.: Definition of the 3D grid

and 5.3(c)). For l, m, n even, all central nodes only have one corner with distance $\sqrt{r^2+t^2+k^2}$ (figure 5.3(d)). Therefore, the following values are upper bounds:

(i) $\sqrt{r^2+t^2+k^2}$ if at least one of l, m, n is odd;

(ii) $\sqrt{(r-1)^2+t^2+k^2}$ if l, m, n are even.

Similar to the 2-dimensional grid, the upper bound can be decreased if n is even and $(l-1)^2+(m-1)^2+(k-1)^2 < r^2+t^2+k^2$. The idea behind this is that there have to be at least two nodes in column $k-1$ which are connected to a node of another column than column $n-1$ in order to avoid subtours. Then $\sqrt{(l-1)^2+(m-1)^2+(k-1)^2}$ is a closer upper bound which is the case

(i) if either l, m, n even and $k \geq 1-2t-r+\frac{3}{2}(t^2+r^2)$;

(ii) or if either l odd, m, n even and $k \geq 1-2t+\frac{3}{2}(t^2+r^2)$;

(iii) or if m odd, l, n even and $k \geq 1-2r+\frac{3}{2}(t^2+r^2)$;

(iv) or if l, m odd, n even and $k \geq \frac{1}{2}(1+3(t^2+r^2))$.

The following theorem summarizes all results that we will yield in this section.

Theorem 2. *Let $l, m, n \in \mathbb{N}$ with $l \leq m \leq n$ and let $r = \lfloor \frac{l}{2} \rfloor$, $t = \lfloor \frac{m}{2} \rfloor$ and $k = \lfloor \frac{n}{2} \rfloor$. If n is odd,* Weave(m,n) *is extended to* Weave_3D(l,m,n). *If l, n are even,* Boeven(m,n) *is extended to* Boeven_3D(l,m,n). *If l odd and n even,* Bobodd(m,n) *is extended to* Bobodd_3D(l,m,n). *There is a linear-time algorithm composed of extensions of* Weave(m,n), Boeven(m,n) *and* Bobodd(m,n) *that specifies a feasible tour for* MSTSP(l,m,n) *that is*

(i) optimal whenever n is odd, or l, m, n even with $k \leq \frac{1}{2}(3r^2-2r+1)$;

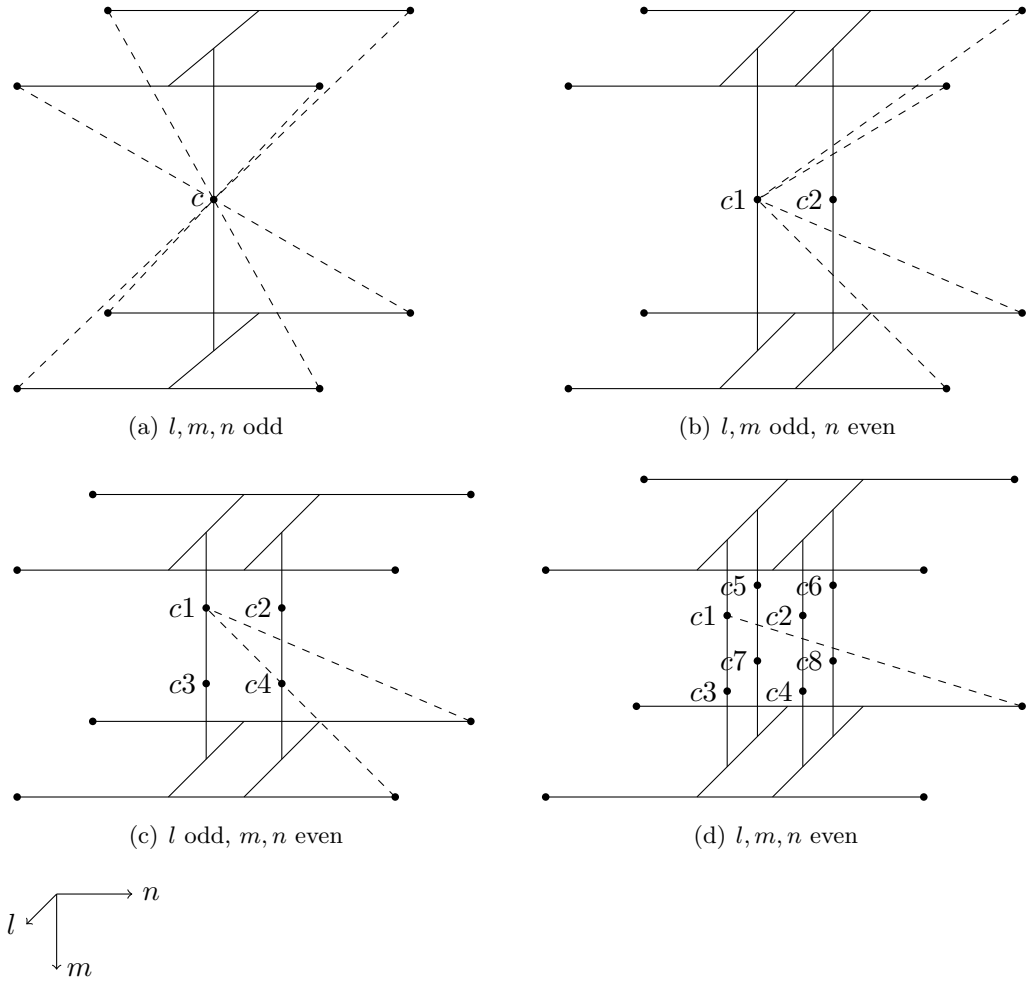

(a) l, m, n odd

(b) l, m odd, n even

(c) l odd, m, n even

(d) l, m, n even

Figure 5.3.: Corners of distance $\sqrt{r^2 + t^2 + k^2}$ from a central node

(ii) an $\frac{1}{\gamma_{rtk}}$*-approximation with the values of* γ_{rtk} *from table 5.2;*

(iii) optimal for $m = 3$ *or* $m = 5$ *with* $k \leq \frac{1}{2}(3t^2 + 1)$ *after some modifications of* BOBODD_3D(l, m, n).

5.2.1. Optimal Procedure for an Odd Number of Columns

If n is odd, we divide the layers into pairs as well (and one triple, if l is odd). We apply the procedures of WEAVE(m, n) for the 2D case on the rows and columns l times while changing the layer after every node. To determine the order of the layers, it turns out that we can shrink each layer to a line and obtain an $(l \times m \cdot n)$-grid. We define $\tau(p) = proj_i(w(p))$.

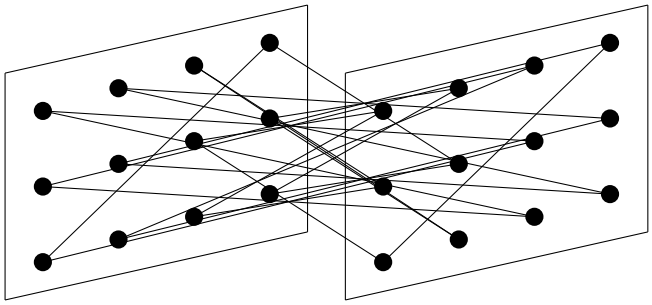

Figure 5.4.: Idea of the extension to 3 dimensions

Applying WEAVE$(l, m \cdot n)$ on the modified grid, $\tau(p)$ indicates the order of the layers. Combining the order of the layers with the order of the rows and columns yields an optimal solution for the MSTSP as we will see hereafter. We call this procedure WEAVE_3D(l, m, n) in the following. WEAVE_3D(l, m, n) can be defined as a mapping with identical components to the two-dimensional components. The basic idea of it is illustrated in figure 5.4.

Definition 9 (WEAVE_3D(l, m, n))**.** *Let l, m, n be the number of layers, rows and columns in a 3D grid. Let $\mathcal{P} = \{0, 1, \ldots, lmn - 1\}$ be the set of positions in a tour, $L = \{0, 1, \ldots, l - 1\}$, $M = \{0, 1, \ldots, m - 1\}$, $N = \{0, 1, \ldots, n - 1\}$.* WEAVE_3D$(l, m, n)$ *is defined as the mapping*

$$\begin{aligned} g : \mathcal{P} &\to L \times M \times N, \\ p &\mapsto (h(p), i(p), j(p)), \end{aligned} \tag{5.2}$$

which maps any position $p \in \mathcal{P}$ to a vertex in an $(l \times m \times n)$-grid.

$h(p)$, $i(p)$ and $j(p)$ are defined in the following way:

If l, m even and n odd, then

$$h(p) = \begin{cases} y + (p \bmod 2) \cdot \frac{l}{2} & \text{if } ymn \le p < (y+1)mn, \\ & y \in \{0, 1, \ldots, \frac{l}{2} - 1\} \\ y - (p \bmod 2) \cdot \frac{l}{2} & \text{if } ymn \le p < (y+1)mn, \\ & y \in \{\frac{l}{2}, \ldots, l - 1\} \end{cases} \tag{5.3}$$

$$i(p) = \frac{q}{2} + [(p \bmod (mn)) \bmod 2] \cdot \frac{m}{2} \quad \begin{array}{l} \text{if } qn \le (p \bmod (mn)) < (q+2)n \\ \text{and } q \in \{0, 2, 4, \ldots, 2(\frac{m}{2} - 1)\} \end{array} \tag{5.4}$$

$$\begin{aligned} j(p) = (((p+1) \bmod n) \bmod 2) \cdot \left(\frac{((p+1) \bmod n) - 1}{2} + \frac{n+1}{2} \right) \\ + (1 - (((p+1) \bmod n) \bmod 2)) \cdot \frac{(p+1) \bmod n}{2}. \end{aligned} \tag{5.5}$$

Let now l be odd, then $h(p)$ is replaced by

$$h(p) = \begin{cases} (p \bmod 3) \cdot \frac{l-1}{2} & \text{if } 0 \le p < 3mn \text{ and } mn \bmod 3 \neq 0 \\ (p \bmod 3) \cdot \frac{l-1}{2} & \text{if } 0 \le p < mn \text{ and } mn \bmod 3 = 0 \\ ((p+1) \bmod 3) \cdot \frac{l-1}{2} & \text{if } mn \le p < 2mn \text{ and } mn \bmod 3 = 0 \\ ((p+2) \bmod 3) \cdot \frac{l-1}{2} & \text{if } 2mn \le p < 3mn \text{ and } mn \bmod 3 = 0 \\ y + (p \bmod 2) \cdot \frac{l-1}{2} & \text{if } (2+y)mn \le p < (3+y)mn, \\ & y \in \{1, 2, \ldots, \frac{l-1}{2} - 1\} \\ y - (p \bmod 2) \cdot \frac{l-1}{2} & \text{if } (1+y)mn \le p < (2+y)mn, \\ & y \in \{\frac{l-1}{2} + 1, \ldots, l-2\}. \end{cases} \tag{5.6}$$

Let now m be odd and let $\eta(p) = p \bmod (mn)$, $\tilde{\eta}(p) = (p+1) \bmod (mn)$. Then $i(p)$ is replaced by

$$i(p) = \begin{cases} (\eta(p) \bmod 3) \cdot \frac{m-1}{2} & \text{if } 0 \le \eta(p) < 3n \\ & \text{and } n \bmod 3 \neq 0 \\ (\eta(p) \bmod 3) \cdot \frac{m-1}{2} & \text{if } 0 \le \eta(p) < n \\ & \text{and } n \bmod 3 = 0 \\ ((\eta(p)+1) \bmod 3) \cdot \frac{m-1}{2} & \text{if } n \le \eta(p) < 2n \\ & \text{and } n \bmod 3 = 0 \\ ((\eta(p)+2) \bmod 3) \cdot \frac{m-1}{2} & \text{if } 2n \le \eta(p) < 3n \\ & \text{and } n \bmod 3 = 0 \\ \frac{q}{2} + (\tilde{\eta}(p) \bmod 2) \cdot \frac{m-1}{2} & \text{if } (q+1)n \le \eta(p) < (q+3)n \\ & \text{and } q \in \{2, 4, \ldots, 2(\frac{m-1}{2} - 1)\} \end{cases} \tag{5.7}$$

and as mn is odd in that case, $h(p)$ is replaced if l is even by

$$h(p) = y + (p \bmod 2) \cdot \frac{l}{2} \text{ if } 2ymn \le p < 2(y+1)mn \text{ and } y \in \{0, 1, \ldots, \frac{l}{2} - 1\} \tag{5.8}$$

and if l is odd by

$$h(p) = \begin{cases} (p \bmod 3) \cdot \frac{l-1}{2} & \text{if } p < 3mn \text{ and } mn \bmod 3 \neq 0 \\ (p \bmod 3) \cdot \frac{l-1}{2} & \text{if } 0 \le p < mn \text{ and } mn \bmod 3 = 0 \\ ((p+1) \bmod 3) \cdot \frac{l-1}{2} & \text{if } mn \le p < 2mn \text{ and } mn \bmod 3 = 0 \\ ((p+2) \bmod 3) \cdot \frac{l-1}{2} & \text{if } 2mn \le p < 3mn \text{ and } mn \bmod 3 = 0 \\ 1 + y + ((p+1) \bmod 2) \cdot \frac{l-1}{2} & \text{if } (3+2y)mn \le p < (3+2(y+1))mn, \\ & y \in \{0, 1, \ldots, \frac{l-1}{2} - 2\}. \end{cases} \tag{5.9}$$

We have to prove that this implementation yields a tour through all nodes.

Theorem 3. *The mapping in definition 9 is a bijection.*

Proof. We have referred to this proof already in previous sections. The technique is demonstrated for one case but can be applied in the same way to the other cases (either 2D or 3D). In this proof, we only consider the case of l, m even and n odd. We have to prove that g is a bijection. By checking the cases, we can easily see that for every position p there is a unique tuple $(h(p), i(p), j(p))$. The case is given by the grid size. We consider the intervals for which $h(p)$ is piecewise defined (equation (5.3)). For any $0 \leq y_1 \leq l-2$ let $y_2 = y_1 + 1$, then $(y_1+1)mn = y_2mn$. So the supremum of one interval is the minimum value of the consecutive interval and there is no gap between the intervals. As the supremum of each interval is excluded, no position gets mapped twice. The smallest and the greatest value of p for which $h(p)$ is defined is 0 and $lmn-1$. This covers all positions. For $i(p)$ (equation (5.4)) the situation is identical. For values of p mod (mn) between 0 and $mn-1$ there is a unique definition of $i(p)$ as there are no gaps between the intervals and the right boundary of the interval is excluded in each interval. $j(p)$ is a function which is defined for any integer p. For the definitions of $h(p)$ and $i(p)$ in other cases, we can check it in the same way.

As we know that the number of positions $|\mathcal{P}| = lmn$ equals the number of nodes lmn, it is sufficient to prove either surjectivity or injectivity. We prove injectivity, i.e. for any node $(h, i, j) \in L \times M \times N$ there is at most one $p \in \mathcal{P}$ such that $(h(p), i(p), j(p)) = (h, i, j)$.

Injectivity in a set of n positions: We first have a look at $j(p) = 0$. This can only hold for $(p+1) \bmod n = 0$, that means $p = a \cdot n + n - 1$ with $a \in \mathbb{N}_0$. Let us now consider $p_1, p_2 \in \{0, \ldots, n-2\}$. We prove for this subset that $j(p_1) = j(p_2) \Rightarrow p_1 = p_2$: Let us assume $p_1 \neq p_2$ with $j(p_1) = j(p_2)$, that means

$$\begin{aligned} &((p_1+1) \bmod 2) \cdot \left(\frac{(p_1+1)-1}{2} + \frac{n+1}{2} \right) \\ &+ (1 - ((p_1+1) \bmod 2)) \cdot \frac{(p_1+1)}{2} \\ =&((p_2+1) \bmod 2) \cdot \left(\frac{(p_2+1)-1}{2} + \frac{n+1}{2} \right) \\ &+ (1 - ((p_2+1) \bmod 2)) \cdot \frac{(p_2+1)}{2}. \end{aligned} \tag{5.10}$$

If $(p_1+1) \bmod 2 = 0$ and $(p_2+1) \bmod 2 = 1$, we get

$$\frac{(p_1+1)}{2} = \frac{(p_2+1)-1}{2} + \frac{n+1}{2} \tag{5.11}$$

$$\Leftrightarrow \quad p_1 = p_2 + n > n - 2. \tag{5.12}$$

Therefore, p_1 is not part of the set $\{0, \ldots, n-2\}$ in contradiction to our assumption. If $(p_1 + 1) \bmod 2 = 1$ and $(p_2 + 1) \bmod 2 = 0$, the result is analogous. The remaining cases are $(p_1 + 1) \bmod 2 = (p_2 + 1) \bmod 2 = 1$ where we have

$$\frac{(p_1 + 1) - 1}{2} + \frac{n+1}{2} = \frac{(p_2 + 1) - 1}{2} + \frac{n+1}{2} \Leftrightarrow \; p_1 = p_2 \tag{5.13}$$

and $((p_1 + 1) \bmod n) \bmod 2 = ((p_2 + 1) \bmod n) \bmod 2 = 0$ which also leads to $p_1 = p_2$. We can conclude that $j(p)$ is injective for $p \in \{cn, cn + 1, \ldots, cn + n - 1\}$ for a given $c \in \{0, \ldots, lm - 1\}$.

Injectivity in a set of mn positions: Let us now consider $i(p)$. We first prove that the values of $i(p)$ are always different for p_1, p_2 in different intervals of the piecewise defined function. Let $q_1 n \leq p_1 < (q_1 + 2)n$ and $q_2 n \leq p_2 < (q_2 + 2)n$ with $q_1 \neq q_2$. We assume $i(p_1) = i(p_2)$:

$$\frac{q_1}{2} + [(p_1 \bmod (mn)) \bmod 2] \cdot \frac{m}{2} = \frac{q_2}{2} + [(p_2 \bmod (mn)) \bmod 2] \cdot \frac{m}{2}. \tag{5.14}$$

If $(p_1 \bmod (mn)) \bmod 2 = (p_2 \bmod (mn)) \bmod 2 = 0$, we get $q_1 = q_2$ which is a contradiction to the assumption. $(p_1 \bmod (mn)) \bmod 2 = (p_2 \bmod (mn)) \bmod 2 = 1$ yields the same contradiction. Remains

$$(p_1 \bmod (mn)) \bmod 2 = 0 \text{ and } (p_2 \bmod (mn)) \bmod 2 = 1 \tag{5.15}$$

and vice versa. In that case $q_1 = q_2 + m$ and therefore $q_1 > m - 2$, so there is no interval of positions belonging to q_1.

So it remains to show that within one interval from the definition of $i(p)$ the tuples (i, j) are different. Each interval consists of $2n$ positions. As the value of $j(p)$ recurs only each n nodes, it is sufficient to prove that $i(p) \neq i(p + n)$ within one interval.

Let $qn \leq p \bmod (mn) < (q + 1)n$

$$i(p) = \frac{q}{2} + ((p \bmod (mn)) \bmod 2)\frac{m}{2}; \tag{5.16}$$

$$i(p + n) = \frac{q}{2} + (((p + n) \bmod (mn)) \bmod 2)\frac{m}{2}. \tag{5.17}$$

As n is odd and m is even according to our assumptions, $p + n$ is odd if p is even and vice versa and $p \bmod (mn)$ is even if p is even and vice versa. So we know that if p is even $p + n$ is odd and

$$i(p) = \frac{q}{2} \neq \frac{q}{2} + \frac{m}{2} = i(p + n). \tag{5.18}$$

Now we know that any node in one plane is at most visited once and therefore we know for the 2D case that Weave(m, n) yields a tour for an even number of rows and an odd number of columns. In the 3D case the proof has to be continued.

Injectivity in a set of lmn positions: For $S_y := \{s \in \mathcal{P} : ymn \leq s < (y+1)mn\}$ we know that $g|_{S_y}$ is injective for any $y \in \{0, \ldots, \frac{l}{2} - 1\}$ because $(i(p), j(p))$ is injective on S_y. Aside from that, we get from the definition of $i(p)$ and $j(p)$ that both values recur for $p_1, p_2 \in \mathcal{P}$ with $p_2 = p_1 + amn$ with a being any positive integer number. We first prove that $h(p_1) \neq h(p_2)$ for p_1 and p_2 from two different intervals of $h(p)$ with

$$\begin{aligned} y_1 mn \leq p_1 < (y_1+1)mn \quad &\text{and} \\ y_2 mn \leq p_2 < (y_2+1)mn \quad &\text{and} \\ y_1 < y_2 < \frac{l}{2}, \text{ in particular } p_1, p_2 < \frac{1}{2}lmn. & \end{aligned} \tag{5.19}$$

Assume

$$h(p_1) = y_1 + (p_1 \bmod 2) \cdot \frac{l}{2} = y_2 + (p_2 \bmod 2) \cdot \frac{l}{2} = h(p_2). \tag{5.20}$$

If p_1 and p_2 were both odd or even, y_1 would be y_2. If p_1 was odd and p_2 even, we would get $y_1 + \frac{l}{2} = y_2$, but this contradicts the assumption $y_2 < \frac{l}{2}$. The case "p_1 even and p_2 odd" works analogously. So we get a contradiction in any case. The proof in the case of $p_1, p_2 \geq \frac{1}{2}lmn$ works analogously.

Let now $p_1 < \frac{1}{2}lmn$ and $p_2 \geq \frac{1}{2}lmn$ and $h(p_1) = h(p_2)$:

$$h(p_1) = y_1 + (p_1 \bmod 2) \cdot \frac{l}{2} = y_2 - (p_2 \bmod 2) \cdot \frac{l}{2} = h(p_2). \tag{5.21}$$

If p_1 and p_2 are both even, we get $y_1 = y_2$, if they are both odd, we get $y_1 + l = y_2 > l - 1$ which is not in the feasible set of y. If p_1 is even and p_2 is odd, we get $y_1 = y_2 - \frac{l}{2}$ and if p_1 odd and p_2 even, the relation is the same. We conclude that for two positions p_1 and p_2 of different intervals of the piecewise defined function $h(p)$, the value of $g(p) = (h(p), i(p), j(p))$ can only be the same if $p_2 = p_1 + \frac{1}{2}lmn$.

Hence, it remains to prove that $h(p) \neq h(p + \frac{1}{2}lmn)$ for $p < \frac{1}{2}lmn$. As l and m are even, we know that $\frac{1}{2}lmn$ is even, so the positions p and $p + \frac{1}{2}lmn$ are either both odd or both even. Let y^* be the corresponding y to p. As $y^*mn \leq p < (y^*+1)mn$, also $(y^* + \frac{l}{2})mn \leq p + \frac{1}{2}lmn < (y^* + \frac{l}{2} + 1)mn$ holds. Thus, $y^{**} = y^* + \frac{l}{2}$ is the corresponding y to $p + \frac{1}{2}lmn$. We receive the following expressions:

$$h\left(p + \frac{1}{2}lmn\right) = y^{**} - \frac{l}{2} = y^* \neq y^* + \frac{l}{2} = h(p) \text{ if } p \text{ odd}; \tag{5.22}$$

$$h\left(p + \frac{1}{2}lmn\right) = y^{**} = y^* + \frac{l}{2} \neq y^* = h(p) \text{ if } p \text{ even}. \tag{5.23}$$

This proves Theorem 3 for l, m even and n odd.

If l, n odd and m even, the proof works identical for i and j. It remains to prove that for any $p_1 \in \{0, \ldots, mn - 1\}$ the values of $h(p_1 + amn)$ differ for any $a \in \{0, \ldots, l-1\}$, that means $h(p_1 + a_1 mn) \neq h(p_1 + a_2 mn)$. We will first consider

the positions from 0 to $3mn-1$ and prove the statement for them. Afterwards, we will consider the intervals of positions with $p \geq 3mn$. The second part of the proof works similar to the proof with l even. In a third step, we will prove that the values of h from the first 3mn positions and those of the later positions are different.

Let us choose any $p_1 \in \{0, \ldots, mn-1\}$. First, we prove that $h(p_1) \neq h(p_2)$, $h(p_2) \neq h(p_3)$ and $h(p_1) \neq h(p_3)$ for $p_2 = p_1 + mn$ and $p_3 = p_1 + 2mn$. We get the following two expressions for $mn \bmod 3 \neq 0$:

$$((p_1 + mn) \bmod 3) \cdot \frac{l-1}{2} \neq (p_1 \bmod 3) \cdot \frac{l-1}{2} \neq (p_1 + 2mn) \bmod 3 \tag{5.24}$$

$$p_2 \bmod 3 \neq p_3 \bmod 3. \tag{5.25}$$

If $mn \bmod 3 = 0$, the following holds:

$$\begin{aligned} h(p_2) &= ((p_2+1) \bmod 3) \cdot \frac{l-1}{2} = ((p_1 + mn + 1) \bmod 3) \cdot \frac{l-1}{2} \\ &= ((p_1+1) \bmod 3) \cdot \frac{l-1}{2} \neq h(p_1) \end{aligned} \tag{5.26}$$

and

$$\begin{aligned} h(p_3) &= ((p_3+2) \bmod 3) \cdot \frac{l-1}{2} = ((p_2 + 2mn + 2) \bmod 3) \cdot \frac{l-1}{2} \\ &= ((p_1+2) \bmod 3) \cdot \frac{l-1}{2} \neq h(p_1) \text{ and } \neq h(p_2). \end{aligned} \tag{5.27}$$

Now we consider p_1 and p_2 from two different intervals of $h(p)$ with $3mn \leq p_1 < p_2 < \frac{l+3}{2}mn$. We first prove that $h(p_1) \neq h(p_2)$. Assume

$$h(p_1) = y_1 + (p_1 \bmod 2) \cdot \frac{l-1}{2} = y_2 + (p_2 \bmod 2) \cdot \frac{l-1}{2} = h(p_2). \tag{5.28}$$

If p_1 and p_2 were both odd or even, y_1 would be y_2. If p_1 was odd and p_2 even, we would get $y_1 + \frac{l-1}{2} = y_2$, but $p_2 < \frac{l+3}{2}mn$ leads to $y_2 < \frac{l-1}{2}$. As $y_1 \geq 1$, there is no y_2 in the required size. For p_1 even and p_2 odd, the argumentation works analogously. So we get a contradiction in any case. The proof in the case of $p_1, p_2 \geq \frac{l+3}{2}mn$ works analogously.

Let now $3mn \leq p_1 < \frac{l+3}{2}mn$ and $p_2 \geq \frac{l+3}{2}mn$ and $h(p_1) = h(p_2)$. Then

$$h(p_1) = y_1 + (p_1 \bmod 2) \cdot \frac{l-1}{2} = y_2 - (p_2 \bmod 2) \cdot \frac{l-1}{2} = h(p_2). \tag{5.29}$$

If p_1 and p_2 are both even, we get $y_1 = y_2$, if they are both odd, we get $y_1 + 2\frac{l-1}{2} = y_2 > l-1$ which is not in the feasible set of y. If p_1 is even and p_2 is odd, we get $y_1 = y_2 - \frac{l-1}{2}$ and if p_1 odd and p_2 even, the relation is the same. In order to compute the associated positions, we have to count how many positions are between y_1 and y_2. Because of the missing value $\frac{l-1}{2}$ of y (see equation (5.6)), there are $\left(3 + \frac{l-1}{2} - 1 - 3\right) mn = \left(\frac{l-1}{2} - 1\right)$ positions in between. We conclude that for

two positions p_1 and p_2 with $3mn \leq p_1 < p_2$ of different intervals of the piecewise defined function $h(p)$, the value of $g(p) = (h(p), i(p), j(p))$ can only be the same if $p_2 = p_1 + \left(\frac{l-1}{2} - 1\right) mn$.

So it remains to prove that $h(p) \neq h\left(p + \left(\frac{l-1}{2} - 1\right) mn\right)$ for $3mn \leq p < \frac{l+3}{2}mn$. As m is even, we know that $\left(\frac{l-1}{2} - 1\right) mn$ is even, so the positions $p + \left(\frac{l-1}{2} - 1\right) mn$ and p are either both odd or both even. Let $y^* \neq y^{**}$ be the corresponding y to p and $p + \frac{1}{2}lmn$. For the two cases odd and even, we receive the following statements

$$h(p_1) = y^{**} - \frac{l-1}{2} \neq y^* + \frac{l-1}{2} = h(p_2) \text{ if } p_1, p_2 \text{ odd;} \tag{5.30}$$

$$h(p_1) = y^{**} \neq y^* = h(p_2) \text{ if } p_1, p_2 \text{ even.} \tag{5.31}$$

Finally, we have to check if the values of $h(p)$ for $p \geq 3mn$ differ from $p < 3mn$. Therefore, we consider the value set of h: If $p < 3mn$, the value set is $\{0, \frac{l-1}{2}, l-1\}$. If $3mn \leq p < \frac{l+3}{2}mn$, the values of $h(p) = y + (p \bmod 2) \cdot \frac{l-1}{2}$ are > 0 ($y \geq 1$) and $< l - 1$ ($y \leq \frac{l-1}{2}$). If p is even, the largest value is $\frac{l-1}{2} - 1$ and the smallest value for p odd is $\frac{l-1}{2} + 1$. If $\frac{l+3}{2}mn \leq p < lmn$, the value set is the same as for $3mn \leq p < \frac{l+3}{2}mn$. So the value set of positions $p < 3mn$ is disjoint to the value set of positions $p \geq 3mn$. The cases with m even can be proved with the same procedure. □

We now have to consider the lengths of the edges appearing in the tours created by WEAVE_3D(l, m, n). As we have already mentioned the distances for WEAVE(m, n), we will just consider the number of layers between consecutive nodes. In the following, we use the previously defined $r = \left\lfloor \frac{l}{2} \right\rfloor$. Within one pair of layers the distance is always r. In the triple there are distances of r and $2r$. When the pair or triple of layers is changed, the list of distances between consecutive layers is dependent on l, m and n.

- If l even and $m \cdot n$ even, the distances are either $r - 1$ or $r + 1$.
- If l is odd and $m \cdot n$ even, the distances are either $r - 1$ or $r + 1$ or $l - 2$ or $r - 2$.
- If l is even and $m \cdot n$ odd, the distances are either $r - 1$ or $l - 1$.
- If l is odd and $m \cdot n$ odd, the distances are either $r - 1$ or $l - 2$.

The last move in WEAVE(m, n) is a $(m - 1, k + 1)$-move if m is even and a $(m - 2, k+1)$-move if m is odd. As the changes between pairs and triples of layers always take place after one or two runs of WEAVE(m, n), only the last edge is matched to the previously mentioned layer distances. All other edges of WEAVE(m, n) get matched to r. Thus, the candidates for the shortest edge are

- (r, t, k), $(r - 1, m - 1, k + 1)$ if l, m even, n odd;
- (r, t, k), $(r - 2, m - 1, k + 1)$ if l, n odd, m even;

- (r, t, k), $(r-1, m-2, k+1)$ if l even, m, n odd;
- (r, t, k), $(r-1, m-2, k+1)$ if l, m, n odd.

For each case, we compute the minimum of both candidates by subtracting the first squared Euclidean length from the second one and determine whether the difference is positive or negative. Because of the monotonicity of the square root, we can determine the smaller edge in that way. For example in the case of l, m even, n odd this is:

$$\begin{aligned}&(r-1)^2 + (m-1)^2 + (k+1)^2 - r^2 + t^2 + k^2 = 3t^2 + 2k + 3 - 4t - 2r \\ &\geq 3t^2 + 2t + 3 - 4t - 2t = \underbrace{3t^2 - 4t + 3}_{p(t)} \overset{*}{\geq} 0\end{aligned} \tag{5.32}$$

* $p(1) = 2 > 0$, the roots of this polynomial are conjugate-complex ($t_{1/2} = \frac{2}{3} \pm \frac{\sqrt{-5}}{3}$), so $p(t) > 0$ for $t \in \mathcal{R}$.

With analogous transformations we can prove for all four cases that the shortest edge is the (r, t, k)-edge which yields the deduced upper bound for the 3D grid. This results in the following lemma.

Lemma 4. WEAVE_3D(l, m, n) *yields an optimal solution to the MSTSP for grids with* n *odd.*

5.2.2. Approximations for an Even Number of Columns

If n is even, it is not always possible to get an optimal solution by extending our optimal algorithm of a 2D grid. If l, m, n are even, there are optimal solutions for certain kinds of grids. We can apply BOBEVEN(l, n) to the layers and columns while moving between the rows as the first component of WEAVE$(m, l \cdot n)$ would do. We will start at node $(1, 1, k+2)$. We call this new procedure BOBEVEN_3D(l, m, n).

BOBEVEN_3D(l, m, n) is defined as a mapping of previously defined components of algorithms:

Definition 10 (BOBEVEN_3D(l, m, n))**.** *Let* $l \leq m \leq n$ *be the number of layers, rows and columns respectively in a 3D grid with* l, n *even,* m *even or odd. Let* $\mathcal{P} = \{0, 1, \ldots, lmn - 1\}$ *be the set of positions in a tour,* $L = \{0, 1, \ldots, l-1\}$, $M = \{0, 1, \ldots, m-1\}$, $N = \{0, 1, \ldots, n-1\}$. BOBEVEN_3D$(l, m, n)$ *is defined as the mapping*

$$\begin{aligned}g_{even} : \mathcal{P} &\to L \times M \times N, \\ p &\mapsto (h(p), i(p), j(p))\,.\end{aligned} \tag{5.33}$$

In the case of m *even,* $i(p)$ *is defined in the same way as* $h(p)$ *in equation (5.3) and as* h *in equation (5.6) if* m *is odd (with* $\hookleftarrow$ *from notation 1):*

$$h(p) = \begin{cases} 0 & \text{if } p \bmod l = 0 \\ l-1 & \text{if } p \bmod l = l-1 \\ r-1-(p \bmod 2)\cdot\left(\left\lfloor \frac{p \bmod l}{2} \right\rfloor\right) \hookleftarrow & \\ +(1-(p \bmod 2))\cdot(r-\left\lfloor \frac{p \bmod l}{2} \right\rfloor) & \text{if } p \bmod l \in \{1,\ldots,l-2\} \end{cases} \tag{5.34}$$

$$j(p) = \begin{cases} (k+1)+q-(p \bmod 2)\cdot k & \text{if } ql \le p \bmod (ln) < (q+1)l, \\ & q \in \{0,\ldots,k-2\} \\ q-(k-1)+(p \bmod 2)\cdot k & \text{if } ql \le p \bmod (ln) < (q+1)l, \\ & q \in \{k-1,\ldots,n-2\} \\ k-(p \bmod 2)\cdot k & \text{if } p \bmod (ln) = l(n-1) \end{cases} \tag{5.35}$$

if m even

$$i(p) = \begin{cases} y+(p \bmod 2)\cdot\frac{m}{2} & \text{if } yln \le p < (y+1)ln, \\ & y \in \{0,1,\ldots,\frac{m}{2}-1\} \\ y-(p \bmod 2)\cdot\frac{m}{2} & \text{if } yln \le p < (y+1)ln, \\ & y \in \{\frac{m}{2},\ldots,m-1\} \end{cases} \tag{5.36}$$

and if m odd

$$i(p) = \begin{cases} (p \bmod 3)\cdot\frac{m-1}{2} & \text{if } 0 \le p < 3ln \text{ and } ln \bmod 3 \neq 0 \\ (p \bmod 3)\cdot\frac{m-1}{2} & \text{if } 0 \le p < ln \text{ and } ln \bmod 3 = 0 \\ ((p+1) \bmod 3)\cdot\frac{m-1}{2} & \text{if } ln \le p < 2ln \text{ and } ln \bmod 3 = 0 \\ ((p+2) \bmod 3)\cdot\frac{m-1}{2} & \text{if } 2ln \le p < 3ln \text{ and } ln \bmod 3 = 0 \\ y+(p \bmod 2)\cdot\frac{m-1}{2} & \text{if } (2+y)ln \le p < (3+y)ln, \\ & y \in \{1,2,\ldots,\frac{m-1}{2}-1\} \\ y-(p \bmod 2)\cdot\frac{m-1}{2} & \text{if } (1+y)ln \le p < (2+y)ln, \\ & y \in \{\frac{m-1}{2}+1,\ldots,m-2\}. \end{cases} \tag{5.37}$$

Theorem 4. *The mapping g_{even} is a bijection.*

The proof of theorem 4 works analogously to the proof in the last subsection. We match the edges of BOBEVEN(l,n) to the length component of rows. As we have already introduced both procedures before, this is only shortly mentioned to get the result for 3D grids.

The shortest edge for grids with $k \le \frac{1}{2}(3r^2-2r+1)$ is the $(r-1,t,k)$-edge. The edges with a short move in the second component are $(l-1,t-1,k+1)$-edges which are longer than $(r-1,t,k)$-edges according to equation (4.16) and some transformations. The shortest edge of the tour yields in this case the upper

bound and therefore BOBEVEN_3D(l, m, n) is optimal for l, m, n even with $k \leq \frac{1}{2}(3r^2 - 2r + 1)$. In the appendix C.1, it is proved that the edges which connect two pairs of rows are always longer than the shortest edge in the algorithm.

For l odd and n even, BOBODD(m, n) can be extended in a similar way. For l odd and m, n even with $l \geq 5$, we can apply BOBODD(l, n) and combine its $(l-3, k+1)$-edge to a move between rows of $t - 1$. In order to terminate with such an edge in BOBODD(l, n), we shift each $p \bmod (ln)$ to $(p \bmod (ln) - (l - 3)) \bmod (ln)$ in the current procedure of BOBODD(l, n) (definition 6). For $l = 3$, the $(l - 1, n - 1)$-edge is matched to the $(t - 1)$-move. The new procedure for the 3D grid will be called BOBODD_3D(l, m, n) in the following.

When we restrict all constructed tours to combinations of WEAVE(m, n) and BOBODD(m, n) or BOBEVEN(m, n), we receive gaps between the upper bound and the shortest edge of those tours for most of the remaining grids. Thus, we will compute the approximation ratio for those grids. For BOBEVEN_3D(l, m, n) or BOBODD_3D(l, m, n), we calculate for which k the edges with a $(k - 1)$-component become smaller than the $(r - 1, t, k)$-edge by transforming the inequality of the squared lengths of the two edges. For certain grids the upper bound changes to a smaller value as was mentioned at the beginning of this section. The values of k where either the upper bound or the lower bound changes constitute the three categories for which we will now compute the approximation ratio.

Let us start with l, m, n even and the case where $(r-1)^2 + t^2 + k^2 > (l-1)^2 + t^2 + (k-1)^2$, that means $k > \frac{1}{2}(3r^2 - 2r + 1)$. There are two cases to distinguish: For $k < 1 - 2t - r + \frac{3}{2}(t^2 + r^2)$, the upper bound is still $\sqrt{(r-1)^2 + t^2 + k^2}$ but the shortest edge of the tour of BOBEVEN_3D(l, m, n) is an $(l - 1, t, k - 1)$-edge, so BOBEVEN_3D(l, m, n) yields a $\sqrt{\frac{(r-1)^2+t^2+k^2}{(l-1)^2+t^2+(k-1)^2}}$-approximation. For greater k, the new upper bound is $\sqrt{(l-1)^2 + (m-1)^2 + (k-1)^2}$ and BOBEVEN_3D(l, m, n) yields a $\sqrt{\frac{(l-1)^2+(m-1)^2+(k-1)^2}{(l-1)^2+t^2+(k-1)^2}}$-approximation.

For l, n even and m odd, we do the same considerations except that the order of rows for WEAVE$(m, l \cdot n)$ differs for m odd.

For l odd and m, n even with $l \geq 7$ and $k \leq \frac{1}{2}(3r^2 + 2r)$, the shortest edge of BOBODD_3D(l, m, n) is the $(r - 1, t, k)$-edge, therefore this algorithm yields a $\sqrt{\frac{r^2+t^2+k^2}{(r-1)^2+t^2+k^2}}$-approximation. For $\frac{1}{2}(3r^2 + 2r) < k \leq 1 - 2t + \frac{3}{2}(t^2 + r^2)$, the shortest edge is the $(l - 1, t, k - 1)$-edge but the upper bound stays the same which results in an $\sqrt{\frac{r^2+t^2+k^2}{(l-1)^2+t^2+(k-1)^2}}$-approximation. For greater k, the upper bound changes and we get an $\sqrt{\frac{(l-1)^2+(m-1)^2+(k-1)^2}{(l-1)^2+t^2+(k-1)^2}}$-approximation.

Analogous considerations are done for l, m odd and n even. A list of the inverses of all approximation ratios is given in table 5.2 ($\gamma_{rtk} = \frac{\text{Extended Algorithm}(l,m,n)}{\text{Upper Bound}(l,m,n)}$). For a very small number of layers ($l < 7$ odd), the approximation is closer than stated in the list as in these cases BOBODD(l, n) yields an optimal solution for the plane, so the approximation is even better.

If $m = 3$ or $m = 5$, we can receive an optimal tour or at least a smaller

	$k \leq a$	$a < k \leq b$	$k > b$
γ_{rtk} (Case 1)	1	$\sqrt{1 - \frac{2k-1-3r^2+2r}{(r-1)^2+t^2+k^2}}$	$\sqrt{1 - \frac{3t^2-4t+1}{(l-1)^2+(m-1)^2+(k-1)^2}}$
γ_{rtk} (Case 2)	$\sqrt{1 - \frac{2r-1}{r^2+t^2+k^2}}$	$\sqrt{1 - \frac{2k-1-3r^2}{r^2+t^2+k^2}}$	$\sqrt{1 - \frac{3t^2-4t+1}{(l-1)^2+(m-1)^2+(k-1)^2}}$
γ_{rtk} (Case 3)	$\sqrt{1 - \frac{2r-1}{r^2+t^2+k^2}}$	$\sqrt{1 - \frac{2k-3r^2+4r-2}{r^2+t^2+k^2}}$	$\sqrt{1 - \frac{3t^2}{(l-1)^2+(m-1)^2+(k-1)^2}}$
γ_{rtk} (Case 4)	$\sqrt{1 - \frac{2r-1}{r^2+t^2+k^2}}$	$\sqrt{1 - \frac{2k-1-3r^2}{r^2+t^2+k^2}}$	$\sqrt{1 - \frac{3t^2}{(l-1)^2+(m-1)^2+(k-1)^2}}$
Case 1: l, m, n even	$a = \frac{1}{2}(3r^2 - 2r + 1)$	$b = 1 - 2t - r + \frac{3}{2}(t^2 + r^2)$	
Case 2: l odd, m, n even	$a = \frac{1}{2}(3r^2 + 2r)$	$b = 1 - 2t + \frac{3}{2}(t^2 + r^2)$	
Case 3: m odd, l, n even	$a = \frac{1}{2}(3r^2 - 2r + 1)$	$b = 1 - 2r + \frac{3}{2}(t^2 + r^2)$	
Case 4: l, m odd, n even	$a = \frac{3}{2}r^2 + r$	$b = \frac{1}{2}(1 + 3(t^2 + r^2)$	

Table 5.2.: $\frac{1}{\gamma}$-approximation for different cases of 3D grids ($l \geq 7$ if l odd)

gap. In the following, we will shortly explain a variation of the defined procedures for the 3D case which yields an optimal solution for some grids with 3 or 5 rows. If $m = 3$ or $m = 5$, we apply BOBODD(m, n) and the proper order of the layers is component i of WEAVE$(l, m \cdot n)$. The proof of the tour can be done analogously to the representative proof and the shortest edges are either (r, t, k)-edges or $(r, m-1, k-1)$-edges. In those cases when (r, t, k)-edges are the shortest edges of the tour, the lower bound yields the upper bound and the tour created by this variation is optimal. If $(r, m-1, k-1)$ is the shortest edge of the tour, the variation yields a $\sqrt{1 + \frac{2k-1-3t^2}{r^2+(m-1)^2+(k-1)^2}}$-approximation. Dependent on l being odd or even, the following distinctions can be made for the approximation. If $\frac{1}{2}(3t^2 + 1) < k \leq \frac{1}{2}(3(r^2 + t^2) + 1)$ (or $\frac{1}{2}(3t^2 + 1) < k \leq \frac{1}{2}(3(r^2 + t^2) - 4r + 1)$), it yields a $\sqrt{1 + \frac{3r^2}{r^2+(m-1)^2+(k-1)^2}}$-approximation (or a $\sqrt{1 + \frac{3r^2-4r+1}{r^2+(m-1)^2+(k-1)^2}}$-approximation). Some computations in regards to this case are explained in sections C.2 and C.3. As this extension only concerns very particular grid sizes, these cases are not mentioned in the general table 5.2.

5.3. Application to the TSP with Forbidden Neighborhoods

Instead of the shortest edge appearing in a tour, we will now consider the length of the tour in the two dimensional grid. We are interested in the shortest tour which is an optimal solution for the MSTSP. This question corresponds to one of the models in section 3: the TSPN.

Definition 11. *The TSPN with mstsp-edge defines the traveling salesman problem with forbidden neighborhoods (TSPN) where the minimum edge length is the objective value of the MSTSP. The TSPN with quasi-mstsp-edge defines the the TSPN where the minimum edge length is the shortest edge of* Bobodd(m, n).

The tours of Bobeven(m, n), Bobodd(m, n) and Weave(m, n) are approximations of the TSPN with mstsp-edge or quasi-mstsp-edge as the lengths of these constructed tours mainly consist of edges of a "medium length", i.e. about half of the rows in vertical direction and half of the columns in horizontal direction. In this section, we will prove an asymptotical optimality in many cases and we will examine how close the tour lengths of the combinatorial algorithms are to a solution of the TSPN with mstsp-edge.

At the time this thesis was written, Fischer and Hungerländer [38] were doing research on the lengths of the shortest TSP tour when certain edges are forbidden as was described in section 3.4. While they start at very small minimum lengths and try to get patterns for combinatorial solutions and bounds, we will start at the longest possible minimum edge length for which there is a possible tour. With the tours from our combinatorial algorithms Weave(m, n), Bobeven(m, n) and Bobodd(m, n), we determine an upper bound for the length of the shortest tour with mstsp-edge or quasi-mstsp-edge. This section supplements the research of Fischer and Hungerländer.

5.3.1. Length of Bobeven(m, n), Bobodd(m, n), Weave(m, n) and Path_Algorithm(m, n)

In order to compute the length of the tours constructed by our algorithms, we will first list the lengths of the edges that are used in our algorithms together with their frequency in the tour. Then, we will write the formula of the length which is the sum of all edge lengths, each multiplied with its frequency. We obtained the edges and their frequency by going through the algorithm and counting the number of edges. The variables t and k are defined like in the previous sections. We can test if all edges in a tour have been observed by taking the sum of the frequencies of all edges in the tour. If the sum is $m \cdot n$, the number of edges is appropriate for a tour through $m \cdot n$ nodes.

We will label the algorithms and list for each of them the appearing edges and their frequencies:

1. Boboven(m, n) for $m \geq 6$:
   - $n \cdot (\frac{m}{2} + 1)$ times $(t - 1, k)$-edges;
   - $n \cdot (\frac{m}{2} - 2)$ times (t, k)-edges;
   - $\frac{n}{2} + 1$ times $(m - 1, k - 1)$-edges;
   - $\frac{n}{2} - 1$ times $(m - 1, k + 1)$-edges.
2. Boboven(m, n) for $m = 4$:

- $3n$ times $(t-1,k)$-edges;
- $\frac{n}{2}+1$ times $(m-1,k-1)$-edges;
- $\frac{n}{2}-1$ times $(m-1,k+1)$-edges.

3. BOBODD(m,n) for $m \geq 5$:
   - $\frac{n}{2}(m+1)$ times (t,k)-edges;
   - $\frac{n}{2}\left(\frac{m-1}{2}\right)$ times $(t+1,k)$-edges;
   - $\frac{n}{2}-1$ times $(m-1,k-1)$-edges;
   - 2 times $(m-2,k)$-edges;
   - $\frac{n}{2}\left(\frac{m-1}{2}-2\right)$ times $(t-1,k)$-edges;
   - $\frac{n}{2}-1$ times $(m-3,k+1)$-edges.
4. BOBODD(m,n) for $m=3$:
   - $2n$ times (t,k)-edges;
   - $\frac{n}{2}$ times $(m-1,k)$-edges;
   - $\frac{n}{2}-1$ times $(m-1,k-1)$-edges;
   - 1 times $(m-1,n-1)$-edges.
5. NEAR_QUADRATIC(m,n) for $m=n-1$:
   - $n\cdot(2+\frac{m-3}{2})$ times (t,k)-edges;
   - $\frac{n}{2}+1$ times $(t+1,k-1)$-edges;
   - $\frac{n}{2}-2$ times $(t+1,k+1)$-edges;
   - $n\cdot\frac{m-3}{2}$ times $(t+1,k)$-edges;
   - 1 times $(t+1,n-1)$-edges.
6. WEAVE(m,n) for m even, n odd: see table 5.3.
7. WEAVE(m,n) for m even, n even: see table 5.3.
8. WEAVE(m,n) for m odd, n odd, $n \bmod 3 \neq 0$: see table 5.3.
9. WEAVE(m,n) for m odd, n odd, $n \bmod 3 = 0$: see table 5.3.
10. WEAVE(m,n) for m odd, n even, $n \bmod 3 \neq 0$: see table 5.4.
11. WEAVE(m,n) for m odd, n even, $n \bmod 3 = 0$: see table 5.4.
12. Path algorithm for m odd and n even:
    We also consider the length of the optimal solution of the path version for m odd and n even, as it seems to be quite close to the optimum. The edges which appear in the tour are:

- $\frac{n}{2}(m+1)$ times (t,k)-edges;
- $\frac{n}{2}(m-2)$ times $(t+1,k)$-edges;
- $\frac{n}{2}-1$ times $(t-1,k+1)$-edges.

Let $T^a(m,n)$ define the tour through an $m \times n$-grid which was created by algorithm $a \in \{1,\ldots,12\}$, let d_{ij} be the Euclidean distance between node i and node j. We define the length of a tour dependent on t and k:

$$\begin{aligned} L^a &: \mathbb{N}^2 \to \mathbb{R}^+ \\ (m,n) &\mapsto \sum_{(i,j)\in T^a(m,n)} d_{ij}. \end{aligned} \tag{5.38}$$

Edge	Case 6	7	8	9
(t,k)	$m(\lfloor\frac{n}{2}\rfloor+1)$	$2m$	$(m-1)(\lfloor\frac{n}{2}\rfloor+1)$	$\lfloor\frac{m}{2}\rfloor(\lfloor\frac{n}{2}\rfloor+1)$
$(t,k+1)$	$\frac{m}{2}(n-2)$	$m(\frac{n}{2}-2)$	$\lfloor\frac{m}{2}\rfloor(n-2)+1$	$\lfloor\frac{m}{2}\rfloor(n-2)+1$
$(t-1,k+1)$	$\frac{m}{2}-1$	$\frac{m}{2}+1$	$\lfloor\frac{m}{2}\rfloor-2$	$\lfloor\frac{m}{2}\rfloor-1$
$(t-2,k+1)$	0	0	0	0
$(m-1,k-1)$	0	0	0	0
$(m-1,k)$	0	0	$\lfloor\frac{n}{2}\rfloor+1$	$\lfloor\frac{n}{2}\rfloor+1$
$(m-1,k+1)$	1	0	$\lfloor\frac{n}{2}\rfloor-1$	$\lfloor\frac{n}{2}\rfloor-1$
$(m-2,k+1)$	0	0	2	1
$(t+1,k+1)$	0	$\frac{m}{2}-1$	0	0
$(t,k-1)$	0	$m(\frac{n}{2}-1)$	0	0

6 = Case of m even, n odd
7 = Case of m even, n even
8 = Case of m odd, n odd, $n \bmod 3 \neq 0$
9 = Case of m odd, n odd, $n \bmod 3 = 0$

Table 5.3.: Edges appearing in WEAVE(m,n) for $m,n \geq 4$ – Part I

For procedure 1, for example, the length of the tour is the following:

$$\begin{aligned} L^1(m,n) = n \cdot \left(\frac{m}{2}+1\right) \cdot \sqrt{(t-1)^2+k^2} + n \cdot \left(\frac{m}{2}-2\right) \cdot \sqrt{t^2+k^2} \\ + \left(\frac{n}{2}+1\right) \cdot \sqrt{(m-1)^2+(k-1)^2} + \left(\frac{n}{2}-1\right) \cdot \sqrt{(m-1)^2+(k+1)^2}. \end{aligned} \tag{5.39}$$

For the sake of consistency with previous sections, we have defined the edges by m,n,t,k. As t and k are dependent on m and n, this notation is in accord with $L^1(m,n)$.

Edge	Case 10	Case 11
(t, k)	$m-2$	$m-2$
$(t, k+1)$	$(m-1)(\frac{n}{2}-2)+2$	$(m-1)(\frac{n}{2}-2)$
$(t-1, k+1)$	$\lfloor \frac{m}{2} \rfloor - 1$	$\lfloor \frac{m}{2} \rfloor$
$(t-2, k+1)$	1	1
$(m-1, k-1)$	$\frac{n}{2}-1$	$\frac{n}{2}-1$
$(m-1, k)$	2	2
$(m-1, k+1)$	$\frac{n}{2}-2$	$\frac{n}{2}-2$
$(m-2, k+1)$	1	0
$(t+1, k+1)$	$\lfloor \frac{m}{2} \rfloor - 2$	$\lfloor \frac{m}{2} \rfloor - 2$
$(t, k-1)$	$m(\frac{n}{2}-1)$	$m(\frac{n}{2}-1)$

10 = Case of m odd, n even, $n \bmod 3 \neq 0$
11 = Case of m odd, n even, $n \bmod 3 = 0$

Table 5.4.: Edges appearing in WEAVE(m, n) for $m, n \geq 4$ – Part II

When we compute the length of the tour for each procedure from 1 to 12, we derive upper bounds for a shortest tour with the minimum edge of the respective algorithm.

5.3.2. Lower Bound for a Tour with Forbidden Edges

A trivial lower bound for the tour length is the length of a tour consisting only of edges of the minimum feasible length. When we consider any of our procedures with a minimum edge of length a, any tour consisting of edges which are longer than a has at least the length mna. For WEAVE(m, n), it is $mn\sqrt{t^2+k^2}$ if n is odd and $mn\sqrt{t^2+(k-1)^2}$ if n is even. For BOBODD(m, n) with $m > 5$ and BOBEVEN(m, n), it is $mn\sqrt{(t-1)^2+k^2}$ for grids with $k \leq \frac{1}{2}(3t^2 - 2t + 1)$ and $mn\sqrt{(m-1)^2+(k-1)^2}$ for all other grids. NEAR_QUADRATIC(m, n), BOBODD(m, n) for $m = 3$ or $m = 5$ and PATH_ALGORITHM(m, n) are compared to the lower bound $mn\sqrt{t^2+k^2}$.

For most cases, this lower bound mna cannot be achieved by a tour, but as the approximate solutions get quite close to this value according to our computations in section 5.3.3, we assume it to be an appropriate lower bound to determine how close our approximations get to the optimum. Moreover, this bound can be easily computed, so we will use this trivial lower bound as the optimum in the following steps.

5.3.3. Comparison of the Lengths of the Approximated Shortest Tours

When we consider the different kinds of edges that are used in WEAVE(m,n) and the special cases BOBEVEN(m,n) and BOBODD(m,n), NEAR_QUADRATIC(m,n) and PATH_ALGORITHM(m,n), we see that they mainly use edges of similar size. Particularly for grids with many rows and columns, the difference between the appearing edges gets tiny in comparison to the edge lengths.

In WEAVE(m,n) – depending on the case – there are mainly edges in the size of the shortest appearing edge. The longest edge appears at most one time and has a length of about $2-3$ times the length of the mstsp-edge. Thus, its influence on the tour length is negligible. All other edges are much shorter. First, we will only consider grids with an odd number of columns and its approximation ratio:

$$\alpha_{tk} = \frac{\text{Tour Length of Combinatorial Algorithm}}{\text{Lower Bound of Tour Length}}. \tag{5.40}$$

For the TSPN the approximation ratio is α_{tk} according to definition 4 with $\alpha_{tk} = k$. We state the following theorem.

Proposition 11. *The length of the tour computed by* WEAVE(m,n) *in an* $(m \times n)$*-grid with* m *even and* n *odd is asymptotically optimal for the classical TSP with a minimum edge length of* $\sqrt{(\frac{m}{2})^2 + (\frac{n-1}{2})^2}$ *and is at least a* 1.78*-approximation.*

Proof. Let $t = \lfloor \frac{m}{2} \rfloor$ and $k = \lfloor \frac{n}{2} \rfloor$ as in the previous sections. Thus, if m even and n odd, $m = 2t$ and $n = 2k+1$ and the lower bound for a tour with minimum edge (t,k) is $2t(2k+1) \cdot \sqrt{t^2+k^2}$. We can compute the approximation ratio of WEAVE(m,n) for an even number of rows and an odd number of columns in the following way (the coefficients of the edge lengths can be received by transforming the coefficients of table 5.3) :

$$\begin{aligned}\alpha_{tk} = {} & \frac{2t(k+1)}{2t(2k+1)} \cdot 1 + \frac{t(2k-1)}{2t(2k+1)} \sqrt{\frac{t^2+(k+1)^2}{t^2+k^2}} \\ & + \frac{t-1}{2t(2k+1)} \sqrt{\frac{(t-1)^2+(k+1)^2}{t^2+k^2}} \\ & + \frac{1}{2t(2k+1)} \sqrt{\frac{(2t-1)^2+(k+1)^2}{t^2+k^2}}.\end{aligned} \tag{5.41}$$

This equals the following:

$$\begin{aligned}\alpha_{tk} = {} & \frac{k+1}{2k+1} \cdot 1 + \frac{2k-1}{2(2k+1)} \sqrt{1 + \frac{2k+1}{t^2+k^2}} \\ & + \frac{1}{2(2k+1)} (1 - \frac{1}{t}) \sqrt{1 + 2\frac{k-t+1}{t^2+k^2}} \\ & + \frac{1}{2t(2k+1)} \sqrt{1 + \frac{3t^2-4t+2+2k}{t^2+k^2}}.\end{aligned} \tag{5.42}$$

We calculate the asymptotic behavior of α_{tk} if $t, k \to \infty$:

$$\begin{aligned}\lim_{t,k\to\infty} \alpha_{tk} = \lim_{t,k\to\infty} \Bigg[& \underbrace{\frac{k+1}{2k+1}}_{\to\frac{1}{2}} \cdot 1 + \underbrace{\frac{(2k-1)}{2(2k+1)}}_{\to\frac{1}{2}} \sqrt{1 + \underbrace{\frac{2k+1}{t^2+k^2}}_{\to 0}} \\ & + \underbrace{\frac{1}{2(2k+1)}}_{\to 0} \underbrace{(1-\frac{1}{t})}_{\to 1} \sqrt{1 + 2\underbrace{\frac{k-t+1}{t^2+k^2}}_{\to 0}} \\ & + \underbrace{\frac{1}{2t(2k+1)}}_{\to 0} \sqrt{1 + \underbrace{\frac{3t^2-4t+2+2k}{t^2+k^2}}_{<\infty}} \Bigg] = 1.\end{aligned} \tag{5.43}$$

So, the tour computed by WEAVE(m, n) with m even and n odd is asymptotically optimal for the TSP with forbidden edges smaller than $\sqrt{t^2+k^2}$.

In order to get the ratio of the worst case, we have a look at the behavior of α_{tk}. We consider the single summands of α_{tk} with $0 < t \leq k$ and compute their partial derivatives with respect to k:

$$\left(\frac{k+1}{2k+1}\right)' = -\frac{1}{(2k+1)^2} < 0 \tag{5.44}$$

$$\begin{aligned}&\frac{\partial}{\partial k}\left(\frac{(2k-1)}{2(2k+1)}\sqrt{1+\frac{2k+1}{t^2+k^2}}\right) = \\ &= \frac{4k^3+12t^2k^2+5k^2+8t^2k+k+4t^4+3t^2}{2(2k+1)^2(t^2+k^2)^2\sqrt{\frac{k^2+2k+t^2+1}{t^2+k^2}}} > 0\end{aligned} \tag{5.45}$$

$$\begin{aligned}&\frac{\partial}{\partial k}\left(\frac{1}{2(2k+1)}(1-\frac{1}{t})\sqrt{1+2\frac{k-t+1}{t^2+k^2}}\right) = \\ &= (1-\frac{1}{t})(\frac{\overbrace{-4k^4+4k^2(t-1)}^{<0}+\overbrace{2t^2k-2t^2k^2}^{<0}-k^2+\overbrace{2k(t-1)-2t^2k^2}^{<0}-3t^2}{2(2k+1)^2(t^2+k^2)^2\sqrt{1+2\frac{k-t+1}{t^2+k^2}}} \\ &- \frac{(4k^2+2t^4+4t^2(k-t)+4k^2(k-t))}{2(2k+1)^2(t^2+k^2)^2\sqrt{1+2\frac{k-t+1}{t^2+k^2}}}) < 0\end{aligned} \tag{5.46}$$

$$\frac{\partial}{\partial k}\left((1-\frac{1}{t})\frac{1}{2t(2k+1)}\sqrt{1+\frac{3t^2-4t+2+2k}{t^2+k^2}}\right) = \\ \frac{-2k^4-6k^3+k^2(-16t^2+16t-9)+k(-5t^2+4t-2)+t^2(-8t^2+8t-3)}{2(2k+1)^2(t^2+k^2)^2\sqrt{1+\frac{3t^2-4t+2+2k}{t^2+k^2}}} < 0. \tag{5.47}$$

All summands except the second one are monotonically decreasing if k increases. The expression under the square root of the second component is also monotonically decreasing as its changing part is monotonically increasing ($\frac{\partial}{\partial k}\left(\frac{2k+1}{t^2+k^2}\right) = 2\frac{-k^2+t^2-k}{(t^2+k^2)^2} < 0$). The monotonically increasing coefficient $\frac{(2k-1)}{2(2k+1)} < \frac{1}{2}$ is bounded from above. Therefore, we can estimate the greatest ratio with the smallest possible k which is t because of $m \leq n$ and the value $\frac{1}{2}$ instead of the coefficient in front of the square root in the second summand:

$$\begin{aligned}\alpha_{tk} \leq & \frac{t+1}{2t+1}\cdot 1 + \frac{1}{2}\sqrt{1+\frac{2t+1}{2t^2}} \\ & + \frac{1}{2(2t+1)}(1-\frac{1}{t})\sqrt{1+\frac{1}{t^2}} \\ & + \frac{1}{2t(2t+1)}\sqrt{1+\frac{3t^2-2t+2}{2t^2}} = \tilde{\alpha}_t.\end{aligned} \tag{5.48}$$

It remains to determine the values of t for which $\tilde{\alpha}_t$ yields large values and compute an upper bound for them. Therefore, we consider the behavior of the summands of $\tilde{\alpha}_t$ for increasing values of t.

For the first two summands of equation (5.48), it is clear that they are either independent of t or definitely decreasing, so we only have a look at the last two summands and compute their derivative:

$$\left(\frac{1}{2t(2t+1)}\sqrt{1+\frac{1}{t^2}}\right)' = \frac{-2t^4+4t^3-3t^2+5t+2}{2t^4\sqrt{1+\frac{1}{t^2}}(2t+1)^2}\begin{cases}<0 & \text{if } t<2\\ \geq 0 & \text{if } t\geq 2\end{cases} \tag{5.49}$$

and

$$\left(\frac{1}{2t(2t+1)}\sqrt{1+\frac{3t^2-2t+2}{2t^2}}\right)' = \frac{-20t^3+5t^2-9t-4}{4t^4\sqrt{1+\frac{3t^2-2t+2}{2t^2}}(2t+1)^2} < 0. \tag{5.50}$$

Thus, we can do another rough estimation by setting t to 1 in all summands except in the third one. In the third summand, we set $t = 2$, which is the local maximum of this summand. Then, we estimate

$$\begin{aligned}\alpha_{tk} \leq & \frac{2}{3}\cdot 1 + \frac{1}{2}\sqrt{1+\frac{3}{2}} + \frac{1}{20}\sqrt{1+\frac{1}{4}} \\ & + \frac{1}{6}\sqrt{1+\frac{3}{2}} \approx 1.78.\end{aligned} \tag{5.51}$$

□

Thus, we get at least a 1.78-approximation for m even and n odd. Furthermore, the following proposition holds:

Proposition 12. *If the solution of the $MSTSP(m,n)$ is not an $(m-1,k-1)$-edge, the orders created by* Weave(m,n), Bobeven(m,n), Near_Quadratic(m,n) *and* Path_Algorithm(m,n) *are asymptotically optimal solutions for the TSPN with mstsp-edge and the solutions of* Bobodd(m,n) *are asymptotically optimal for the TSPN with quasi-mstsp-edge.*

Proof. For the case of m odd, n odd we have already proved this in proposition 11. For the remaining cases, we split the definition of α_{tk} into single summands:

$$\alpha_{tk}^{alg(m,n)} = \sum_{\text{e: edges in alg(m,n)}} g_e \cdot \sqrt{h_e} \tag{5.52}$$

with $\sqrt{h_e}$ being the quotient of the length of an edge from the considered algorithm

$$alg(m,n) \in \{\text{Weave}(m,n), \text{Beveven}(m,n), \text{Bobodd}(m,n), \\ \text{Near\_Quadratic}(m,n), \text{Path\_Algorithm}(m,n)\}$$

and (quasi-)mstsp-edge edge, g_e being the quotient of the number of occurrences of that edge and the complete number of edges of the tour. First, we check if h_e converges to 1 or if h is at least finite. Therefore, we consider all edges which appear in any of the algorithms which we get from section 5.3.1.

Let (t,k) be the shortest edge of the algorithm. Then the quotient of any edge with $(t \pm x_1, k \pm x_2)$ is $1 + \frac{at+bk+c}{t^2+k^2}$ which converges to 1 for $t,k \to \infty$. It remains to check any edge with $(m-x_1, k \pm x_2)$ or $(m-x_1, n-x_2)$. In this case the quotient has the following form: $1 + \frac{\pm at^2 \pm bk^2 \pm ct \pm dk \pm e}{t^2+k^2}$ (in the first case $b=0$) with $a,b,c,d,e \geq 0$. We determine that its absolute value is finite by

$$1 + \underbrace{\frac{at^2}{t^2+k^2}}_{<\frac{a}{2}} \pm \underbrace{\frac{bk^2}{t^2+k^2}}_{<b} \pm \underbrace{\frac{ct}{t^2+k^2}}_{<c} \pm \underbrace{\frac{dk}{t^2+k^2}}_{<d} \pm \underbrace{\frac{e}{t^2+k^2}}_{<e} < \infty. \tag{5.53}$$

The same holds for a denominator of $(t-1)^2 + k^2$ or $t^2 + (k-1)^2$.

In a second step, we determine the limit of the coefficients. We realize that for any rate f from section 5.3.1 which is only dependent on either m and t or n and k

$$\lim_{t,k \to \infty} \frac{f}{mn} = 0. \tag{5.54}$$

We then compute the limit of the remaining coefficients. If we sum up the limit of all coefficients g_e of one procedure, we realize that this sum is one for all mentioned algorithms. Furthermore, we see that the limit of all edges with a positive (> 0) limit of the coefficient is 1. Thus, we have proved

$$\lim_{t,k \to \infty} \frac{\text{Tour length } alg(m,n)}{\text{Lower Bound}} = 1. \tag{5.55}$$

□

For grids whose upper bound for the MSTSP is the length of an $(m-1, k-1)$-edge, we have not succeeded in proving an asymptotical optimality with the current lower bound. Although the coefficients are the same, it was impossible to prove $\lim_{t,k\to\infty} \frac{t^2+k^2}{(m-1)^2+(k-1)^2} = 1$. For those grids, it remains open whether the tour from the new algorithms are asymptotically optimal.

After some theoretical considerations, we will now compute the tour length of the combinatorial algorithms for several grids and describe the behavior of the approximation ratio. We computed the length of the tours for grids from 3 to 99 rows and columns and plotted some samples. Having a closer look at figure 5.6(a) where the approximation ratio is plotted for WEAVE(m, n) with n odd dependent on the number of rows and columns of the grid, we see that the computed ratio points towards a better approximation ratio for the set of samples. The graphs are monotonically decreasing for all values and even the values for the quadratic grid, where the single curves start, have monotonically decreasing values for increasing $t = k$. However, the graphs differ for an odd and an even number of rows. If m is odd, the graphs start at a greater ratio which is decreasing for greater values of m. For grids from 3 to 99 rows and columns, the greatest appearing ratio is < 1.33 for m, n odd and < 1.114 for m even, n odd.

We received from our computations that for those grids with $m > 80$ odd, the approximation ratio is smaller than 1.0133 for the computed grids, for $m \geq 80$ even, it is smaller than 1.0053.

For all evaluated grids, the approximation of the TSPN with mstsp-edge using BOBEVEN(m, n) is not worse than a 1.135-approximation. Leaving out the values of the quadratic grids, we even receive a better approximation ratio than 1.1. For some different m, the ratio α_{tk} is plotted in figure 5.6(b). From this figure we can also see that the curves are first decreasing, before they increase again on a certain interval and finally decrease to 1. The graph of $m_2 > m_1$ is below the graph of m_1 after the change of the shortest edge.

If a grid has an even number of columns n, the shortest edge differs for grids with a small number or a large number of columns. This change of the shortest edge at a certain size of n or k (see table 4.5) can be observed in figures 5.6(b) where the curve starts to increase. For BOBODD(m, n) the change of the shortest edge is apparent in figure 5.7(a).

Figure 5.7(a) shows some plotted examples for the ratio α_{tk} for BOBODD(m, n). We can observe the change of the shortest edge length from $\sqrt{(t-1)^2+k^2}$ to $\sqrt{(m-1)^2+(k-1)^2}$ at the point where the curves start to increase. According to our computations, all ratios yield values which are smaller than 1.1134. The graph has the same behavior as described for BOBEVEN(m, n).

The ratio of the tour length of NEAR_QUADRATIC(m, n) for grids with $n = m+1$ columns is monotonically decreasing for an increasing m and therefore n (see figure 5.5). The maximum ratio that is yielded for the tested grid sizes with a minimum edge length of $\sqrt{t^2+k^2}$ is $\alpha_{max} < 1.07$ which is better than all other computed maxima.

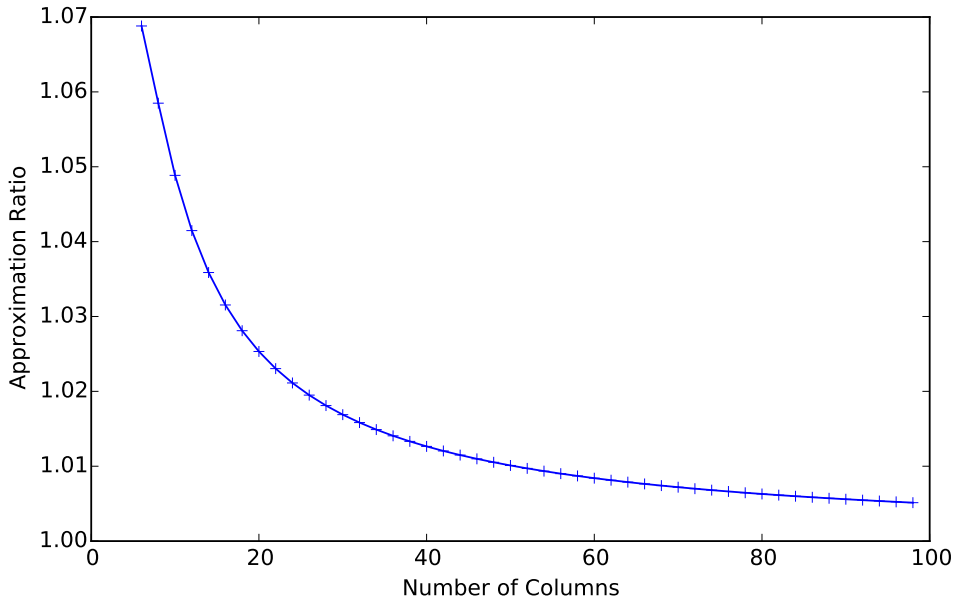

Figure 5.5.: Approximation ratio α of NEAR_QUADRATIC(m, n) ($m = n - 1$ and n even) for the TSPN

We also consider PATH_ALGORITHM(m, n) as it contains very few different kinds of edges with very similar lengths. For this algorithm, we compute the tours for grids with odd $m = 5, \ldots, 21$ and even $n = 6, \ldots, 70$ ($m \leq n$) and compare it with the lower bound of a path with minimum edge length $\sqrt{t^2 + k^2}$. The maximum ratio of the computed grid sizes is $\alpha_{tk} = 1.098$. The graph illustrated in figure 5.7(b) is monotonically decreasing and the graph of the ratio of a larger m lies below the graphs of the smaller m.

Even though we did not succeed to prove that BOBEVEN(m, n) and BOBODD(m, n) are asymptotically optimal for tours with edges longer than $\sqrt{(m-1)^2 + (k-1)^2}$, the figures indicate it. They also point to a much better approximation ratio than proved in proposition 11.

5.3.4. Approximation of the TSPN in a Three-Dimensional Grid

In this section, we will prove a theorem about the approximation of the TSPN with mstsp-edge for the three-dimensional grid ($l \leq m \leq n$). As the algorithms for n involve a lot of case analysis and include the change of the shortest edge length which we could not prove to be asymptotically optimal in the two-dimensional case, we restrict our considerations in this section on grids with an odd number of columns n. The following expression will be used in the following:

Definition 12. *Any distance in the three-dimensional grid can be defined by three components: the l-distance, the m-distance and the n-distance. The l-distance is the component of the distance which is perpendicular to the plane of rows and columns, the m-distance is the component perpendicular to the plane of layers and columns and the n-distance is the component perpendicular to the plane of layers and rows.*

We start with a proposition which deals with a grid with an even number of layers and rows and an odd number of columns.

Proposition 13. *Let l even, m even and n odd.* WEAVE_3D(l, m, n) *yields an asymptotically optimal solution to the TSPN with mstsp-edge.*

Proof. We will start by listing the edges that appear in WEAVE_3D(l, m, n): From table 5.3, we get the edges appearing in WEAVE(m, n). Considering equation (5.3), we see that within an interval $[ymn, (y+1)mn[$ with $y \in \{0, \dots l-1\}$ the l-distances are r and they are $r-1$ at the transition from one interval to the next in the first half of intervals, as well as at the transition from the first half to the second half and at the transition from the last interval to the first one. In the second half of intervals, the l-distance is $r+1$. As one interval contains the same number of positions as one plane of a two-dimensional grid, all edges except the last one of the algorithm in the plane are combined with an r-move. Thus, we obtain the list of edges with their respective rate of table 5.5.

As the shortest edge is always an (r, t, k)-edge, the lower bound of a TSP tour with that minimum edge can be set to $l \cdot m \cdot n \cdot \sqrt{r^2+t^2+k^2} = (2r) \cdot (2t) \cdot (2k+1) \cdot \sqrt{r^2+t^2+k^2}$. The approximation ratio is defined as

$$\begin{aligned}
\gamma_{rtk} &= \frac{\text{Length of WEAVE_3D}(l, m, n)}{\text{Lower Bound}} \\
&= \frac{(2r) \cdot (2t) \cdot (k+1)}{(2r) \cdot (2t) \cdot (2k+1)} \cdot \sqrt{\frac{r^2+t^2+k^2}{r^2+t^2+k^2}} \\
&+ \frac{(2r) \cdot t \cdot ((2k+1)-2)}{(2r) \cdot (2t) \cdot (2k+1)} \cdot \sqrt{\frac{r^2+t^2+(k+1)^2}{r^2+t^2+k^2}} \\
&+ \frac{(2r) \cdot (t-1)}{(2r) \cdot (2t) \cdot (2k+1)} \cdot \sqrt{\frac{r^2+(t-1)^2+(k+1)^2}{r^2+t^2+k^2}} \\
&+ \frac{r+1}{(2r) \cdot (2t) \cdot (2k+1)} \cdot \sqrt{\frac{(r-1)^2+(2t-1)^2+(k+1)^2}{r^2+t^2+k^2}} \\
&+ \frac{r-1}{(2r) \cdot (2t) \cdot (2k+1)} \cdot \sqrt{\frac{(r+1)^2+(2t-1)^2+(k+1)^2}{r^2+t^2+k^2}}.
\end{aligned} \tag{5.56}$$

Computing the limit of γ_{rtk} leads to

$$
\begin{aligned}
\lim_{r,t,k\to\infty} \gamma_{rtk} = \lim_{r,t,k\to\infty} \Bigg[& \overbrace{\frac{k+1}{2k+1}}^{\to\frac{1}{2}} \\
& + \underbrace{\frac{2k-1}{2\cdot(2k+1)}}_{\to\frac{1}{2}} \cdot \underbrace{\sqrt{1+\frac{2k+1}{r^2+t^2+k^2}}}_{\to 1} \\
& + \underbrace{\left(\frac{1}{2\cdot(2k+1)} - \frac{1}{2t\cdot(2k+1)}\right)}_{\to 0} \cdot \underbrace{\sqrt{1+2\frac{k-t+1}{r^2+t^2+k^2}}}_{<\infty} \\
& + \underbrace{\left(\frac{1}{4t\cdot(2k+1)} + \frac{1}{4rt\cdot(2k+1)}\right)}_{\to 0} \cdot \underbrace{\sqrt{1+\frac{3t^2-4t+2(k-r)+3}{r^2+t^2+k^2}}}_{<\infty} \\
& + \underbrace{\left(\frac{1}{4t\cdot(2k+1)} - \frac{1}{4rt\cdot(2k+1)}\right)}_{\to 0} \cdot \underbrace{\sqrt{\frac{(r+1)^2+(2t-1)^2+(k+1)^2}{r^2+t^2+k^2}}}_{<\infty} \Bigg] \\
& = \frac{1}{2} + \frac{1}{2} = 1.
\end{aligned}
\tag{5.57}
$$

Edge	Rate
(r,t,k)	$2r\cdot 2\cdot t\cdot(k+1)$
$(r,t,k+1)$	$2r\cdot t\cdot((2k+1)-2)$
$(r,t-1,k+1)$	$2r\cdot(t-1)$
$(r-1,2t-1,k+1)$	$r+1$
$(r+1,2t-1,k+1)$	$r-1$

Table 5.5.: Edges in WEAVE_3D(l,m,n) with l, m even, n odd

□

This can be extended to the following theorem:

Theorem 5. *Let l, m be even or odd and n be odd.* WEAVE_3D(l, m, n) *yields an asymptotically optimal solution to the TSPN with mstsp-edge.*

Proof. When extending the two-dimensional edges to three-dimensional edges, we know from the definition of $h(p)$ that nearly all 2D-edges are combined with an l-distance of r if l is even. Only the edge which completes the tour in the two-dimensional case can be merged to an l-distance of $r-1$, r, $r+1$, $m-2$ or $m-1$. The edges within one layer, which are combined with an l-distance of r, appear l times the frequency that they have in the 2D-procedures. If l is odd, there is also a greater number of edges which include an l-distance of $m-1$. However, the number of these edges is not dependent on the number of layers but only on the numbers of rows and columns.

When we compute γ_{rtk} we sum up the length of all appearing edges multiplied with their frequency and divide it by a lower bound of the tour length. This lower bound is lmn times the length of the shortest edge of the current algorithm. Two important facts need to be considered here:

1. If a 2D-edge has a frequency f_e which is not dependent on both dimensions m and n, $\lim_{t,k\to\infty} \frac{f_e}{mn} = 0$. Then, also $\lim_{r,t,k\to\infty} \frac{f_e^{3d}}{lmn} = 0$ with f_e^{3d} being the frequency of any extension of e to a 3D-edge. The ratio of any edge length of the tour and the shortest edge length of the tour is always finite.

2. Considering table 5.3 (without case 7) we can state that all edges e_{fin} which complete the tour in WEAVE(m, n) for grids with n odd have a frequency that is not dependent on the grid size. These are either $(m-1, k+1)$-edges or $(m-2, k+1)$-edges in WEAVE(m, n) with n odd. Those edges which are dependent on both the number of rows and columns are only the (t, k)-edges and the $(t, k+1)$-edges. When extending them to 3-dimensional edges and considering their components in γ_{rtk}, we can recognize that both expressions under the square root converge to 1 and each coefficient converges to $\frac{1}{2}$.

Thus, $\lim_{r,t,k\to\infty} \frac{f_e^{3d}}{lmn} = 1$. □

For the other $3D$-procedures, similar studies could be made, but as the shortest edge is not that easily determined, we leave it open whether the algorithms produce an asymptotically optimal solution to the TSPN with mstsp-edge.

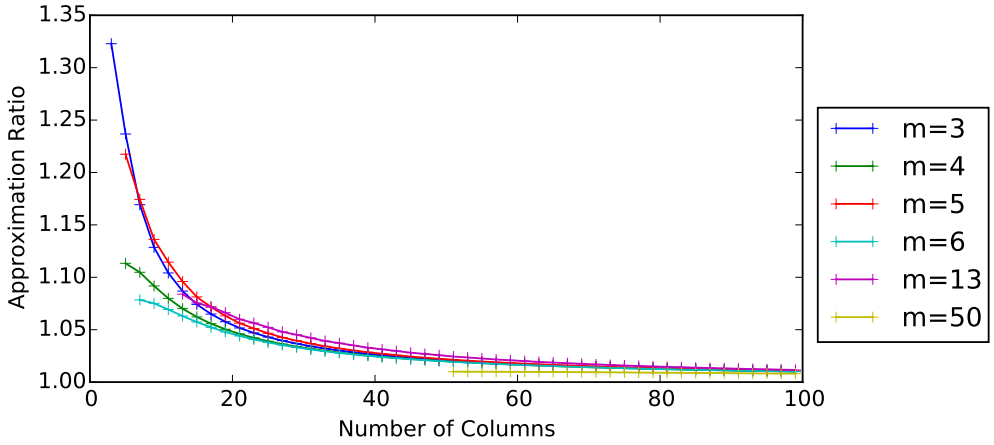

(a) Weave(m, n) with odd n

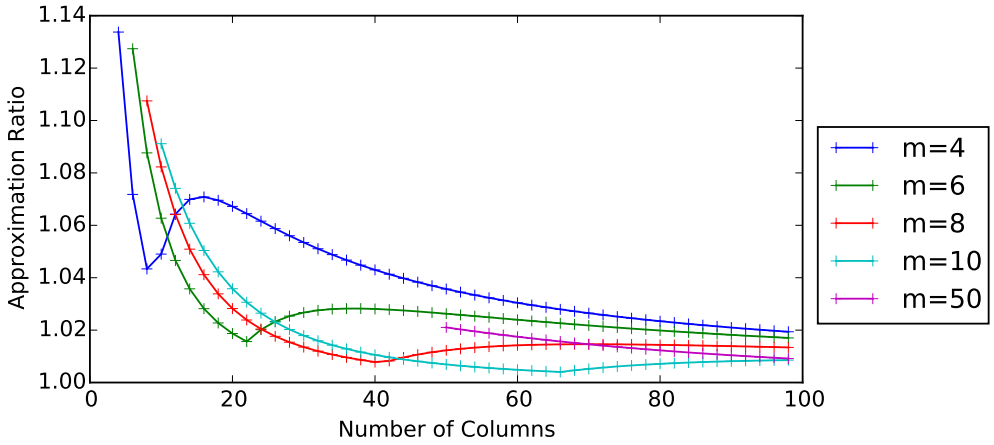

(b) Boeven(m, n)

Figure 5.6.: Approximation ratio α of the grid algorithms for the TSPN – part 1

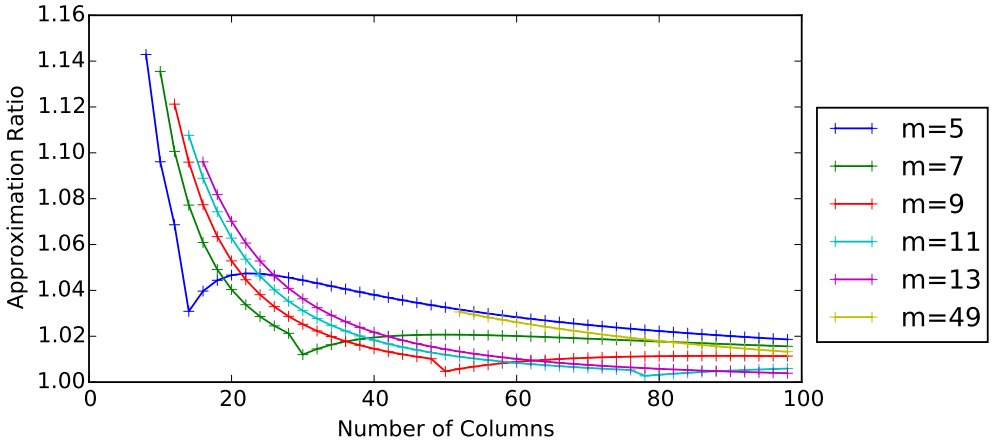

(a) Bobodd(m, n)

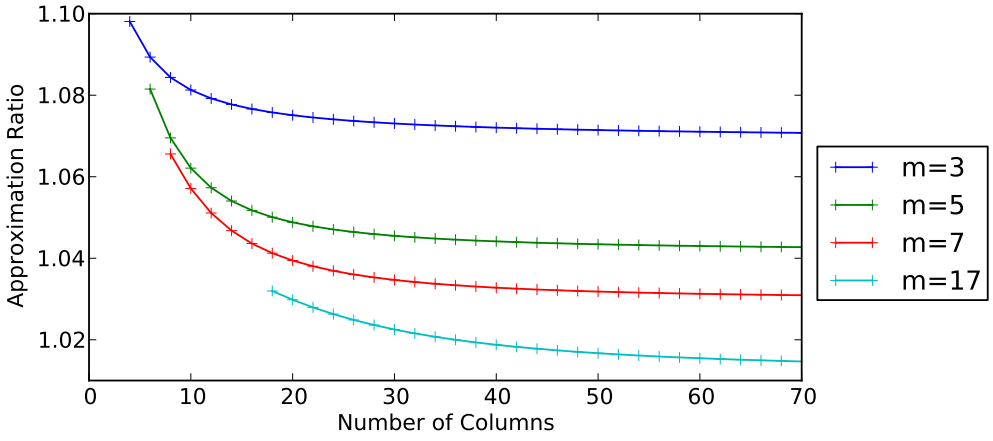

(b) Path_Algorithm$(m, n)$for odd m and even n

Figure 5.7.: Approximation ratio α of the grid algorithms for the TSPN – part 2

6. Heuristics for the Maximum Scatter and the Max-Min 2-Neighbor TSP

After the examination of linear time methods for the MSTSP on a regular grid, we will now have a look at a heuristic which we have deduced and which solves the MSTSP approximately. This procedure can even be extended to a heuristic for the MM2NTSP. Currently it is a local search containing solely 2-opt moves. According to Applegate et al. [6] (chapter 15.1), one of the most successful tour-finding approaches is the algorithm of Lin and Kernighan. In this section, we will deal with this heuristic as our local search heuristic could be extended to such a procedure.

6.1. Background: Lin-Kernighan Heuristic for the Classic TSP

The description of the Lin-Kernighan heuristic together with its precursors refers mainly to Applegate et al. [6] (chapter 15) and Reinelt [73] (chapters 2.4 and 7.3) and there are some parallels to part of my master thesis [47]. The precursor of the algorithm of Lin and Kernighan is the nearest neighbor algorithm of Flood [39]. Building on Dantzig, Fulkerson and Johnson [31], he solved the assignment relaxation of the traveling salesman problem which ignores the constraint of a cycle without subtours and got the dual solution $u_0, \ldots, u_n$, which he reused to compute the so called reduced-cost matrix. This matrix consists of the difference between the original costs of travel for each pair of cities (i, j) and $(u_i + u_j)$. For the following algorithm, the edge cost is the reduced cost of an edge. The algorithm starts at one city and then proceeds to the closest city that has not been visited yet. Having thus found a tour, the procedure is followed by an improvement phase. This phase builds on the fact that in any optimal tour $(i_0, \ldots, i_{n-1})$ for an n-city TSP, for each $0 \leq p < q < n$, the inequality

$$c_{i_{p-1}i_p} + c_{i_q i_{q+1}} \leq c_{i_{p-1}i_q} + c_{i_p i_{q+1}} \tag{6.1}$$

is fulfilled with c_{ij} being the entries of the reduced-cost matrix. That means that if two edges are taken from the optimal tour and the adjacent nodes are connected in another way such that there is again one cycle, the costs of this new cycle cannot be lower than the original costs.

A special kind of exchange of edges (*flip(p,q)*) is used in the advanced algorithm by Croes [30]. If there is a pair of indices (p, q) that violates the previous inequality

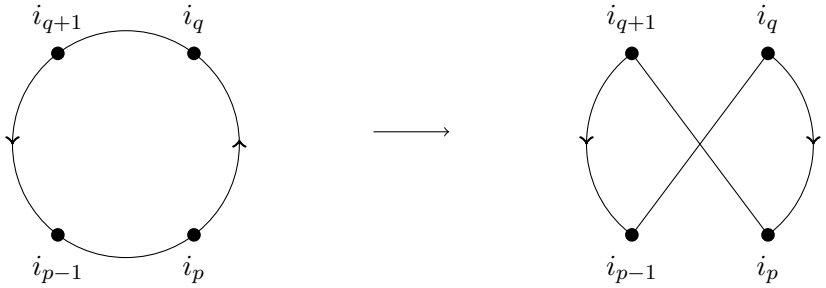

Figure 6.1.: The $flip(p, q)$-operation [according to Applegate et al. [6],fig. 15.1]

(6.1) in the current tour, the edges $(p-1, p)$ and $(q, q+1)$ are replaced by the edges $(p-1, q)$ and $(p, q+1)$. This exchange is also called inversion and can be repeated until all pairs (p, q) fulfill inequality (6.1). Under the assumption that the tours are oriented, this operation is well defined.

If a $flip$-operation reduces the cost of the tour, it is a 2-opt move which means that two edges are removed from the current tour and the resulting paths are reconnected in the best possible way (Reinelt [73], section 2.4.5). Analogously, also k-opt moves can be defined. Lin [56] went on with this idea and expanded it. He provided a very useful framework to describe intersectionless tours and tours which are optimal with respect to flip-operations. He did not only exchange the edges between two pairs of adjacent nodes, but took even more pairs together for an exchange of edges.

A tour is called *k-optimal* if no abatement of costs is possible by replacing any k of its edges by any other set of k-edges which is adjacent to the same nodes (Lin [56]). The algorithm of Lin and Kernighan [57] is "variable k-optimal", it is an effective search method to find a sequence of flips, such that the costs at the final state of the tour decrease compared to the initial state. Every k-optimal move can be achieved by a number of flips. The length of the sequence varies, as the sequence is chosen as long as possible. Some of the intermediate tours may have costs that are greater than those of the initial tour. If an improving sequence is found, the flips are applied and the algorithm continues with the new tour. Reinelt [73] states that it takes $\mathcal{O}(n^k)$ to completely check if there is an improving k-move. In his implementation he focused on 2-opt moves and node insertion moves, which means that a node is deleted from the tour and reinserted at the best possible position.

Lin and Kernighan describe the general idea of iterative improvement of a set of randomly selected feasible solutions in their article [57] on page 499 (C being some criterion that has to be satisfied in the optimization problem):

1. Generate a pseudorandom feasible solution, that is, a set T that satisfies C.

2. Attempt to find an improved feasible solution T' by some transformation of T.

3. If an improved solution is found, i.e., $f(T') < f(T)$, then replace T by T' and repeat from Step 2.

4. If no improved solution can be found, T is a locally optimum solution. Repeat from Step 1 until computation time runs out, or the answers are satisfactory.

Following the approach of iterative improvement, the last gained locally optimal tour is changed and set as the new initial order for the next iteration. For the modifications of the current solution, Martin et al. [61] suggest a double bridge which is a move replacing four edges (see figure 6.2). This configuration does not arise from *flip*-operations as it is not possible to reach it while preserving a tour at any time. An advantage of this new configuration is that it consists of very similar edges to the latest locally optimal tour.

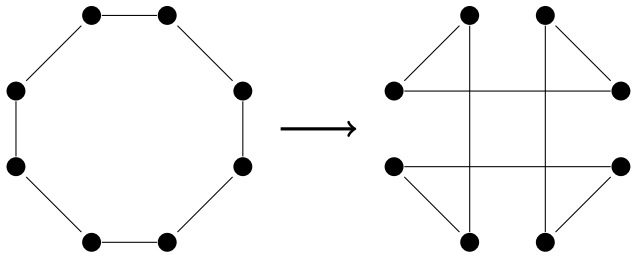

Figure 6.2.: Double-bridge [according to Applegate et al.[6], fig. 15.7]

Algorithm 1 is a very short notation of the heuristic of Lin and Kernighan. For more detailed information, we refer to their paper [57].

For the implementation several components are needed like the selection rule of the most-out-of place pair, a function which represents the total profit from a set of exchanges, a stopping rule as well as further criteria such as a criterion which guarantees that the edges $x_1, \ldots, x_k$ and $y_1, \ldots, y_k$ are disjoint and one which guarantees a feasible exchange.

There are quite a lot of different implementations. Helsgaun [46] solved transformed equality generalized traveling salesman problems with an effective implementation of the Lin-Kernighan Traveling Salesman Heuristic which he describes in [45]. Some further examples are the implementations of Bland and Shallcross [17], Johnson [49], Mak and Morton [59], Perttunen [69].

Furthermore, Martin et al. [61] combine the Lin-Kernighan heuristic with simulated annealing and thus create a chained Lin-Kernighan which works for larger instances. Simulated annealing samples solutions iteratively and stochastically with a Markov chain. It is a very slow approximation, but is well suited to preserve properties of previous locally optimal solutions. The classical Lin-Kernighan heuristic runs faster, but sometimes skips information of near optimal solutions when perturbing the tour. Chained Lin-Kernighan does an annealing between locally optimal tours and has larger Lin-Kernighan steps in between.

Algorithm 1 Heuristic of Lin and Kernighan [57]

Let S be the set of edges, $x_i, y_i \in S$.

1. Generate a random initial solution T.
2. (a) Set $i = 1$.
   (b) Select x_i and y_i as the most-out-of-place pair at the ith step. This generally means that x_i and y_i are chosen to maximize the improvement when $x_1, \ldots, x_i$ are exchanged with $y_1, \ldots, y_i$. x_i is chosen from $T - \{x_1, \ldots, x_{i-1}\}$ and y_i from $S - T - \{y_1, \ldots, y_{i-1}\}$.
   (c) If it appears that no more gain can be made, according to an appropriate stopping rule, go to Step 3; otherwise, set $i = i + 1$ and go back to Step 2(b).
3. If the best improvement is found for $i = k$, exchange $x_1, \ldots, x_k$ with $y_1, \ldots, y_k$, to give a new T, and go to Step 2; if no improvement is found, go to Step 4.
4. Repeat from Step 1 if desired.

Applegate et al. [5] work on the Chained Lin-Kernighan heuristic based on Martin et al. [61] applying it to larger instances. They state that there are three particular issues which have a great impact on the efficiency of implementations of Chained Lin-Kernighan. These issues are the breadth of the Lin-Kernighan search, the structure of the kick and the choice of the initial tour especially for large instances. They introduce improvements to the Lin-Kernighan heuristic that enable them to better cope with these issues. As a result, they are able to compute solutions for instances with up to 25,000,000 nodes. Estimates for the exact optimal value prove that these solutions are within 1% of the optimum.

6.2. The Algorithm LS_MSTSP

In this section, we will consider a local search method which is an approximation heuristic for the MSTSP. It could certainly be extended to a Lin Kernighan heuristic. In our current implementation, we focus primarily on a local search algorithm with exclusively 2-optimal moves and without repeating the procedure several times with different initial solutions. We stop when the procedure fails to yield an improving flip for the first time. A further modification of the local search methods for the classic TSP is included in the criteria for $flip(p, q)$-operations. Only if all shortest edges can be replaced by longer edges, the objective value increases. Starting from an initial tour, we always take the shortest edge and try to eliminate it by $flip(p, q)$-operations. Having found one edge (i, j) of the shortest length, we search for a second edge (g, h) to do a $flip(j, g)$-operation. The following inequalities have

to hold for the pair of edges:

$$d_{ij} < d_{ig} \tag{6.2}$$
$$d_{ij} < d_{hj} \tag{6.3}$$

with the length of an edge (i, j) being given by d_{ij}. After the exchange of edges, the procedure restarts with the new tour. This is done until there is either no second edge (g, h) fulfilling the inequalities (6.2) and (6.3) to do a $flip(j, g)$-operation or a maximum number of iterations (MAXITER) is reached. A draft of the procedure is given in algorithm 2.

Algorithm 2 Local search heuristic for the MSTSP (LS_MSTSP)

Given: n vertices, initial order $(v_1, \ldots, v_n)$ and distances d_{ij}, maximum number of iterations MAXITER;
iteration counter $iter = 0$;

while $iter <$ MAXITER **do**
Find current shortest edge $(v_{i_s}, v_{i_{s+1}})$ such that

$$d_{v_{i_s},v_{i_{s+1}}} = \min\{\min_{k\in\{1,\ldots,n-1\}} \{d_{v_{i_k},v_{i_{k+1}}}\}, d_{v_{i_n},v_{i_1}}\};$$

Find an edge $(v_{i_t}, v_{i_{t+1}})$ to flip like in figure 6.1 such that the following inequalities hold:

$$d_{v_{i_s},v_{i_t}} > d_{v_{i_s},v_{i_{s+1}}} \tag{6.4}$$
$$d_{v_{i_{s+1}},v_{i_{t+1}}} > d_{v_{i_s},v_{i_{s+1}}}; \tag{6.5}$$

if impossible to find such a set of edges **then**
TERMINATE;
else
Execute a $flip$-operation (see figure 6.1);
Increment $iter$;
end if
end while

6.2.1. Analysis and Comparisons

We can state the following proposition

Proposition 14. *The complexity of LS_MSTSP is* $\mathcal{O}(n^3)$.

One iteration of the LS_MSTSP heuristic, which is counted by $iter$, runs in $\mathcal{O}(n)$ time, n standing for the number of nodes. When storing the edges of the tour in a heap (Fibonacci heap), it takes $\mathcal{O}(\log n)$ ($\mathcal{O}(1)$) time to find the shortest edge of

the current tour consisting of n edges [29]. But it is not sufficient to receive the shortest edge in a fast manner. As the reordering after a flip operation requires $\mathcal{O}(n)$ and there are at most $n-2$ candidate nodes to reconnect the endpoints of the shortest edge, it also takes $\mathcal{O}(n)$ in each turn to find a suitable edge for a $flip$-operation and to conduct a $flip$. MAXITER has to be somehow adapted to the maximum size of the problems which are applied such that there is a variety of possible iterations in which shortest edges can be eliminated. Therefore, it is dependent on n. If MAXITER is hypothetically set to ∞, the number of iterations lies in $\mathcal{O}(n^2)$. The number of all edges between n nodes is $\frac{n(n-1)}{2}$. In the worst case, we start with a tour consisting of the shortest edges and replace them step by step with the next longer edges. So each single short edge has to be deleted from the tour. The complexity of this step is $\mathcal{O}(n^2)$. From Reinelt [73] (section 7.5) we know that it takes $\mathcal{O}(n^k)$ to completely check if there is an improving k-move for the classic TSP; the heuristic of Lin and Kernighan limits the set of exchange candidates in order to obtain reasonable running times. For a 2-opt move this would mean a complexity of $\mathcal{O}(n^2)$. As we fix the first edge to the shortest edge, we reduce the number of possible checks. LS_MSTSP checks all 2-moves in $\mathcal{O}(n)$ in the current version. In the first draft of the implementation the data structure is not ideally chosen, but this would be changed in an advanced implementation.

LS_MSTSP compares both new inserted edges with the current shortest edge before executing a $flip$-operation. As for the objective value each single short edge has a great impact which cannot be compensated by other edges, it is not reasonable to leave out one of the comparisons or to take the difference of the sum of the initial and the modified tour as is usually done in the Lin Kernighan heuristic for classical TSP.

In our current version, we only do 2-opt moves, but the strategy could also be extended to k-opt moves. In that case, it would not be important to have a shorter tour after the exchange of edges, but to have included only longer edges than the previous shortest edge. Within the complete move, there could also be included shorter edges but they would have to be eliminated again within the move in another $flip$. To find out which k to choose and how to restrict the candidate set where the $flip$-candidates are searched, further examinations are needed. What we can state in advance is that the set of candidate nodes for a $flip$-operation should not consist of the nearest nodes to an adjacent node of the shortest edge, but of nodes of a greater distance. Considering the influence of different initial tours on the approximation could be a further aspect to study in order to improve the heuristic. As an outlook on possible refinements of LS_MSTSP we give an example for a possible 3-opt move in figure 6.3. In this figure, which does not use Euclidean distances, the shortest edge in the initial tour is (c,d). By $flip(d,e)$ the even shorter edge (c,e) is included, but is eliminated in the next $flip$. Finally, both shorter edges (c,d) and (e,f) of the initial tour do no longer belong to the tour, all newly inserted edges are longer than (c,d) and so the shortest edge of the final tour is longer than the one of the initial tour. It is also possible that the shorter edge

which is included by a $flip$-operation is the other edge (in the example edge (d, f)). The $flip$-operations which lead to this case should either be rejected or they should be continued by a further step which eliminates the second included edge if this one is shorter. This new kind of step, however, would be a non-sequential step. In the picture this was a $flip$-operation such as $flip(f, g)$. It is important that all inserted edges which are shorter than the initial shortest edge get eliminated in the step as otherwise the objective value deteriorates. The concrete implementation of such a combined $flip$ is not done in this work.

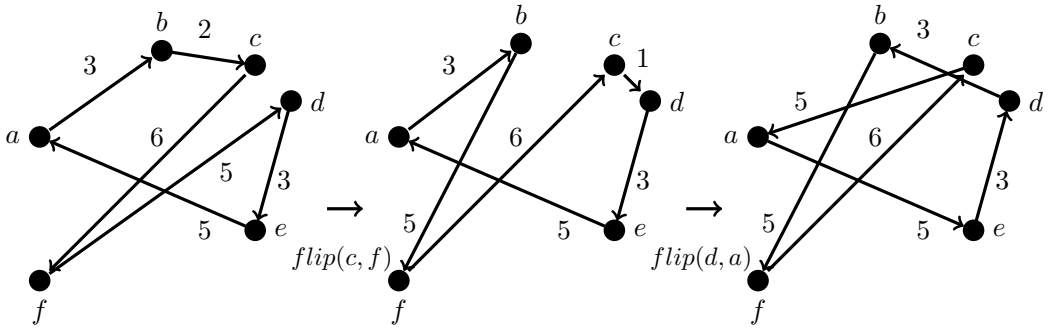

Figure 6.3.: A 3-opt move in LS_MSTSP

Arkin et al. [7] have introduced a 2-approximation algorithm for the MSTSP on a complete graph with weighted edges of non-negative lengths satisfying the triangle inequality, which returns in $\mathcal{O}(n^2)$ a tour with a shortest edge of at least half the length of the longest possible shortest edge. A basic theorem for the idea of their algorithm is theorem 3 of Dirac [33] which states that if the degree of every node in a connected graph with n nodes is at least $\lceil \frac{n}{2} \rceil$, the graph is Hamiltonian. If we wanted to ensure our algorithm to yield an $\frac{1}{2}$-approximation, we could combine the two strategies and first compute an approximation following the strategy of Arkin et al. [7] and improve their tour by taking it as an initial tour for LS_MSTSP. For the tested samples which are described in the next subsection, we did not implement this combination but already received solutions which were better than a $\frac{1}{2}$-approximation for all but 7 samples. As we computed the approximation with a rough upper bound, the real value is likely to be even better. Arkin et al. [7] also determined an upper bound ub for the solution of the MSTSP. This bound can be received by taking all subsets R of nodes containing $\lfloor \frac{n}{2} \rfloor$ nodes. They prove that in any Hamiltonian cycle there is at least one edge connecting two nodes of R. Their upper bound is obtained by taking the longest edge within any subset and choosing the shortest edge of these:

$$ub = \min_{R:|R|=\lfloor \frac{n}{2} \rfloor} \{\max_{i,j \in R} d_{ij}\}. \tag{6.6}$$

But as the number of such subsets $\binom{n}{\lfloor \frac{n}{2} \rfloor}$ is exponential $\binom{n}{\frac{n}{2}}$, the computation of

this bound is quite complicated. That is why we use a more imprecise bound which is easy to compute.

6.2.2. Computational Results

We test LS_MSTSP on a set of $(m \times n)$-grids. As we already know an optimal solution or at least a very close upper bound for all of them, we can better determine the quality of the approximation which is yielded by LS_MSTSP. Moreover, we apply our procedure on a set of TSP instances from the TSPLIB [72]. For those samples, we do not know an optimal solution, but we compare the approximate solution of LS_MSTSP to a rough upper bound. We receive this upper bound by considering for each node the second longest edge to which it is incident. As a tour visits every node two times, the minimum of these second longest edges is an upper bound. All results were computed on an OSX 10.9.4 system with a CPU of 2.8 GHZ Intel Core 2 Duo and a stack of 8GB 1067MHz DDR3. The approximation ratio of the considered grids and of the instances of the TSPLIB are illustrated in figure 6.4. The computational results of the instances of the TSPLIB are listed in the appendix in tables D.1 and D.2. The names of the computed instances can be found in those tables. We define α analogous to $\alpha_{t,k}$.

We computed the solutions for grids from 2 to 19 rows and from 2 to 99 columns. The initial order was the enumeration of all nodes from 1 to $m \cdot n$. For all of the computed grids except for three relatively small ones (3×8, 4×5 and 5×10), the approximation ratio ($\frac{1}{\alpha}$) is better than 1.2 ($\alpha = 0.83$). For greater grids the approximation ratio decreases. One can argue that the regular grid has a very special structure, where each distance, especially the small ones, appears several times. That is why we tested LS_MSTSP also on 63 instances from the TSPLIB. For all tested instances, the coordinates of the nodes are given and the distances have to be computed as Euclidean distances in the two dimensional space. Even though we use a general upper bound for the computation of α, our heuristic found a solution with $\alpha > 0.5$ ($\frac{1}{\alpha} < 2$) for all but 6 samples. For more than 80% of the samples $\alpha > 0.8$ ($\frac{1}{\alpha} < 1.25$) and for half of the instances $\alpha > 0.9$ ($\frac{1}{\alpha} < 1.12$).

When we consider the ratio between the number of iterations counted by *iter* in algorithm 2 and the number of nodes n in our computations, we see that it generally increases, so the number of iterations increases more than linearly compared to the number of nodes. The ratio between the number of iterations and the squared number of nodes seems to decrease. This is consistent with the complexity of the algorithm which was discussed in the previous section. There is one further use that we can get from this approximation. When solving the MSTSP formulated as a linear program with SCIP [2] (default parameters), we can use the approximation as a lower bound and a feasible solution. The linear program is described in section 3.2. The solving process was very much accelerated. Some instances, for which SCIP took several days to yield a close solution, were solved in a few hours with the primal solution from LS_MSTSP. We have not systematically tested it, but the simple improvements make us suggest this lower bound for the solution. The optimal

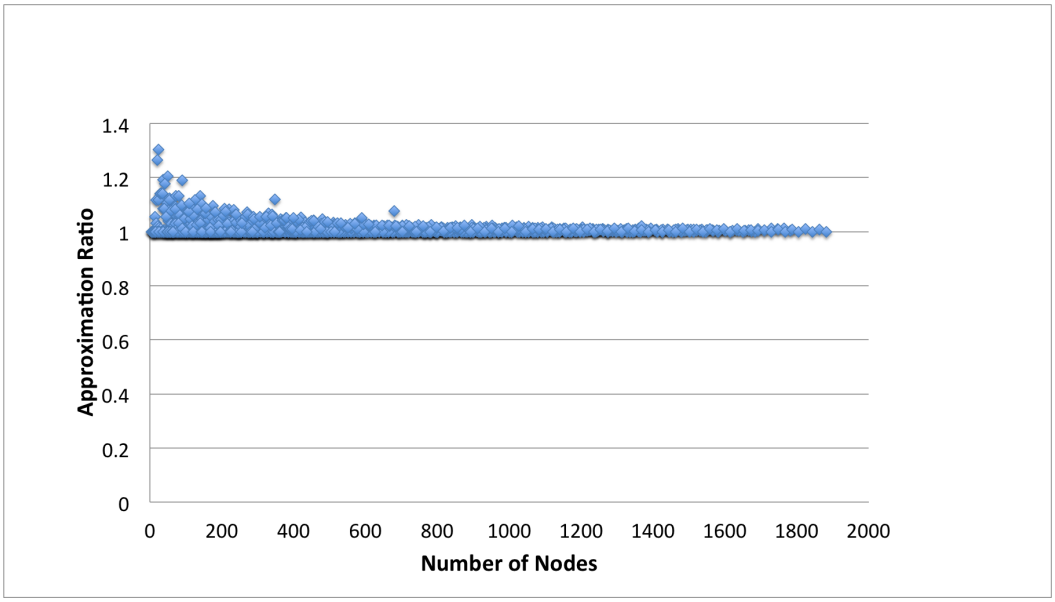

(a) Grid samples

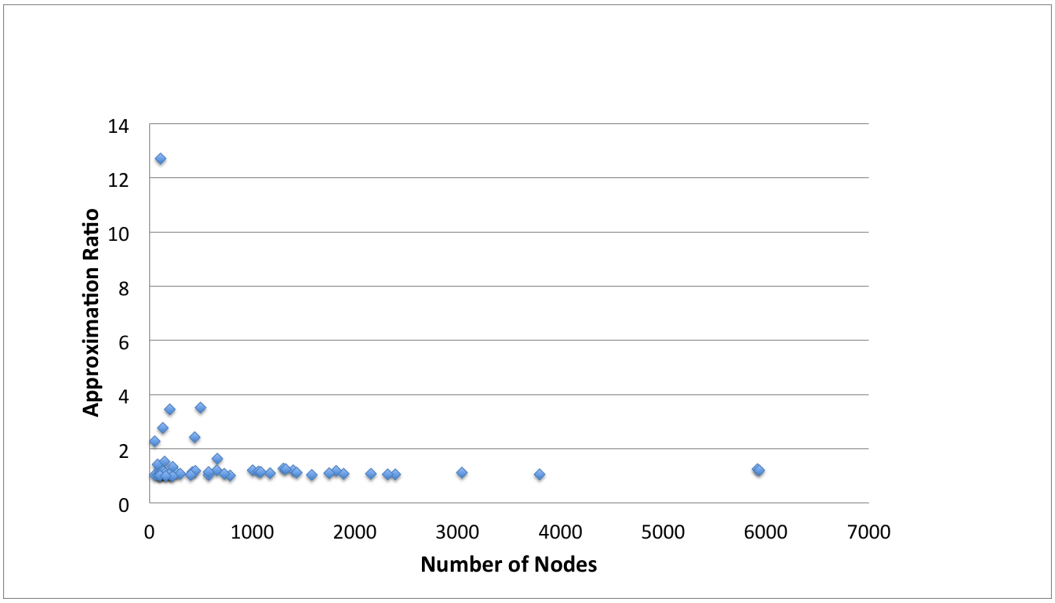

(b) Samples from the TSPLIB

Figure 6.4.: Approximation ratio ($\frac{\text{Upper Bound}}{LS\_MM2NTSP}$) of LS_MSTSP for the MSTSP

solutions or at least the new upper bounds which we got from this computation were significantly closer to the primal bound from LS_MSTSP. For instance, for pr76 the approximation obtains 97% of the upper bound instead of $\approx 71\%$ and pr107 obtains an optimal solution instead of a value of 7% of the upper bound which differs tremendously. It is not yet known whether pr76 is optimal as after about 7 hours of computation time the primal bound is still the bound from LS_MSTSP. In some cases, we could decrease the upper bound to the solution of LS_MSTSP. These cases are also highlighted in the table.

6.3. The Algorithm LS_MM2NTSP

In this section, we will extend the LS_MSTSP-heuristic for the MSTSP to the MM2NTSP with an equal weight 1 of the edges and the 2-edges in the tour as it was already mentioned in section 3.2. After that, we will do another computational study with grids and the instances of the TSPLIB. We will first deduce closer upper bounds for the MM2NTSP on a regular grid.

6.3.1. Upper Bounds for the Max-Min 2-Neighbor TSP

Arkin et al. [7] and Chiang [23] also determined upper bounds for the MM2NTSP. They stated that for any subset S of $\lfloor \frac{n}{3} \rfloor$ at least one pair of nodes are 2-neighbors in a Hamiltonian cycle. As the number of subsets is exponential we use a simpler but looser upper bound which is described in subsection 6.3.3.

Upper bounds on a regular grid can be received in a similar way to the MSTSP. We consider the nodes in the middle of a grid which we illustrated already when we examined the upper bounds of Weave(m, n) in figure 4.3. For the MM2NTSP, we need to consider four edges for each node (instead of two for the MSTSP) as each node has two neighbors and two 2-neighbors in the tour. Furthermore, we include the fact that after going from a node in the middle to one at the corners, we have to get on to a node which is a 2-neighbor of the first node and then to a node which is a 2-neighbor to the node at the corner. We distinguish the following four cases with m, n, t, k being defined as in chapter 4.

Theorem 6. *Let m, n be the number of rows and columns of a regular grid and let $m \leq n$ with $m > 1, n > 2$. Furthermore, let $k = \lfloor \frac{n}{2} \rfloor$ and $t = \lfloor \frac{m}{2} \rfloor$. For the MM2NTSP, the following upper bounds can be claimed considering the distances between corners and central points as well as the direct distance between a potential*

successor of a central point and the potential successors of the successor:

$$(x^*, y^*) = \begin{cases} (t, k) & \text{if } m \text{ and } n \text{ odd}, k \leq \frac{1}{2}(3t^2+1) \\ (m-1, k-1) & \text{if } m \text{ and } n \text{ odd}, k > \frac{1}{2}(3t^2+1) \\ (t-1, k) & \text{if } m \text{ even and } n \text{ odd}, k \leq \frac{1}{2}(3t^2-2t+1) \\ (m-1, k-1) & \text{if } m \text{ even and } n \text{ odd}, k > \frac{1}{2}(3t^2-2t+1) \\ (t-1, k) & \text{if } m \text{ odd and } n \text{ even}, k \leq \sqrt{t(3t-2)} \\ (m-2, 0) & \text{if } m \text{ odd and } n \text{ even}, \\ & \sqrt{t(3t-2)} < k \leq 1 + \sqrt{3t^2-4t+1} \\ (t, k-1) & \text{if } m \text{ odd and } n \text{ even}, k > 1 + \sqrt{3t^2-4t+1} \\ (t, k-1) & \text{if } m, n \text{ even}, k \leq 1 + \sqrt{3t^2-4t+2)} \\ (m-1, 1) & \text{if } m, n \text{ even}, \\ & 1 + \sqrt{3t^2-4t+2} < k \leq 1 + \sqrt{3t^2-2t+1} \\ (t-1, k-1) & \text{if } m, n \text{ even}, k > 1 + \sqrt{3t^2-2t+1)}. \end{cases} \tag{6.7}$$

Proof. The proof is constructive and it is split into four different cases.

m, n **odd:** If the number of rows and columns are odd, the node in the middle has the distance $\sqrt{t^2+k^2}$ to the four corners of the grid. If $k > \frac{1}{2}(3t^2+1)$, the length of any edge with horizontal length $k-1$ is shorter than $\sqrt{t^2+k^2}$. If we used only edges of at least the length $\sqrt{t^2+k^2}$, we could only move between the first, the central and the last column as we would have to consider two predecessors and could not have any horizontal distance of less than $k-1$. So one edge of the tour can be at most as long as the longest edge with $k-1$ as horizontal component. For $k > \frac{1}{2}(3t^2+1)$ such an edge is shorter than $\sqrt{t^2+k^2}$. Thus, the upper bound can be reduced to $\sqrt{(m-1)^2+(k-1)^2}$.

m **even and** n **odd:** For an even number of rows and an odd number of columns we have $\sqrt{(t-1)^2+k^2}$ as an upper bound. If $k > \frac{1}{2}(3t^2-2t+1)$ all edges of horizontal length $k-1$ are shorter than this bound. For the same reason as in the previous case the upper bound can be reduced in this case to $\sqrt{(m-1)^2+(k-1)^2}$.

m **odd and** n **even:** For an odd number of rows and an even number of columns the upper bound is at most $\sqrt{(t-1)^2+k^2}$. There are two central nodes. W.l.o.g. let us consider the left one of the two. If we try to avoid any $(t, k-1)$-move and smaller moves, we need to chose the successor of the central node and the successor of the successor in the right column. Also the predecessor of the left central node and the predecessor of the predecessor have to be chosen from the right column. So we need to take at least two $(m-2, 0)$-edges (see case a in figure 6.6(a)). For $k \leq \sqrt{t(3t-2)}$, $(t-1, k)$ is shorter than $(m-2, 0)$,

for $k > \sqrt{t(3t-2)}$ it is $(m-2,0)$. But if $k > 1+\sqrt{3t^2-4t+1}$, we avoid $(m-2,0)$-edges and take $(t,k-1)$ as an upper bound for the shortest edge like in case b in figure 6.6(a).

m,n **even:** If the number of rows and columns are even and $m \geq 4$, the longest edges which can connect central nodes to other nodes but are shorter than $\sqrt{(t-1)^2+k^2}$ are either $(t-2,k)$-edges or $(t,k-1)$-edges. If $k > 2t-\frac{3}{2}$, the longer edge of the two is $(t-2,k)$. We get the constraints for k in this case and in the following by transformations of an inequality which compares the lengths of two edges. As for each central node we only have one node with a distance of $\sqrt{t^2+k^2}$ and two with a distance of $\sqrt{(t-1)^2+k^2}$, we need at least one further node with a shorter edge. Let us first assume that $(t-2,k)$ is the longest edge that is used in a tour and that $k > 2t-\frac{3}{2}$. There are 5 or 4 nodes respectively for $m \geq 6$ and $m = 4$ respectively in the right column which could be a neighbor of the lower left central node. In order to keep a shortest edge of $\sqrt{(t-2)^2+k^2}$, two pairs of those neighbors need to have a distance between them of at least $\sqrt{(t-2)^2+k^2}$. As we can also see in figure 6.6(b), this is only the case if the $(m-2,0)$-edge is longer than $\sqrt{(t-2)^2+k^2}$ which would be the case for $k \leq \sqrt{3t^2-4t}$. This contradicts the constraint $k > 2t-\frac{3}{2}$. Therefore, there is no optimal tour for MM2NTSP containing edges of a length of at least $\sqrt{(t-2)^2+k^2}$. However, we can prove by transformation that an $(m-2,0)$-edge is only strictly longer than a $(t,k-1)$-edge for $k < 1+\sqrt{3t^2-8t+4}$ and this bound always lies below the domain with $k > 2t-\frac{3}{2}$ which we have restricted. This means that there is no optimal tour for the MM2NTSP which exclusively consists of strictly longer edges than a $(t,k-1)$-edge.

Therefore, we may start with an upper bound of $\sqrt{t^2+(k-1)^2}$ for all grids with m,n even, but can even decrease the value for several cases. In the following, we use the fact that $(0,n-1)$ is longer than $(t-1,k)$ for $n > 2$:

$$(n-1)^2 \geq (t-1)^2+k^2 \tag{6.8}$$
$$\Leftrightarrow \quad 4k^2-4k+1 \geq t^2-2t+1+k^2 \tag{6.9}$$
$$\Leftrightarrow \quad 3k^2-4k-t^2+2t \geq 0 \tag{6.10}$$
$$\Leftrightarrow \quad k(3k-4)-t(t-2) \geq t(3k-2-t) = t(2k-2+k-t) \geq 0. \tag{6.11}$$

In grids with $n \leq 2$, we have to use even the shortest possible edge, so any tour is optimal and we do not have to consider them. The following considerations are structured in figure 6.5. If an $(m-1,1)$-edge is longer than a $(t,k-1)$-edge, that means for $k \leq 1+\sqrt{3t^2-4t+2}$, we keep the current upper bound of $\sqrt{t^2+(k-1)^2}$ as we can connect the left upper corner to the right upper corner and the first node in column $n-1$ to the last node in column n

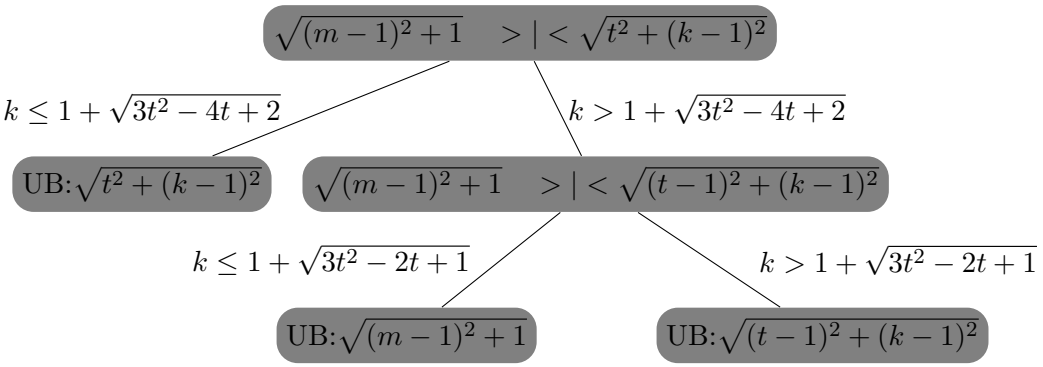

Figure 6.5.: Different upper bounds for m, n even

and the distances of the four nodes to the lower left central node is smaller than $\sqrt{t^2+(k-1)^2}$. For $k > 1+\sqrt{3t^2-4t+2}$ we can decrease the upper bound. Candidate edges for a possible shortest edge in a tour are $(m-1,1)$, $(t-1,k-1)$ and $(t,k-2)$. $(t-2,k)$ is not a candidate as including this edge does not enable any two connections longer than $\sqrt{(m-1)^2+1}$ between the neighbors. We prove that $(t,k-2)$ is not immediately a candidate for an upper bound for the shortest edge when we only consider the neighbors of the left lower central node.

$$\sqrt{t^2+(k-2)^2} \leq \sqrt{(t-1)^2+(k-1)^2} \tag{6.12}$$

$$\Leftrightarrow \quad t^2+k^2-4k+4 \leq t^2-2t+1+k^2-2k+1 \tag{6.13}$$

$$\Leftrightarrow \quad 0 \leq -2t-2+2k \tag{6.14}$$

$$\Leftrightarrow \quad k \geq t+1. \tag{6.15}$$

The only case for which $(t,k-2)$ is longer than $(t-1,k-1)$ is for a quadratic grid ($t=k$). But for this grid, we can get all neighbors and 2-neighbors of the lower left central node with $\sqrt{(m-1)^2+1} > m-1 = n-1 \geq \sqrt{(t-1)^2+k^2} = \sqrt{t^2+(k-1)^2}$. So we can ignore that edge as a candidate until there is another reason to decrease the upper bound.

It remains to check which of the two candidate edges is the longer one. By transformations of the stated inequality, we receive that an $(m-1,1)$-edge is longer than a $(t-1,k-1)$-edge for $k \leq 1+\sqrt{3t^2-2t+1}$. So we get the cases as they are listed in the theorem.

For $m=2$ the considerations do not work in the same way as there are no $(t-2,k)$-edges or others and $m-1$ is already 1. Here we see according to figure 6.6(c) that $(t,k-1)$ is not the closest upper bound and we can decrease it to $(t-1,k-1)$ or $(1,k-2)$. If $k \geq 2$, a closer upper bound is $k-1$. In a (2×2)-grid, it is $\sqrt{1+(k-2)^2} = 1$.

Of course, we could still decrease some of the upper bounds by considering the common neighbors of the central nodes. This is the case if m, n even and the current upper bound is the length of a $(t, k-1)$-edge. Then the four central nodes do not have enough candidate nodes to connect without getting subtours or visiting some nodes several times. But we think that we are close enough to have better upper bounds than before and that the distinctions would lead to many special cases without gaining a lot of decrease. Therefore, we stop at that state and use the bounds of theorem 6 for the following comparisons.

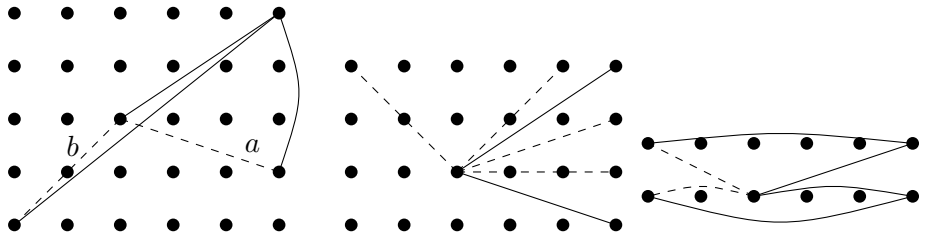

(a) m odd and n even (a for small n, b for large n) (b) m, n even (c) $m = 2, n$ even

Figure 6.6.: Upper bounds for the MM2NTSP

□

6.3.2. Extension of LS_MSTSP to the Max-Min 2-Neighbor TSP

We can extend LS_MSTSP to the MM2NTSP. The approximation procedure – called LS_MM2NTSP in the following – additionally tests if a flip of edges does improve the shortest edge between 2-neighbors as well. The shortest edge that is determined in each iteration is chosen from the set of all edges of a tour and of all its 2-edges. So a $flip(p, q)$-operation is only applied if the added edges and edges between the new 2-neighbors are all longer than the shortest current one. LS_MM2NTSP is defined in algorithm 3. We could choose either the lexicographical order of the nodes or the solution of the MSTSP or any random order as initial order.

The parameter c in LS_MM2NTSP stands for the weight of the 2-neighbor edges. For the computational results of the heuristic, it is always set to 1, but for the samples in CHAMP, it was set to 1.5. This value is chosen if the influence of 2-neighbor edges is not as severe as of the direct edges.

We can deduce the following proposition in the same way as for LS_MSTSP.

Proposition 15. *The complexity of LS_MM2NTSP is* $\mathcal{O}(n^3)$.

As there are more tests in each iteration than in LS_MSTSP, the constant however increases.

We also used this heuristic in CHAMP. As we thought that the distances between 2-neighbors are less important than the direct edges, we set $c = 1.5$. Thus, only the distances between consecutive nodes had to be shorter than the objective value. When we computed the strategies for the tests at Concept Laser GmbH, the solutions for the MM2NTSP were received by applying the Lin Kernighan heuristic, starting with the order that is a solution for the MSTSP. Although this was not the optimal solution for the MM2NTSP, it was an approximation that sufficed to test if this type of strategy caused less deflection than other strategies. The tests on real world workpieces will be described in chapter 7. But in the following, we do the examinations of the approximation ratio only for the MM2NTSP with equal weights of both kinds of edges as treated in Arkin et al. [7] and Chiang [23].

6.3.3. Computational Results

We also do computations for LS_MM2NTSP with the previously mentioned instances. The instances are grids of 2 to 19 rows and 2 to 99 columns and a set of examples of the TSPLIB. For each instance, we take two different initial orders, one time the enumeration of the nodes and the second time the approximate solution of the MSTSP. For the grids, we take the upper bound of theorem 6 being aware that they are in several cases greater than the optimal value. The upper bound for the instances of the TSPLIB is the shortest fourth longest incident edge of a node, a very general bound.

Nevertheless, $\alpha \geq 0.34$ for all solutions for the grids for the MM2NTSP. As for the grids the approximation ratio is identical for both initial orders, we only illustrate one of the two cases in figure 6.7, the average approximation ratio being less than 2 ($\alpha \geq 0.52$). in both cases. All tested grids with at least 10 rows have an approximation ratio smaller than 2.3 ($\alpha > 0.43$). Less than 2% of all tested grids has a greater approximation ratio than 2.5 ($\alpha < 0.4$).

For the TSPLIB instances, the approximation ratio is not as good as for the grids but at least for about 30% of the instances LS_MM2NTSP the solution is better than a 2-approximation ($\alpha < 0.5$) and less than 5% of the instances had an approximation ratio greater than 10 ($\alpha < 0.1$). The approximation ratio $\frac{1}{\alpha}$ is illustrated dependent on the number of nodes in figure 6.8. The computation times, solutions of LS_MM2NTSP and the inverse approximation ratio α are listed in tables D.3 and D.4 for an enumerated initial solution and in tables D.5 and D.6 with the approximation of the MSTSP as initial solution. For about 60% of the instances the enumerated initial order leads to a better approximation ratio, but the difference of the approximation ratio for the same instance with different initial orders is smaller than 1.9, i.e. the difference between two different values of α is at most 0.08. So we claim that the two different initial solutions yield similar results which are a first general approximation to the MM2NTSP but still need to be improved. Probably some progress could already be gained by decreasing the current upper bound. The current results do not retain the quality of the approximate algorithm for the MM2NTSP of Arkin et al. [7] and Chiang [23] which

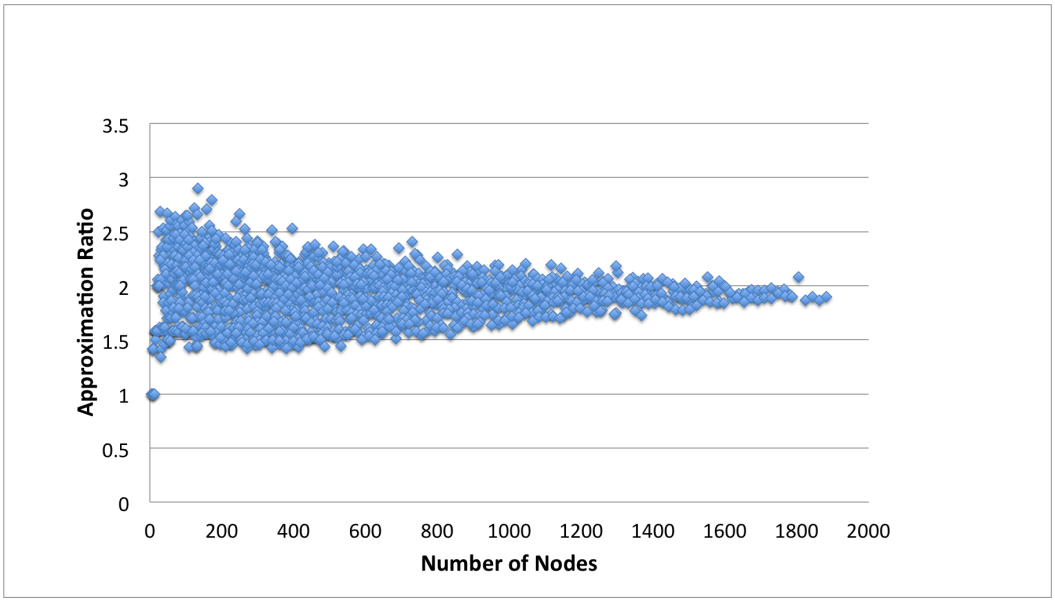

Figure 6.7.: Approximation ratio ($\frac{\text{Upper Bound}}{LS\_MM2NTSP}$) of LS_MM2NTSP for regular grids

is at least an 18-approximation in $\mathcal{O}(n^{2.5})$. But nevertheless, our procedure is rather general yet promising.

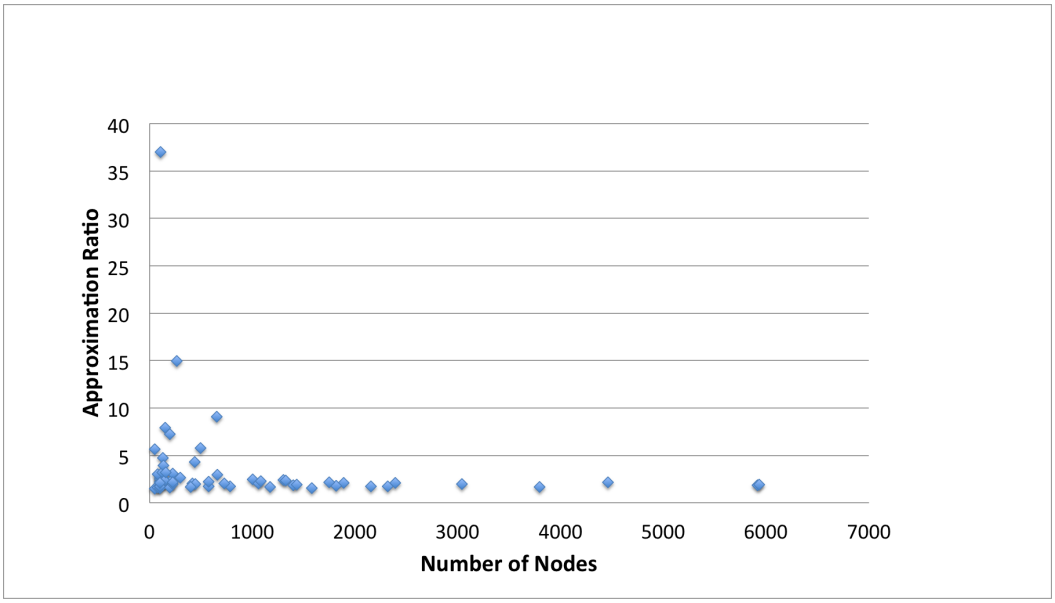

(a) Samples with trivial initial solution

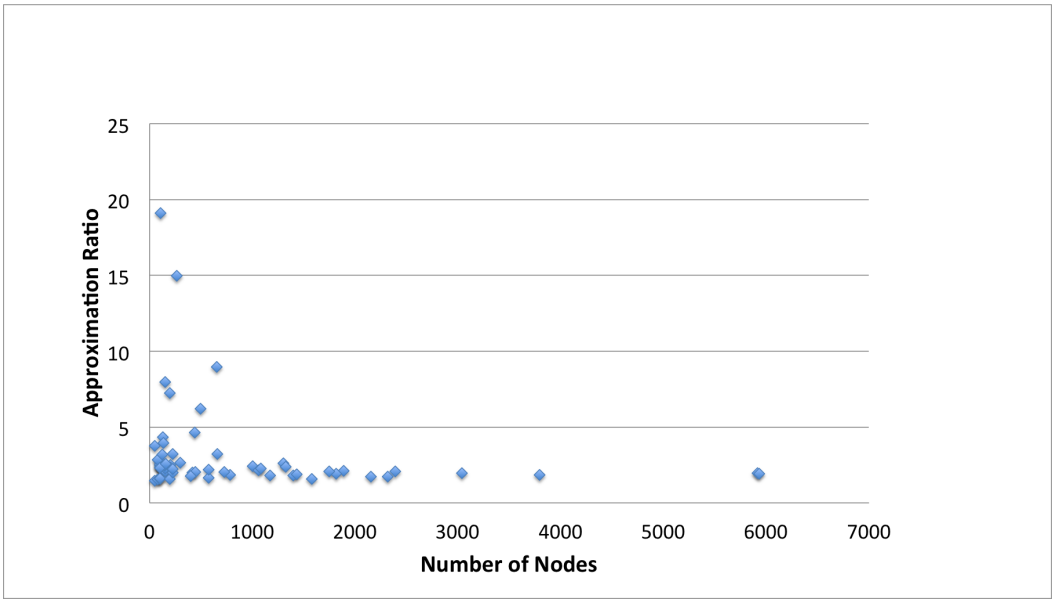

(b) Samples with initial solution from LS_MSTSP

Figure 6.8.: Approximation ratio ($\frac{\text{Upper Bound}}{LS\_MM2NTSP}$) of LS_MM2NTSP for samples of the TSPLIB

Algorithm 3 Local search heuristic for the MM2NTSP(LS_MM2NTSP)

Given: n vertices, initial order $(v_1, \ldots, v_n)$ (directed) and distances d_{ij}, maximum number of iterations MAXITER, weight c;
iteration counter $iter = 0$;

while $iter <$ MAXITER **do**

Find length of current shortest edge or 2-edge $\tilde{d}(v_{i_s}, v_j)$ and the position s of the first node v_{i_s} of that edge such that

$$\begin{aligned}\tilde{d}_{v_{i_s},v_j} = \min\{&\min_{k\in\{1,\ldots,n-1\}}\{d_{v_{i_k},v_{i_{k+1}}}\}, d_{v_{i_n},v_{i_1}},\\ &c\cdot d_{v_{i_{n-1}},v_{i_1}}, c\cdot d_{v_{i_n},v_{i_2}}, \min_{k\in\{1,\ldots,n-2\}}\{c\cdot d_{v_{i_k},v_{i_{k+2}}}\}\};\end{aligned} \tag{6.16}$$

Find an edge $(v_{i_t}, v_{i_{t+1}})$ for a $flip(v_{i_s+1}, v_{i_t})$ such that the following inequalities hold:

$$d_{v_{i_s},v_{i_t}} > \tilde{d}_{v_{i_s},v_j}; \tag{6.17}$$

$$d_{v_{i_{s+1}},v_{i_{t+1}}} > \tilde{d}_{v_{i_s},v_j}; \tag{6.18}$$

$$d_{v_{i_{s-1}},v_{i_t}} > \tilde{d}_{v_{i_s},v_j}; \tag{6.19}$$

$$d_{v_{i_s},v_{i_{t-1}}} > \tilde{d}_{v_{i_s},v_j}; \tag{6.20}$$

$$d_{v_{i_{s+2}},v_{i_{t+1}}} > \tilde{d}_{v_{i_s},v_j}; \tag{6.21}$$

$$d_{v_{i_{s+1}},v_{i_{t+2}}} > \tilde{d}_{v_{i_s},v_j}; \tag{6.22}$$

$$\tag{6.23}$$

if impossible to find such a set **then**
TERMINATE;
else
Execute a $flip$-operation (see figure 6.1);
Increment $iter$;
end if
end while

7. Tests and Results of CHAMP

In order to find out the advantages and disadvantages of certain scan strategies concerning the deflections, it was necessary to conduct tests on the LaserCUSING® machines. This chapter deals with the tests that were conducted in CHAMP. We introduce the geometries of the workpieces and summarize the setup of the tests. Moreover, we present the results and our conclusions.

7.1. Creation of the Data Transmission File for LaserCUSING®

The interface that we used to transmit the order of islands from different strategies and the control of the laser power to the LaserCUSING® machine was the Common Layer Interface (CLI) [21]. This interface is currently the only possibility to manipulate the island order. The files contain a header and a geometry part. In the header part, general information about the scaling, the version, and some settings as well as the different pairs of power and speed is given. After an extension of the interface during the project, the laser power and the laser speed can now be included into the file. In the geometry part, the lines of the contour (polyline) and the scan vectors (hatches) associated with the number of the current layer are listed. A hatch and a polyline can be a polygon of scan vectors. In order to create the CLI-file, all single vectors with their lengths have to be computed in advance. As many islands are only partly covered by the workpiece, there are different sizes and shapes of areas which have to be filled with scan vectors. Considering the orientation of the scan vectors in the current island, the individual length of the island is divided by the ideal distance between hatches. Thus, a fractional number of scan vectors is computed. This number is commercially rounded to the next integer. For this fixed number of hatches, an equal distance between all hatches of this island is computed. In a formula with d being the distance between two hatches and l being the length of the island with perpendicular hatches that distance is

$$d = \frac{l}{\left\lfloor \frac{l}{105} + 0.5 \right\rfloor}. \tag{7.1}$$

The number of hatches n is

$$n = \left\lfloor \frac{l}{105} + 0.5 \right\rfloor + 1. \tag{7.2}$$

The length of each hatch and the direction and length of the short connecting hatch between two longer hatches has to be computed with the help of trigonometric functions.

For the tests in CHAMP, each single workpiece was stored in a separate file. The files were put together at Concept Laser to build the workpieces in one turn. Most of our workpieces consisted of a small base and a tile. Support structures, additional long thin stripes of molten material between the tile and the base plate, stabilize those parts of the tile that are not seated on the base. There was a division of responsibility for the creation of the data for the workpiece. The CLI-file, which I generated, contains only the tile. The base and the support structures were conceived by Concept Laser and were added on the LaserCUSING® machine. The coordinates for the workpieces were fixed in advance such that the left upper corner always lay in the origin of ordinates.

During the project time, the interface was enhanced according to the needs identified in the tests. Currently, every scan vector has to be listed as a separate hatch. The disadvantage of the interface in the current version is that the size of the file grows quite fast and the machine cannot cope well with data greater than 35 MB. For example, listing each single scan vector in Workpiece 1 (100 and 121 islands with a height of 100) takes about 50 MB. As we kept a constant laser power in this test, we could combine several scan vectors to one hatch and thus, reduce the size of the data of this workpiece.

In the new extended version, different pairs of power and speed were applied to one vector. This meant, however, that a vector that should be split into pieces had to be listed twice with different indices. The indices were matched to a certain pair of power and speed. But as this was the only way to communicate with the machine, we had to write the files to be able to test certain strategies. For our purpose, the possible size of the CLI-file was a bound for the complexity and size of the workpieces and the number of levels of laser power. If some laser strategy was regularly applied in the production process, it would be encoded on the machine. However, for the tests this was not profitable. An example of a CLI-file is given in the appendix in section E.

7.2. The Workpieces

In this section, we consider the geometries of the workpieces produced during the project. As all scan vectors had to be computed by us in order to write the CLI-file, we had to choose rather simple geometries for our workpieces. That is why we chose only the following four workpieces to test different order strategies in consultation with Concept Laser. The areas are illustrated in figures 7.1 and 7.2. With the shift of the island grid, it is useful to create workpieces in which each layer has the same shapes such that the data is identical for every fifth layer. For the rectangular workpieces, there are in fact only two kinds of layers concerning the number of islands, the second to the fifth layer are the same except that the parts

of the island belonging to the workpiece are different. The effort of computing the scan vectors can be limited in that way. The first workpiece was chosen because of its simple geometry: it is just a block and was supposed to be a test for the procedure and the use of CLI-files. No measurements of the distortions have been performed for this workpiece as it was completely fixed to the base plate and thus did not have visible distortions at all.

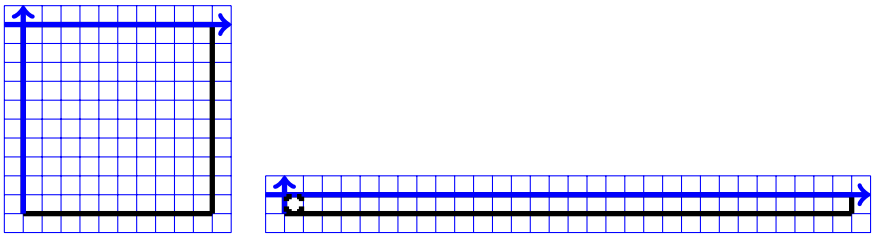

(a) Contour 1 (b) Contour 4 with base (dotted)

Figure 7.1.: The rectangular workpieces

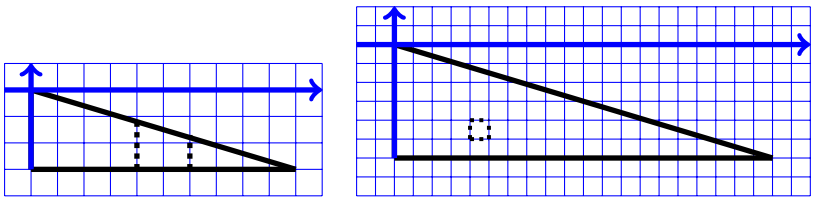

(a) Contour 2 with base (dotted) (b) Contour 3 with base (dotted)

Figure 7.2.: The triangular workpieces

The following workpieces were put on a base whose contour is drawn in figures 7.1 and 7.2 with dashed lines (see figure 7.2). Below the part without base, support structures were put. The support structures are long thin stripes of material connecting the workpiece partially to the base plate. They are removed after the production. The generation of the base and the support structures was done by an employee at Concept Laser as explained in section 7.1. The second workpiece (figure 7.2(a)) was a triangle with one sharp corner and a base in the middle of the length of the workpiece. In Workpiece 3 (figure 7.2(b)), the triangular contour had a larger area and the area of the base was decreased at the same time in order to facilitate the formation of greater distortions and to better distinguish between different order strategies. For the same reasons the last workpiece (figure 7.1(b)), a very long but narrow shape, was chosen. The exact number of islands per layer and the number of layers are listed in table 7.1.

Workpiece	Height[layers]	Area	Islands (I) per layer
Workpiece 1	100	10×10	Every 5th layer: 100 I, the others: 121.
Workpiece 2	$200 + 100$	10×3	In turns: 21, 27, 28, 30 and 31 I.
Workpiece 3	$200 + 100$	20×6	In turns: 72, 83, 85, 89 and 91 I.
Workpiece 4	$200 + 100$	30×1	Every 5th layer: 30 I, the others: 62.

Table 7.1.: Overview on all workpieces

7.3. Tests of the Strategies on Workpieces

During the project, several tests of strategies were conducted on the LaserCUSING® machine. The data transmission was tested with Workpiece 1 in Test 1. In the second test Workpiece 2 was produced and the distortions were measured. As the distortions were not significantly different for several strategies and were also very small, the geometries of Workpieces 3 and 4 were chosen for further tests. As the first two tests did not yield results, but were the preliminary tests of the approach, they are summarized in section 7.3.1. In the third test several samples of Workpieces 3 and 4 were produced (section 7.3.2). The measured deflections, which were not significant, made us choose a two-part final test. On the one hand, we wanted to ensure that there is no significant influence of the island order on the deflection (section 7.3.3); on the other hand we produced samples with different tour lengths where the tour is composed of the distances between consecutive islands and not the lengths within one island. For these samples we measured the scanning time of single layers (section 7.3.4) in order to test if time saving is possible.

7.3.1. Test 1 and 2

The goal of the first job (Workpiece 1) was to test the application of the CLI and to find out if there were problems in understanding or in transmitting data. The workpiece was built with four different strategies. It completely connected to the base plate and we did not measure the distortions. The height of the workpiece had to be reduced enormously – from 666 to 100 layers – in order to reach a suitable file size.

Therefore, the next workpiece had a smaller area with fewer islands and was built on a base to receive some distortions. Normally, one step in the production is to place the workpiece in an optimal way such that the area connected to the base plate is as large as possible and the angles between the perpendicular line to the baseplate and the workpiece are as small as possible. In our tests, this step was omitted to obtain greater distortions and to better see differences between different strategies. In the second test, Workpiece 2 was built eight times with the following strategies:

1. MSTSP;
2. MM2NTSP;
3. TSPSID;
4. Serial order in horizontal lines without meandering;
5. Random order;
6. Serial order in horizontal lines with meandering;
7. Serial order in vertical lines without meandering;
8. Serial order in vertical lines with meandering.

Meandering means continuing the strategy in reverse direction at the end of each line, e.g. left-to-right in the first line, right-to-left in the second line and so on for serial order in horizontal lines with meandering. The number of islands per layer were 21, 27, 28, 30, 31 in turns because of the shift of the grid. The solutions of the MM2NTSP were always approximated with LS_MM2NTSP described in section 6.3, because the computation of the exact solution by solving an Integer Program (IP) would have taken too long. However, approximated solutions are sufficient for this test. The starting tour for the algorithm was the solution of the MSTSP.

After the production process, the support structures were disconnected from the base plate such that the workpieces were only connected to the working platform via their base. At Concept Laser, the distance between the base plate and the top level of the workpiece was measured by a vernier height gauge at four points (see figure 7.3) to determine the distortions. The differences in height at the measuring points were $0.9 - 1.5\%$ of the planned height of the workpiece. As the rank order of heights of the workpieces was completely different at every measuring point, it was not possible to rank the quality of the strategies. Unfortunately, the height had not been evaluated at any reference point above the base and the measuring points had not been coordinated with the project partner. The need of a reference point was communicated for the following workpieces. We did not catch up on the missing reference point in Workpiece 2 as another measurement method would have been necessary and the quality of the strategies could not be specified anyway.

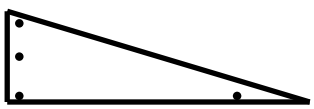

Figure 7.3.: Measuring points on Workpiece 2

7.3.2. Test 3

In addition to a reference point, it was important to have more than one sample of each strategy. As both production time and material were limited, we decided to have at least two samples of each strategy and each following workpiece with a random assignment of position.

The third and the fourth workpiece were designed to receive greater distortions within the workpieces so that we would be able to distinguish the quality of different strategies. Workpiece 3 has twice the length and width of the area of Workpiece 2, but a smaller base and therefore more support structures. The order of islands in the strategies differed more due to the number of islands being much greater than in the second workpiece. As the base was quite small (see figure 7.2), we expected more obvious distortions. A fourth workpiece of a very simple geometry – a base of one island and an array of 30 islands (see figure 7.1(b)) – was chosen to keep out various additional effects and to allow us to observe mainly the distortions in one direction.

In Workpieces 3 and 4, the measuring points were fixed along the long side at equidistant nodes which are illustrated in figure 7.4.

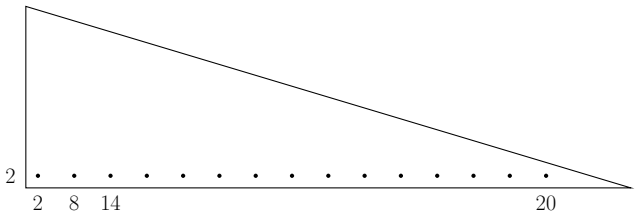

(a) Measuring points on Workpiece 3

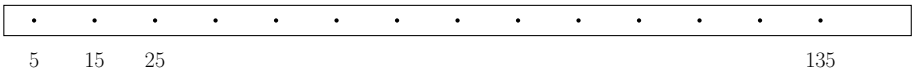

(b) Measuring Points on Workpiece 4

Figure 7.4.: Positions of the measuring points in Workpieces 3 and 4 [mm]

However, the results differed immensely from what we expected. There were greater distortions in the new workpieces indeed, but they did not show significant differences for any strategy.

Workpiece 3 was built 14 times with the following seven strategies

1. MSTSP;
2. MM2NTSP;
3. TSPSID;
4. Random order;

5. Serial order in horizontal lines with meandering;

6. Serial order in vertical lines with meandering;

7. MM2NTSP with a short break after each island.

The last strategy was added in order to get samples in which the heating of the previous islands has as little influence on the heat in the workpiece as possible. Like this, we sought to cover all kinds of strategies. On the one hand, this includes the heating of islands in lines with a great influence of the heat in the surrounding islands. On the other hand, we used a strategy where the heating of the surrounding islands should already have spread enough to have a similar situation like at the beginning of a layer. The MM2NTSP ensures that none of the nearby islands is the predecessor and because of the break there is more cooling time between the heating intervals. The break was implemented by a jump delay. Usually this delay is used for time intervals of less than $1ms$, where it can be set very precisely. For our purposes, we increased the duration of the delay as much as possible in order to get the longest possible break between the heating of two islands. The maximum jump-delay is a little less than $1s$.

The arrangement of seven samples of Workpiece 3 on the plate is illustrated in figure 7.5. There were two base plates on which two samples of each strategy were randomly allocated. After the building process, the support structures were

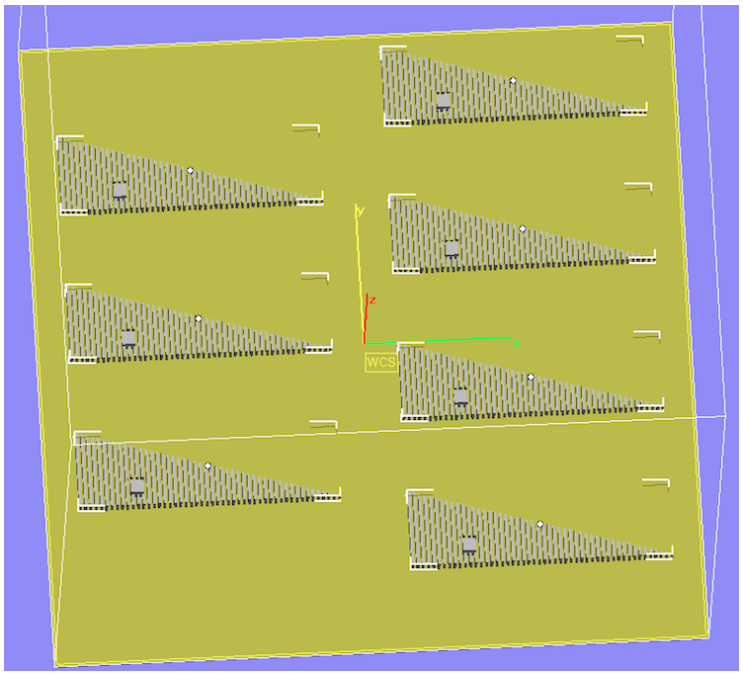

Figure 7.5.: Arrangement of the samples of Workpiece 3 [Concept Laser GmbH]

disconnected from the working platform by wire cutting. That is why the samples had to be positioned in columns. Only the stripe containing the base remained fixed to the base plate. Unfortunately, the company charged by Concept Laser to do the wire cutting, disconnected at the wrong positions in one column with three samples. Therefore, in the workpieces of this column the distortions are not representative for the according strategies. The measuring was performed by a partner of Concept Laser with a 3D scanner, a Gom Atos Core 300.

Leaving out the three defective pieces, the differences between the reference point above the base and the measuring point on the right side were the ones listed in table 7.2.

Strategy	Abs. D [mm]	Rel. D [%]	Max. V [%]
TSPSID	8.9	98.6	0.6
MM2NTSP	8.6	95.4	0.2
Slowly 2-Nb.	9.0	99.8	0.9
Random	8.9	98.6	0.6

Table 7.2.: Average distortions and differences of distortions at the right hand side of the samples of Workpiece 3 (D = distortion, V = variation)

The strategies where both samples were cut off correctly showed a difference in the average distortions of less than $0.4mm$, that is 4.4% of the ideal height of the workpiece. The difference of distortion within one strategy was between 0.2% and 0.9%.

As we can see in figure 7.6, the distortions of the samples which were not cut correctly are completely different as the reference point is at a different position. In order to be able to consider the three defective workpieces as well, we computed the angle between the left end and the right end of a workpiece and for all samples of one strategy the average angle. The average angle for each strategy was in the same order of magnitude, which can be gathered from table 7.3.

Strategy	MSTSP	MM2NTSP	TSPSID
Av. Angle[°]	6.9	7.0	6.7
Horiz. Line	Vertic. Line	Slowly	Random
7.1	6.8	6.7	6.7

Table 7.3.: Average angle in Workpiece 3

Even those samples with completely different strategies – like the ones with serial order in horizontal direction and samples with breaks in the heating – hardly varied

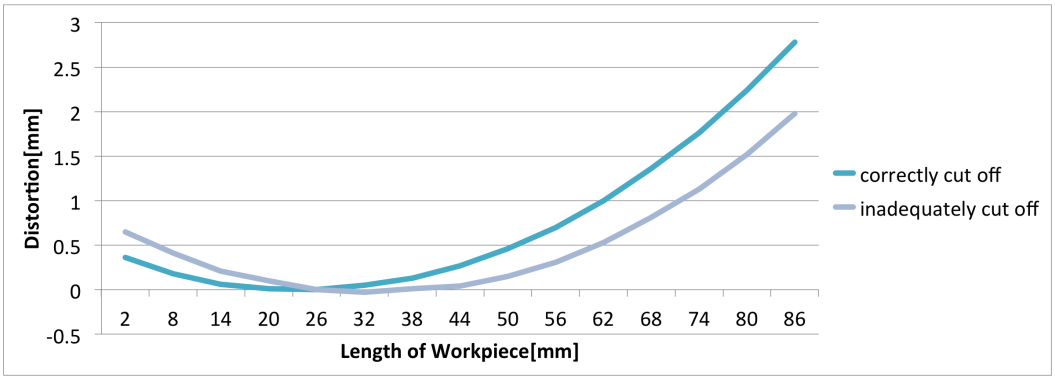

Figure 7.6.: Different profiles in Workpiece 3 after cutting the samples off

in distortions. Therefore, we suspected the order of island to only have a non-relevant influence on the distortions. One possible explanation for that could be that the island order might have been too similar for the different strategies. In order to disprove this, we evaluated the different objective functions for each of the solutions. For every different kind of layer – that means five for the third workpiece – we evaluated the solution of the MSTSP, the MM2NTSP and the TSPSID. We do not mention the evaluations of the orders of the horizontal lines in tables 7.4, 7.5, 7.6, 7.7, and 7.8 as they are virtually the same as for the vertical lines. For the random order it was not possible to evaluate one order, thus we omitted it. As the values for each objective function differed significantly for different island orders, we can assume that the orders themselves are also different. Only the solutions of MSTSP and TSPSID have similar objective values. As the idea of those two optimization problems is similar, also the objectives do not differ very much.

Solution	Objective Value		
	MSTSP	MM2NTSP	TSPSID
MSTSP	33.541	7.5	44414.9
MM2NTSP	21.2132	21.2131	62248.7
TSPSID	32.0156	7.5	39388.6
Vertic. Line	5	5	2.7801e+06

Table 7.4.: Objective values for 72 islands

In Workpiece 4 similar strategies were tested but as the solution of the MSTSP problem coincided at least in one layer with the solution of the TSPSID, only the former was tested. Furthermore, the vertical and horizontal lines of islands would also nearly coincide, thus were summarized in the horizontal lines. Ten samples

Solution	Objective Value		
	MSTSP	MM2NTSP	TSPSID
MSTSP	38.0789	7.5	42364.7
MM2NTSP	25	23.7171	63892
TSPSID	36.0555	7.5	39358.5
Vertic. Line	5	5	3.24009e+06

Table 7.5.: Objective values for 83 islands

Solution	Objective Value		
	MSTSP	MM2NTSP	TSPSID
MSTSP	38.0789	7.5	41547.4
MM2NTSP	25.4951	25.4951	59948.8
TSPSID	36.0555	7.5	39991.8
Vertic. Line	5	5	3.28009e+06

Table 7.6.: Objective values for 85 islands

were built one beneath the other on one base plate. There were two samples of each of the following strategies whose position on the plate was randomly chosen:

1. MSTSP;
2. MM2NTSP;
3. MM2NTSP with a break after each island;
4. Random order;
5. Serial order in horizontal lines without meandering.

Table 7.9 lists the samples with increasing numbers from the top to the bottom of the working platform.

After the building process and the cooling, the samples were partially removed from the plate by wire cutting from the right side. Only the island on the left with the base below it remained fixed to the working platform. As can be seen in figures 7.7 and 7.8, there were clearly visible distortions. The numbers of the samples in the figures are referring to table 7.9. The distortions are normalized, meaning that the distortion of 0 implies that the measuring point has the same height as the reference point on the base, which is not necessarily the planned height of the workpiece. Considering the distortions of all samples, we see that two values of distortions differ at most 9.9% of the planned height of a workpiece, but

Solution	Objective Value		
	MSTSP	MM2NTSP	TSPSID
MSTSP	38.0789	7.5	43636.8
MM2NTSP	25	25	69600.7
TSPSID	36.0555	7.5	40158
Vertic. Line	5	5	3.4201e+06

Table 7.7.: Objective values for 89 islands

Solution	Objective Value		
	MSTSP	MM2NTSP	TSPSID
MSTSP	39.0512	7.5	43827.3
MM2NTSP	28.2843	27.0417	60461.5
TSPSID	36.0555	7.5	40805.9
Vertic. Line	5	5	3.56009e+06

Table 7.8.: Objective values for 91 islands

the distortions are at least 93.7% of the planned height of a workpiece. In table 7.10, the average distortions and the relative difference of distortions are listed for each strategy. Because of these great heights at the right end of the workpiece with only little differences according to the strategies, we assumed that the distortions are not dependent on the order of the islands. Furthermore, this assumption is based on the outcome that the distortions of workpieces with completely different strategies, such as the MM2NTSP with breaks and the serial heating of the islands, do not remarkably differ. This proposition was confirmed by the final test which is described in the following.

7.3.3. The Final Test I – Distortions for Different Strategies

The final test was solely performed on samples of Workpiece 4. In the part of the final test in which the non remarkable influence of the island order on the distortions should be ensured, six samples were produced for each of the chosen strategies and were placed randomly on three plates.

The following strategies were tested:

1. MM2NTSP;
2. Random order;
3. Serial order in horizontal lines without meandering;

Pos.	Strategy
1.	MM2NTSP
2.	MM2NTSP with breaks
3.	MM2NTSP
4.	Serial order
5.	MSTSP
6.	Random order
7.	MSTSP
8.	Serial order
9.	Random order
10.	MM2NTSP with breaks

Table 7.9.: Positions of the samples of Workpiece 4 in the working space

Strategy	Abs. D [mm]	Rel. D [%]	Max. V [%]
MSTSP	8,9	98,6	3,1
MM2NTSP	8,6	95,4	3,4
MM2NTSP with Breaks	9,0	99,8	7,4
Random Order	8,9	98,6	1,3
Serial Heating	9,0	99,6	1,0

Table 7.10.: Distortions and its variations at the rim of Workpiece 4 referring to the height of the workpiece (D = distortion, V= variation)

4. MM2NTSP in combination with a control of the laser power;

5. Random order in combination with a control of the laser power.

As similar strategies had been examined in earlier tests and we wanted the final test to consist of several samples of each strategy, we had to reduce the number of strategies. Therefore, we decided for one optimization strategy, the solution of the MM2NTSP, which seemed to yield slightly less deflections in Workpiece 4 than the other optimization strategies. Moreover, we included the random order, and one trivial strategy, the serial order, into the final test. As the second part of the project concerned the control of the laser power, we decided to take samples for which only the new control of the laser power was applied – the order of the islands being randomly chosen. Other samples were taken whose strategy was a combination of an optimization strategy and a power control. Some more details about the control of the laser power can be found in appendix A.

The distortions of the workpieces are visualized in figures 7.9 and 7.10. There are ten samples on each plate, one below the other. Each sample got a number

Strategy	Abs. D [mm]	Rel. D [%]	Rel. Max. V [%]
Random order	8.71	96.8	4
Serial order	8.84	98.2	6.1
MM2NTSP	8.52	94.7	3.9
PWR+Random order	8.78	97.6	7
PWR+ MM2NTSP	8.74	97.1	2.9

Table 7.11.: Average distortions at the rim of Workpiece 4 in the final test referring to the height of the workpiece (Plates 2-4, D=distortions, V=variation, PWR=control of the laser power)

according to its position, the first digit naming the plate and the others the position on this plate (e.g. 302 is the second sample on the third plate). The plates have the numbers 2, 3, 4. Plate 1 contains the workpieces of the second part of the final test (see section 7.3.4).

The distortions were at least 92.3% of the planned height of the workpiece. The average distortions for the different strategies as well as the variations of the distortions are listed in table 7.11. The difference between the smallest and the greatest distortion in any workpiece was 9.7% of the original height of the workpiece, that is about the same size as the variations within single strategies. So we concluded from our tests that neither the order of the islands nor the control of the laser power visibly influences the distortion of a workpiece made of CL20 ES and probably as well for different kinds of steel.

figure 7.11 gives an idea of how the working platforms with the samples looked like after removing the support structures from the platform.

7.3.4. The Final Test II – Variation of the Tour length

As neither the control of the laser power nor the order of the islands had an influence on the distortions, we shifted our focus on different objectives. The control of the laser power influences the quality of the surface. The examinations about the surface are considered in the Technical Report of CHAMP [13] and briefly in appendix A. Concerning the order of islands, we decided to reduce the length of the tour of the laser by shortening the distances between consecutive islands. We solve a TSP containing the distances between the centers of the islands. For sensitive materials or very complicated geometries with very little connection to the base plate, small edges can be excluded, i.e. the TSPN has to be solved for some minimum edge length. For a small minimum edge length, the tour within one layer is much shorter than the average tour of the current production. In the final test, we wanted to measure the impact of the length of the tour on the production times. The samples of Workpiece 4 for which the scanning time had to be measured were placed on a separate plate as the measurement took place at one single day

and more than one plate a day would not have been practicable. The cases that we considered were optimal tours with a minimum edge of $10mm$, $20mm$, $30mm$, $40mm$. Actually, the laser move between the islands is a path within one layer, but we computed a tour and started at about the first and last node of the tour in the following layer. Like this, the computations were easier to implement than the path version and are still sufficient to our purpose.

We compared the lengths of the tours with a restricted edge set to the average length of a random tour. A relatively easy way to compute this average length is introduced in appendix F. As we were not sure whether the expected value would reflect the tour lengths, we computed the lengths of 300 random tours part of which were taken for the reference workpieces built with a random order. There were 60 samples of a rectangle with 30 islands on a line and 240 with two rows and 31 columns reflecting the ratio of layers in the workpiece. For this set of sample orders, we computed the average deviation of the length from the expected value. The average deviation from the expected value was 7.8% for the layers with 30 islands and 5.8% for the layers with 62 islands. More than 60% of the tours with 30 islands and more than 80% of the tours with 62 islands had a deviation of less than 10%. The results of this computation can be found in table 7.12. Thus, in our samples the random tours had a length close to the expected value.

Number of islands	30	62
Average deviation [%]	7.85	5.75
Max deviation [%]	23.87	22.21
Layers with dev. < 0.05 [%]	33.3	52.9
Layers with dev. < 0.1 [%]	66.7	82.9
Layers with dev. < 0.2 [%]	96.7	99.2

Table 7.12.: Deviation of the length from the expected value of the random tours

The optimal tours with a minimum edge length were computed with Concorde [6]. We set the small and forbidden edges to a large enough value. Computing the average length of a random tour for both kinds of layers (see section F) and comparing it to the lengths of the resulting tours computed by Concorde, we see that the lengths are approximately 20%, 40%, 60% and 90% of the average length of a random tour considering the distances between the islands. Regarding the lengths of the tours, only the distances between the centers of consecutive islands are considered, the scanning path within the islands is neglected even though it is the most time consuming part. The speed of movement of the laser between islands is between $4100\frac{mm}{s}$ and $4200\frac{mm}{s}$. The lengths are listed in table 7.13 and illustrated in figure 7.12.

Two samples of each strategy – including the random order as well – were put in a random position on the plate (see table 7.14). I spent a day at Concept Laser

Length of the tour:

Shortest edge	10	20	25	30	40	ALRT[mm]
Layer of 30 I	330	680	860	1040	1400	1550
Layer of 62 I	663,78	1346,15	1645,94	2102,48	2704	3271,87

Length of the tour related to ALRT:

Shortest edge	10	20	25	30	40	ALRT[mm]
Layer of 30 I	21,29%	43,87%	55,48%	67,10%	90,32%	1
Layer of 62 I	20,29%	41,14%	50,31%	64,26%	82,65%	1

Table 7.13.: Length of the tours of plate 1 (ALRT = average length of random tours, I=islands)

Pos.	Strategy
1.	Random order
2.	Shortest edge 40
3.	Shortest edge 30
4.	Random order
5.	Shortest edge 20
6.	Shortest edge 30
7.	Shortest edge 10
8.	Shortest edge 20
9.	Shortest edge 40
10.	Shortest edge 10

Table 7.14.: Position of the workpieces on plate 1 in the final test

GmbH and measured the duration of 55 layers of each sample using a stop-watch. I distinguished between the five different types of layers due to the shift of the grid from layer to layer. The first type of layer has only 30 islands, all others have 62, but the island sizes differ. There are ten to twelve measurements of each layer.

Taking the time was very difficult as it required a very fast response time and sometimes it was hard to determine the exact moment when the layer of one sample was finished just by watching. Particularly the duration of the first (and the last) sample tends to be too long (too short respectively). But as the arrangement of the samples on the plate was chosen randomly and there were two samples of each strategy, the results are representative. Occasionally, technical problems occurred, for example in case I did not push the button at the change of a sample, took too long to push it or did not see the termination of the workpiece. This resulted in some erroneous measurements in nearly every kind of layer. Those values were sorted out, but we still had at least nine values for each kind of layer of each sample of which we took the average value (see figure 7.13). The samples are sorted in such a way that those of the same strategy have similar colors and are placed beside each other. The x-axis goes from the random tour to the tour with the longest minimum edge to the tour with the shortest minimum edge.

Between every two layers, some time is needed to spread a new powder layer on the working space, which I did not measure. It is about 15 to 30 seconds. This time is rather constant as it is always the same amount of powder and the same movements of the coating blades. What I measured was the scanning duration of one layer of one sample, involving the time of scanning of the islands, the moves between consecutive islands and the scanning of the contour.

Considering the production times we see that the difference within one layer is at most 2 seconds, but a slight decline in the scanning time is recognizable for strategies with shorter tours. In figure 7.13, one can see that for the second to the fifth layer the decline is steeper than for the first layer, which can be explained by the smaller number of islands in that layer. The greater the number of islands and the more they are spread in the working space, the more optimization strategies can differ from random tours and this seems to be the case here after our first test. The very strong decline for sample 10 could possibly be explained by the error in measurement at its position, but sample 7, which is produced by the same scanning strategy, has a remarkably smaller scanning time as well. To determine whether the order of the islands can be relevant to the production time, we computed the relative scanning time of the layers compared to the average scanning time of samples with random order. Not skipping the first and the last workpiece, we get a decrease of $3 - 5\%$ for the strategy with a shortest edge length of 10. When we skip the first and the last sample, there is still a decrease of $2.8 - 5.4\%$. Of course, we may not forget the constant time required to renew the powder surface, but a reduction of the scanning time that is around $4 - 5\%$ is desirable for our project partner Concept Laser.

Having compared the duration of the production process, we should keep in

mind that it has to be made sure that the quality of the workpiece concerning the distortions does not deteriorate. In table 7.15, the distortions of the samples are listed and they are visualized in figure 7.14. The dimension of the distortions is the same as for the other samples of Workpiece 4 and there are no significant differences for different strategies.

Strategy	Abs. distortions (mm)	Rel. distortions (%)
Min. edge 10	9,1	101
Min. edge 20	9,07	101
Min. edge 30	8,85	98,3
Min. edge 40	9,13	101
Random order	8,89	98,7

Table 7.15.: Average distortions at the free end of the workpieces on plate 1

7.4. Results

Concerning the results of CHAMP, the following needs to be mentioned. According to our tests, there is no significant impact of the order of the islands and the control of the laser power on the distortions of the workpieces in the LaserCUSING® process. This is contrary to the original hypothesis. However, there were strong hints that a control of the laser power can improve the quality of the workpiece's surface (see appendix A). Furthermore, the travel length of the laser between the islands can be diminished rigorously, such that a reduction of the production time can be achieved without increasing distortions. The shorter distances can also lead to a better preservation of the machines and abrasion can be decelerated.

The results were surprising for us and Concept Laser. To our knowledge, no one else had stated this before. As we only occupied one alloy of steel, we do not make any assumptions on whether the order of islands influences the distortions when other materials are used. If this were the case, we suppose that a focused heating in one region would deteriorate the quality of the workpiece. Therefore, we propose the invention of geometry- and material-depending minimum distances between consecutive islands which have to be considered when the tour of the laser is determined.

Even though Concept Laser did not immediately implement the new results in their machines, the results will influence further research and some aspects of the control of the laser will indirectly appear in further software. Particularly for the idea of shortening the tour of the laser will also have an effect on the further development.

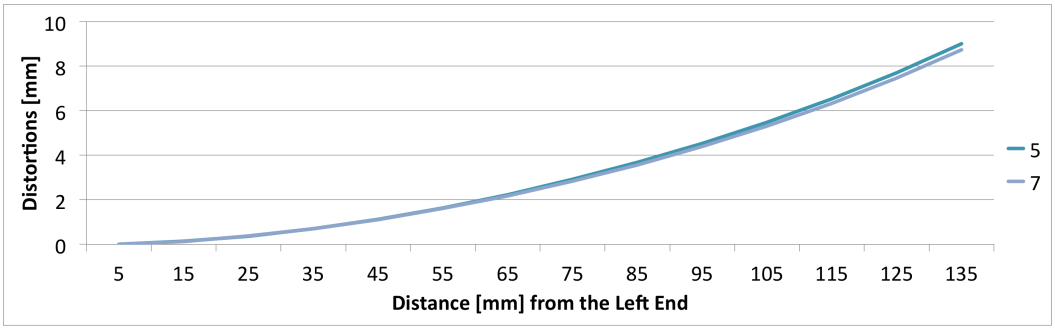

(a) MSTSP

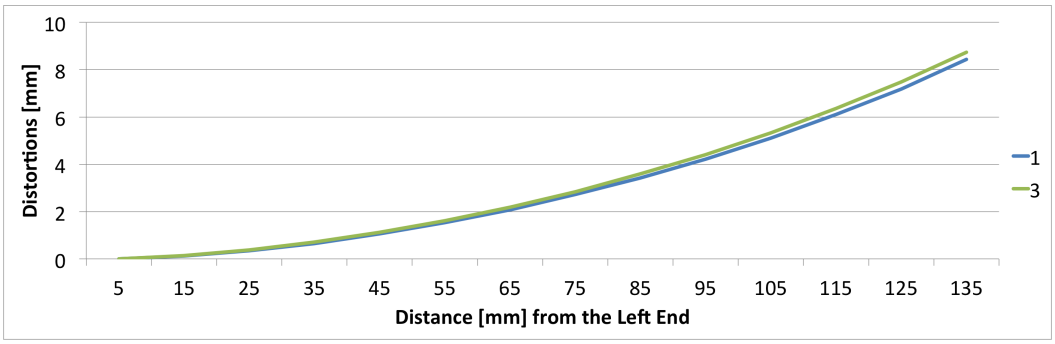

(b) MM2NTSP

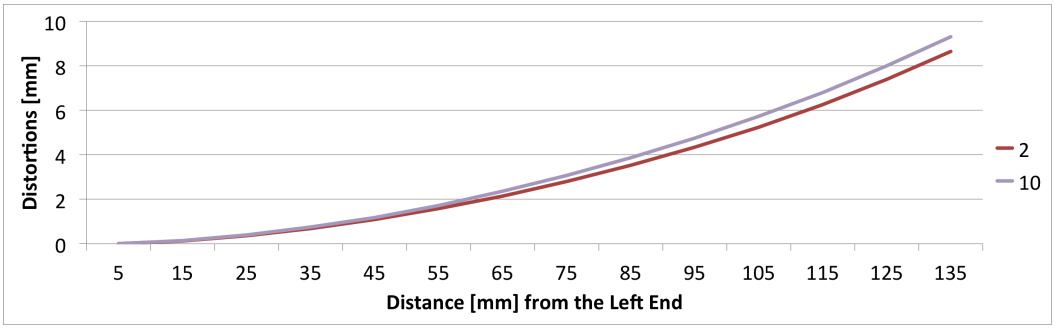

(c) MM2NTSP with breaks

Figure 7.7.: Distortions in Workpiece 4 for the optimization strategies

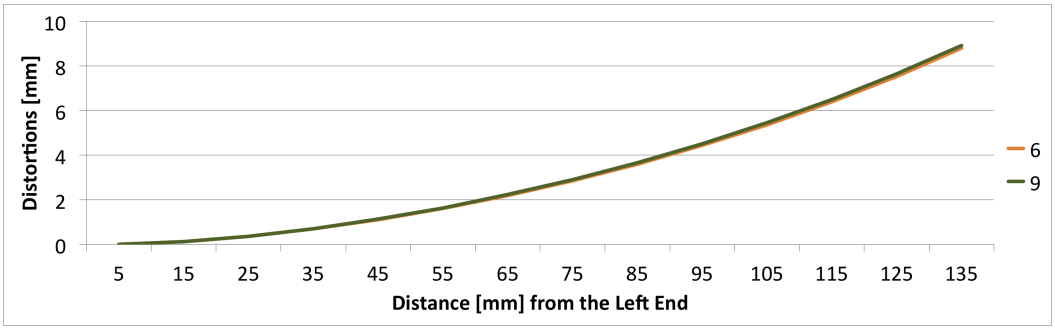

(a) Random order

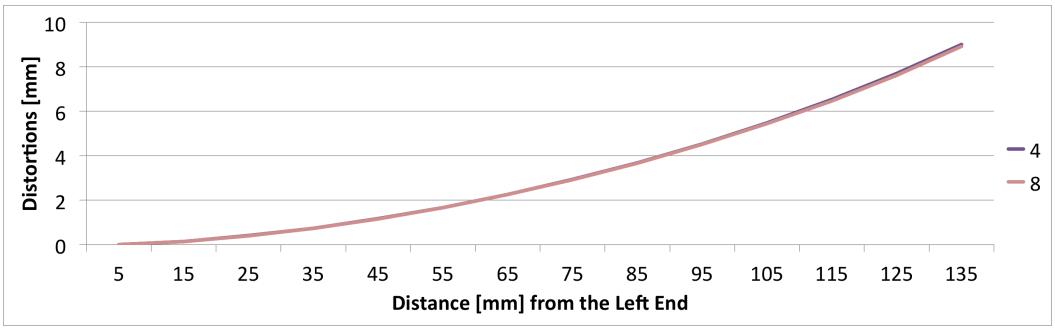

(b) Serial order

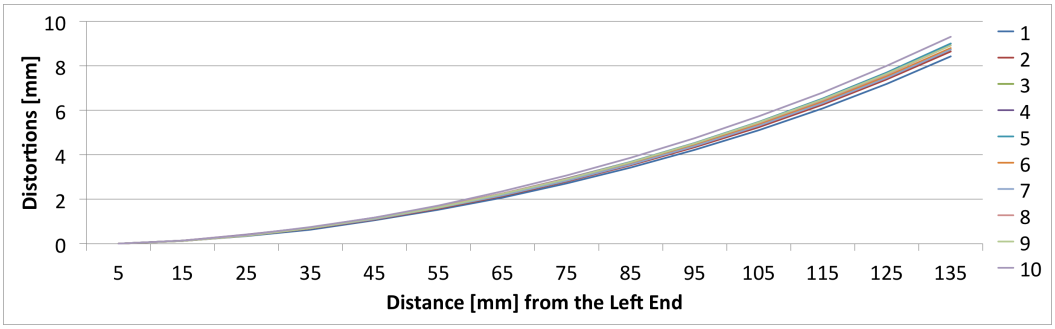

(c) All strategies

Figure 7.8.: Distortions in Workpiece 4 for random and serial orders and all samples

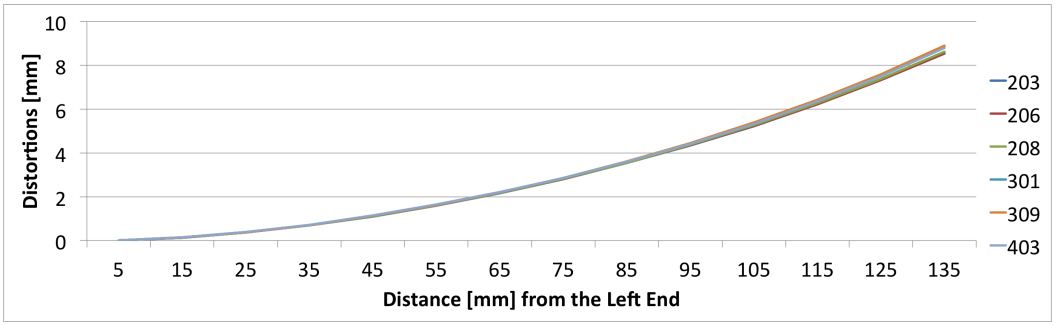

(a) Random order

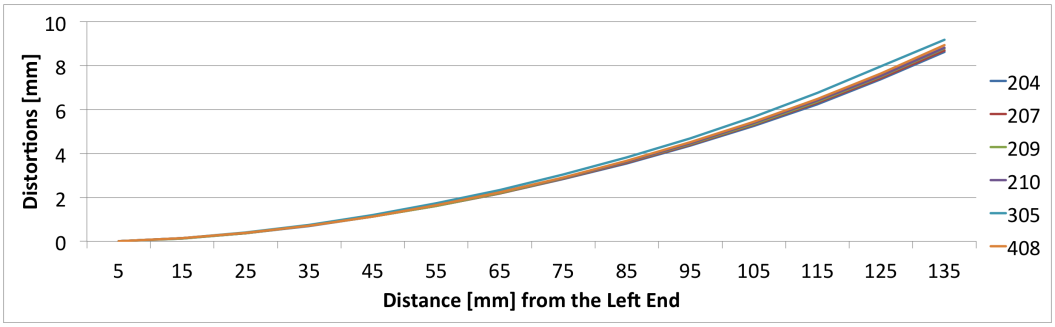

(b) Serial order

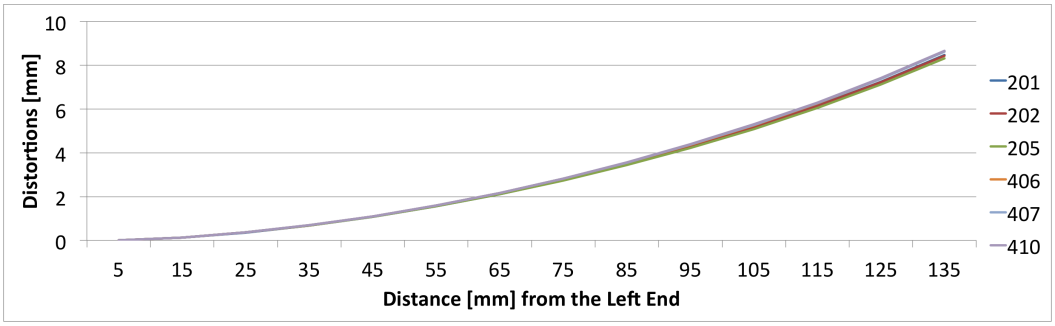

(c) MM2NTSP

Figure 7.9.: Distortions in the samples with different order strategies in the final test (plates 2-4)

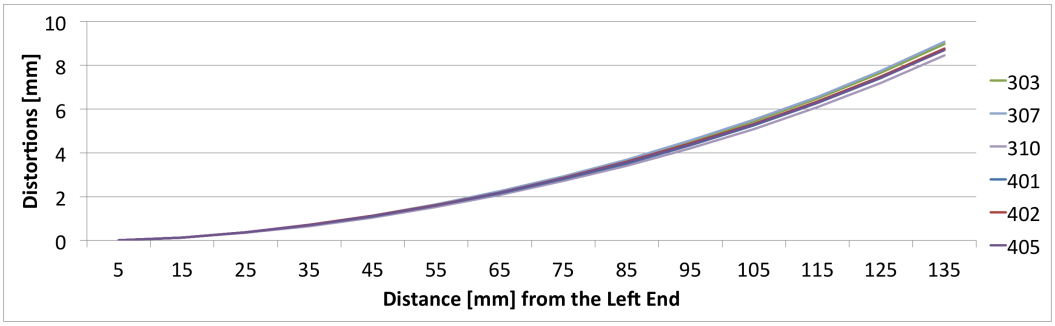

(a) Control of laser power with random order

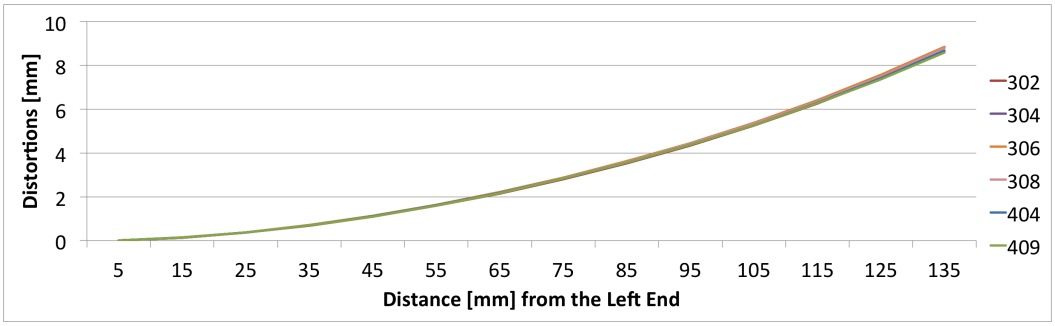

(b) Combination of control of laser power and MM2NTSP

Figure 7.10.: Distortions in the combined samples in the final test (plates 2-4)

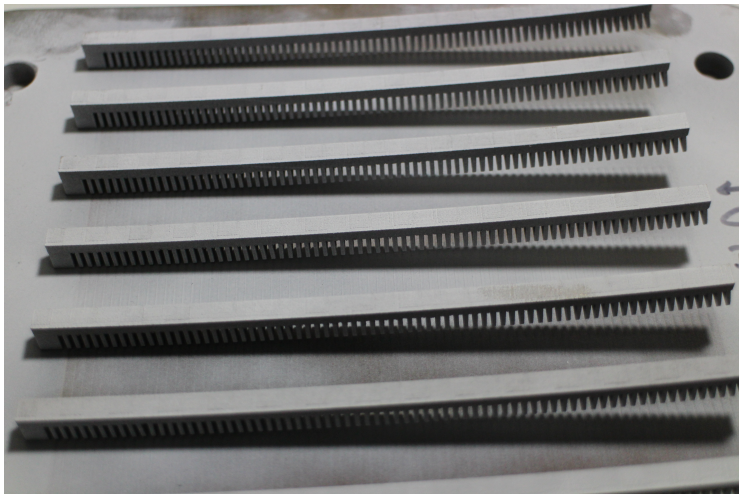

Figure 7.11.: Image of a working platform from the final test

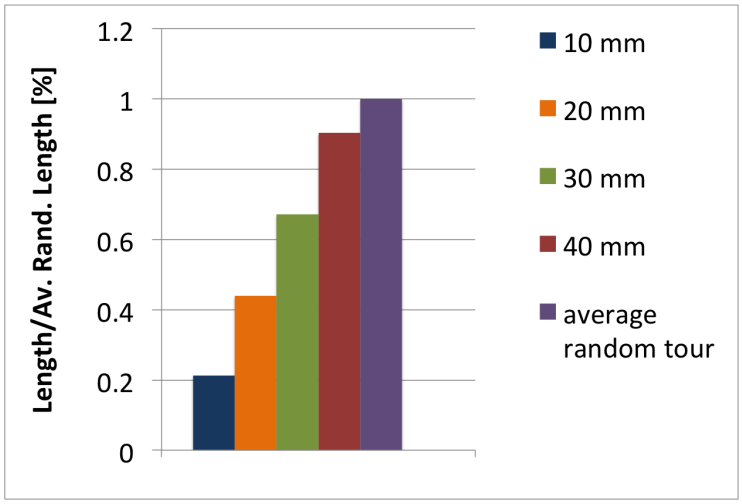

(a) Layer 1

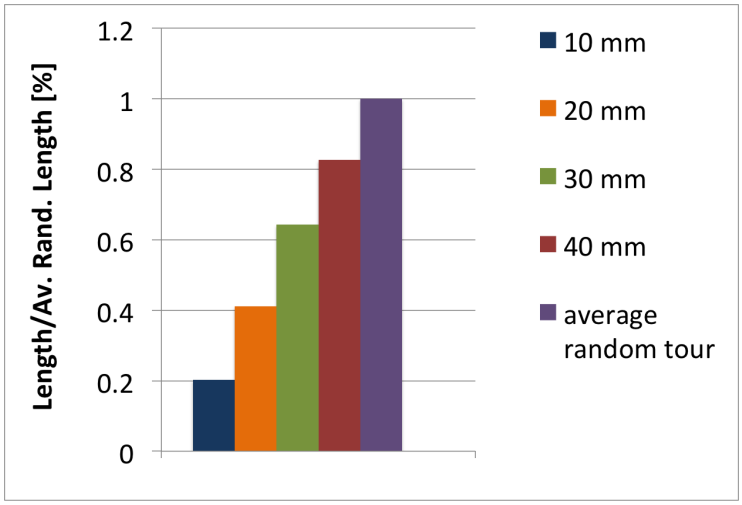

(b) Layer 2-5

Figure 7.12.: Tour length in the final test (plate 1) compared to ALRT for different minimum edge lengths

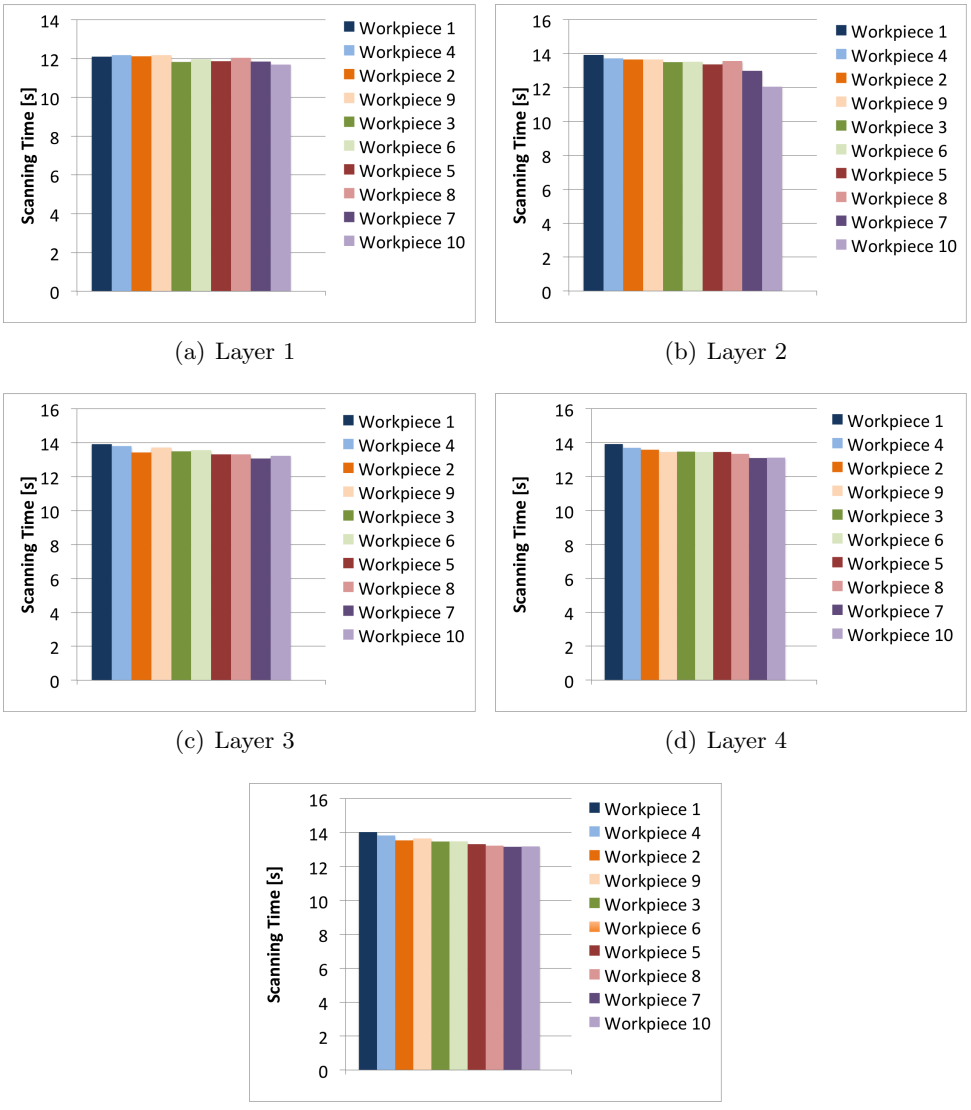

(a) Layer 1

(b) Layer 2

(c) Layer 3

(d) Layer 4

(e) Layer 5

Figure 7.13.: Average measurements of the scanning time in different layers

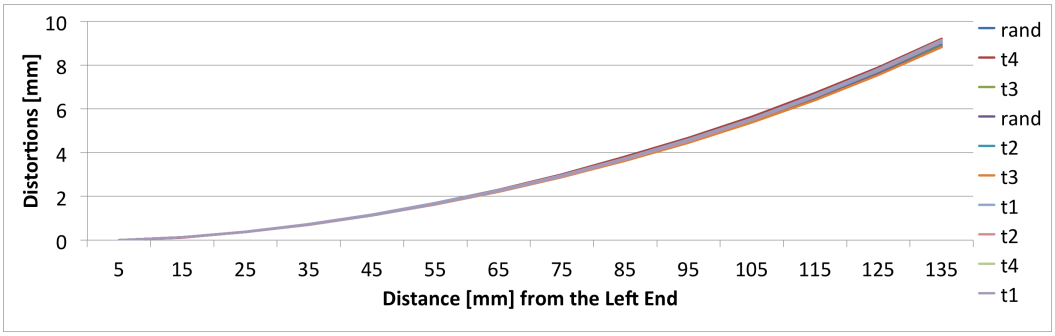

Figure 7.14.: Distortions within the workpieces on plate 1

8. Conclusion

We will now summarize the results which were gained in this work. On the one hand, we yielded exact and approximate solutions for the MSTSP on a regular grid and upper bounds as well as an approximation for the MM2NTSP. On the other hand, we gained practical results for additive manufacturing regarding good scan orders of the islands. Let us first start with the achievements on the MSTSP and the MM2NTSP. We have deduced a linear-time combinatorial solution to the MSTSP on a regular grid. For grids with an odd number of columns n or grids with two rows, this solution can be created by $\textsc{Weave}(m, n)$. For grids with an even number of rows m and columns n, $\textsc{Boboeven}(m, n)$ yields an optimal tour. For grids with an odd number of rows and an even number of columns with either $m = 3$, or $m = 5$ or $k \geq \frac{1}{2}t(3t + 2)$, $\textsc{Bobodd}(m, n)$ with its particular cases returns the optimum. So does $\textsc{Near\_Quadratic}(m, n)$ for grids with n even and $m = n - 1$. We have succeeded in yielding an optimal solution for all grid sizes except for grids with an odd number of rows m and an even number of columns n with $5 < m \neq n - 1$ and $k < \frac{1}{2}t(3t + 2)$. In these cases, the remaining gaps are always smaller than 1 or, in more general terms, smaller than the distance between the two closest vertices. Furthermore, $\textsc{Bobodd}(m, n)$ is asymptotically optimal and has an approximation ratio of $\sqrt{\frac{t^2+k^2}{t^2+k^2-2t+1}}$. We found a further procedure $\textsc{Path\_Algorithm}(m, n)$ which is optimal for a Hamiltonian path on the grid with m odd and n even.

We have also considered the distances of the tours in 1- and ∞-norm. For the ∞-norm, optimal solutions of the MSTSP can be found for any grid size. $\textsc{Weave}(m, n)$ is then optimal for n odd, or $m = n$ or $m = 2$, $\textsc{Boboeven}(m, n)$ for m, n even and $\textsc{Bobodd}(m, n)$ is optimal for m odd, n even. Considering the 1-norm, we derived optimal solutions for n odd with $\textsc{Weave}(m, n)$, for m and n even with $\textsc{Weave}(m, n)$ or $\textsc{Boboeven}(m, n)$, for $m = 3$ or $m = 5$ and n even with $\textsc{Bobodd}(m, n)$ and for $m = n - 1$, n even with $\textsc{Near\_Quadratic}(m, n)$. The procedures can even be extended to a three-dimensional grid of layers, rows and columns by a similar scheme, ensuring that moves between closer layers are combined with long moves between rows and columns. The extension of $\textsc{Weave}(m, n)$ for n odd yields an optimal solution. Depending on the grid size, the extension of $\textsc{Boboeven}(m, n)$ can yield an optimal solution.

The two-dimensional tours of $\textsc{Weave}(m, n)$, $\textsc{Boboeven}(m, n)$ and $\textsc{Bobodd}(m, n)$ are also an approximation of the solution of the TSPN with mstsp-edge or quasi-mstsp-edge. The tours are asymptotically optimal. Therefore, the created tours are useful for two optimization problems. In many applications, this approxima-

tion of the length will be sufficient. We proved that WEAVE_3D(l, m, n) is also asymptotically optimal for the TSPN with mstsp-edge for grids with n odd.

For more general instances than a regular grid, we have tested first ideas of an approximation procedure for MSTSP based on local search and the heuristic of Lin and Kernighan. The procedure does not take into account any information about specific positions or distances. The first draft runs in $\mathcal{O}(n^3)$. For general instances where we had to guess an inaccurate upper bound, the approximation ratio was worse than for the regular grids where we knew the optimum quite exactly. Probably the approximation ratio is actually better. We chose this procedure as it hardly needs information about the instance and works much faster than solving a mixed-integer program with SCIP [2].

We also applied the local search to the MM2NTSP. In order to get closer upper bounds for at least the grids, we deduced upper bounds for MM2NTSP, which could still be improved, but we stopped at a certain point to avoid too much case analysis.

The new heuristic is promising as the computation times are reasonable did not exceed too much even if the search sets have not been restricted. So it is worth putting effort in it.

The reason to start considering the above-mentioned problems was given by CHAMP where we tested different island orders to understand the influence of the island strategy on the deflections in the samples and determine the best one. Instead, we found that the island order does not influence the deflections of a workpiece. Even though this does not make a particular strategy maintainable, it is worth focusing on short tours in order to decrease the production time. Moreover, it is still likely according to long-term experience of Concept Laser that, depending on the material and geometry, deflections can be reduced by using a careful strategy which avoids neighboring islands being molten consecutively. Therefore, we propose the solution of the TSPN as an island order. In most cases, it is likely sufficient to forbid only the smallest or the smallest few edges. But in the worst case, when the minimum edge length is around its maximum such that there still exists a Hamiltonian tour, we could apply our approximation of such a tour to the island order. There are no concrete implementations on the machines for these algorithms. Nevertheless, their implementation is likely in the future.

It was an important step to realize the independence of order and deflections. This enables researchers and developers to concentrate on productivity and requires them to find a completely new leverage point of how to diminish distortions.

A. Control of the Laser Power

The second part of project CHAMP, which is only mentioned briefly in this dissertation was examined by Simon Bechmann. In this section, I will give a short outline of his work on the project. The results are described in the Technical Report [13] and will be published in his dissertation. The hypothesis was that the control of the laser intensity within the islands during the melting process could influence the deflection of the workpiece. This control should be combined with the strategy of order that would best diminish distortions. Therefore, Simon modeled the distribution of heat in a three-dimensional rectangular block which is surrounded by powder. The resulting optimization problem was a state-constrained optimal control problem. The optimal strategies were computed with Comsol Multiphysics 3.5 [26] and Matlab2010 [25] a combination of simulation and optimization in certain parts of the path of the laser. As it is currently not possible to change the speed of the laser beam within the process, Simon focused on the control of the laser power. The path of the laser was taken as it is currently used at Concept Laser, which is a series of anti parallel scan vectors with perpendicular meanders as a connection.

From a continuous control of the laser power resulting from the optimization process, he tested many controls with a different number of discrete steps of different heights and lengths. As a change of the laser power goes along with an overshooting of the laser, the final strategy was chosen to have only two levels of laser power. The result was that the melt structures are better visible in this kind of strategy than in the current procedure with constant laser power.

As already mentioned in section 7.3.3, the deflections in the final test were not reduced. Nevertheless, the quality of the surface can be significantly improved by a specific control of the laser power.

B. Proof concerning the Squared Inverse Distances

When introducing the TSP with squared inverse distances, we stated that $\tilde{d}_{ab} = \frac{1}{d_{ab}^2}$ does not satisfy the relaxed triangle inequality with d_{ab} being the Euclidean distance between node a and node b. Our proof is presented here.

Proposition 16. *There is no τ such that for all a, b, c the following holds:*

$$\tilde{d}(a,c) \leq \tau \left(\tilde{d}(a,b) + \tilde{d}(b,c) \right). \tag{B.1}$$

Proof. We prove the proposition by construction. Let an integer $\tau > 0$ be given. We have to find a $\tilde{d}(a,b)$, $\tilde{d}(a,c)$, $\tilde{d}(b,c)$ such that $\frac{\tilde{d}(a,c)}{\tilde{d}(a,b)+\tilde{d}(b,c)} > \tau$. We construct this counterexample in the following way. We set $\tilde{d}(a,c) = 1$ and $\tilde{d}(a,b) = \frac{1}{x^2}$ and $\tilde{d}(b,c) = \frac{1}{(x-1)^2}$ with $x > 1$ in order to guarantee that the Euclidean distances $d(a,b) = x$, $d(a,c) = 1$ and $d(b,c) = x - 1$ satisfy the triangle inequality. So we have to determine a value of $x > 1$ such that

$$\frac{1}{\frac{1}{x^2} + \frac{1}{(x-1)^2}} > \tau. \tag{B.2}$$

After some transformations of the inequality, we get

$$0 < x^2(x-1)^2 - \tau((x-1)^2 + x^2). \tag{B.3}$$

If we set $x = 3\tau$, this inequality holds:

$$0 < 9\tau^2(9\tau^2 - 6\tau + 1) - \tau(18\tau^2 - 6\tau + 1) \tag{B.4}$$

$$\Leftrightarrow \qquad 0 < \underbrace{\tau}_{>0}(\underbrace{81\tau^3 - 72\tau^2}_{>0} + \underbrace{15\tau - 1}_{>0}). \tag{B.5}$$

Thus, for every $\tau \geq 1$ we can determine at least one $x > 1$ such that inequality B.2 holds. □

C. Computations regarding the Approximation of MSTSP on a 3D Grid

C.1. Computations on the Shortest Edges

The following cases of grids with an even number of columns n can be checked to prove that the edge at the switch of pairs of rows is not the shortest edge in the algorithm. We always compare the squared length of edges. We start with a claim, transform it and find a valid statement from which we can deduce the claim.

C.1.1. l, n even, m arbitrary

$$(l-1)^2+(t-1)^2+(k+1)^2 \geq (r-1)^2+t^2+k^2 \tag{C.1}$$
$$\Leftrightarrow \quad 3r^2-2r-2t+2k+2 \geq 0 \Leftarrow \underbrace{r(3r-2)}_{\geq 0}+2+2\underbrace{(k-t)}_{\geq 0} \geq 0. \tag{C.2}$$

C.1.2. l odd, m arbitrary, n even

In the following, the final steps can always be established by computing the zeros of a polynomial (which are complex conjugated) and choosing any example value for which the value of the polynomial is greater 0. First, we only consider grids with more than five layers: $l > 5$ has to be ensured as otherwise the shortest edge, to which the edge at the flip is combined, differs.

$$(l-3)^2+(t-1)^2+(k+1)^2 \geq (r-1)^2+t^2+k^2 \tag{C.3}$$
$$\Leftrightarrow \quad 3r^2-6r+5\underbrace{-2t+2k}_{\geq 0} \geq 0 \Leftarrow 3r^2-6r+5 \geq 0. \tag{C.4}$$

We continue with grids with $l = 5$:

$$(l-3)^2+(t-1)^2+(k+1)^2 \geq r^2+t^2+k^2 \tag{C.5}$$
$$\Leftrightarrow \quad 3r^2-8r+6\underbrace{-2t+2k}_{\geq 0} \geq 0 \Leftarrow 3r^2-8r+6 \geq 0. \tag{C.6}$$

For grids with $l = 3$, the following holds:

$$(l-1)^2+(t-1)^2+(n-1)^2 \geq r^2+t^2+k^2 \tag{C.7}$$
$$\Leftrightarrow \quad 3r^2-4r+3k^2\underbrace{-4k-2t}_{\geq -6k}+3 \geq 0 \Leftarrow \underbrace{3r^2-4r+1}_{\geq 0}+\underbrace{3k^2-6k+2}_{\geq 0} \geq 0. \tag{C.8}$$

We can state the following for BOBEVEN_3D(l, m, n) and BOBODD_3D(l, m, n):

Lemma 5. *For all grids with l odd, m even (resp. odd) and n even, the connecting edges between pairs of rows are at least as long as one further edge of the tour.*

C.2. Computation of the Approximation for $l = m = 3$, n Even

If $m = 3$, the edges which appear in BOBODD_3D(l, m, n) are (r, t, k)-edges, $(r, m-1, k)$-edges, $(r, m-1, k-1)$-edges, $(r-1, m-1, n-1)$-edges, $(r+1, m-1, n-1)$-edges and $(r, m-1, n-1)$-edges. Candidates for the shortest of those are: (r, t, k) and $(r, m-1, k-1)$ as well as $(r-1, m-1, n-1)$. The last one of the three is never the shortest edge as $(r-1)^2 + (m-1)^2 + (n-1)^2 \geq r^2 + (m-1)^2 + (k-1)^2$ which is proved in the following.

We transform the squared length of $(r-1, m-1, k-1)$:

$$(r-1)^2 + (m-1)^2 + (n-1)^2 = r^2 + (m-1)^2 + k^2 + 3k^2 - 4k + 1 - 2r + 1. \quad \text{(C.9)}$$

As $k > k-1$, it suffices to prove $3k^2 - 4k - 2r + 2 \geq 0$. It is obvious that $3k^2 - 4k + 1 - 2r + 1 \geq 3k^2 - 6k + 2$. This parable, which is opened to the top (coefficient of k^2 is positive), equals 0 at $k_{1,2} = 1 \pm \frac{\sqrt{3}}{3}$ and therefore for all $k \geq 2$ the inequality holds. If $k < 2$, $n = 2k \leq 2$ as n is even in our considerations. As this contradicts $m < n$, this case does not have to be considered.

Thus, the following lemma holds:

Lemma 6. *If $l = m = 3$ and n even, the shortest edges are*

$$(y_1, y_2, y_3) = \begin{cases} (r, t, k) & \text{if } k \leq \frac{1}{2}(3t^2 + 1) = 2 \\ (r, m-1, k-1) & \text{else.} \end{cases} \quad \text{(C.10)}$$

For an $(3 \times 3 \times 4)$-grid, an optimal solution is yielded. For all other cases, the special combination for $m = 3$ yields at least a $\sqrt{\frac{r^2+t^2+k^2}{r^2+(m-1)^2+(k-1)^2}}$-approximation.

C.3. Computation of the Approximation for $l \leq m = 5$ Odd, n Even

The shortest edges of BOBODD(m, n) are in the 2D case: either (t, k) or $(m-1, k-1)$. When applying BOBODD(m, n) in combination with the first component of WEAVE(l, mn), we have to ensure that the edge at which the pair or triple of layers is switched is not the shortest edge of the tour. The change of a pair or triple of layers, yields at least a $(r-1, m-3, k+1)$-edge.

We do the following transformations:

$$(r-1)^2 + (m-3)^2 + (k+1)^2 \tag{C.11}$$
$$= r^2 + 4t^2 + k^2 + 2k + 1 - 8t + 4 - 2r + 1 \tag{C.12}$$
$$= r^2 + t^2 + k^2 + 3t^2 - 8t + 2k - 2r + 6. \tag{C.13}$$

When we compute the values of k for which $|(r-1, m-3, k+1)| \geq |(r,t,k)|$ holds, it suffices to prove that

$$3t^2 - 8t + 2k - 2r + 6 \geq 0 \tag{C.14}$$
$$3t^2 - 8t + 6 + 2k - 2r \geq 3t^2 - 8t + 6 = p(t). \tag{C.15}$$

The curve is a polynomial and thus continuous, the zeros are complex conjugated and as there is at least one positive value for $p(1) = 1$, it is always strictly greater than 0 and the inequality holds. We can conclude the following:

Lemma 7. *The shortest edges are*

$$(y_1, y_2, y_3) = \begin{cases} (r,t,k) & \text{if } k \leq \frac{1}{2}(3t^2+1) = 6.5 \\ (r, m-1, k-1) & \text{else.} \end{cases} \tag{C.16}$$

For $k \leq \frac{1}{2}(3t^2+1)$, the upper bound is yielded and therefore the tour is an optimal solution.

D. Tables about the Computational Results of our Local Search Heuristics

Name	Time [10^{-2}sec]	Iter.	Approx.	Upper bnd.	α
berlin52:	0.0	95	355.01	806.2	0.44
bier127:	0.4	446	2900.62	8004.0	0.36
ch130:	0.3	293	316.43	346.7	0.91
ch150:	0.4	370	328.21	347.3	0.94
d198:	1.7	1206	586.78	2030.1	0.29
d493:	9.8	2930	538.11	1898.4	0.28
d657:	20.0	4692	1230.92	2011.7	0.61
eil51:	0.0	107	33.29	34.2	0.97
eil76:	0.1	227	43.01	44.3	0.97
eil101:	0.3	393	49.65	52.8	0.94
fl417:	7.4	2784	640.29	734.9	0.87
fl1400:	189.7	20006	1042.46	1264.6	0.82
fl1577:	260.3	23918	973.88	1008.5	0.97
fl3795:	2953.3	98606	1943.02	2062.2	0.94
kroA100:	0.1	149	1853.48	2033.3	0.91
kroA200:	0.5	394	1982.08	2033.3	0.97
kroA150:	0.2	216	1829.01	2038.2	0.9
kroB100:	0.1	132	1510.05	1939.1	0.78
kroB150:	0.2	222	1777.01	1923.8	0.92
kroB200:	0.7	488	1897.18	1952.0	0.97
kroC100:	0.1	149	1824.38	1985.0	0.92
kroD100:	0.1	175	1626.42	1947.7	0.84
kroE100:	0.1	121	1649.13	2004.0	0.82
lin105:	0.5	659	1338.9	1504.7	0.89
p654:	32.9	7385	2147.67	2600.3	0.83
pcb442:	15.1	5274	1216.06	1451.0	0.84
pcb1173:	117.9	15720	992.64	1087.3	0.91

Table D.1.: Computations of LS_MSTSP on instances of the TSPLIB – part 1

The computational results from the samples from the TSPLIB are listed in this chapter.

Name	Time [10^{-2}sec]	Iter.	Approx.	Upper bnd.	α
pcb3038:	1708.3	83547	1881.18	2104.0	0.89
pr76:	0.2	373	7050.14	**7260.1**	**0.97**
pr107:	0.3	425	602.08	**602.08**	**1.0**
pr124:	0.5	612	4025.4	4800.4	0.84
pr136:	0.3	270	6133.12	7150.1	0.86
pr144:	0.7	768	4300.59	6550.4	0.66
pr152:	1.0	900	6575.42	7150.4	0.92
pr226:	1.5	1078	6650.17	7550.1	0.88
pr264:	3.5	2140	5550.96	6151.4	0.9
pr299:	2.5	1482	3105.1	3366.1	0.92
pr439:	9.2	2968	2450.94	5950.6	0.41
pr1002:	117.1	17444	6569.21	7914.8	0.83
pr2392:	925.6	55714	4891.88	5190.1	0.94
rat99:	0.3	384	61.85	63.3	0.98
rat195:	1.4	1077	106.25	113.5	0.94
rat575:	22.4	6030	297.98	307.4	0.97
rat783:	47.3	8894	403.0	407.2	0.99
rd100:	0.1	178	482.01	484.8	0.99
rd400:	3.5	1360	505.79	522.1	0.97
rl1304:	103.1	11999	7414.22	9413.9	0.79
rl1323:	117.0	13371	7637.58	9470.4	0.81
rl1889:	251.8	19684	8897.01	9505.8	0.94
rl5915:	3649.2	83059	7901.07	9787.5	0.81
rl5934:	3815.4	85594	8055.32	9781.0	0.82
ts225:	2.4	1583	6000.31	6000.3	1.0
tsp225:	2.2	1567	196.4	260.9	0.75
u159:	0.8	765	2600.31	2600.7	1.0
u574:	28.4	7436	1340.12	1540.0	0.87
u724:	45.9	9541	1365.95	1474.4	0.93
u1060:	136.5	18965	7692.26	8884.0	0.87
u1432:	222.6	23575	2463.26	2731.6	0.9
u1817:	480.9	38545	1397.01	1641.4	0.85
u2152:	764.4	48525	1582.17	1694.7	0.93
u2319:	758.1	47848	2717.4	2865.2	0.95
vm1084:	35.4	5298	8235.98	9376.3	0.88
vm1748:	132.5	11388	8647.72	9452.3	0.91

Table D.2.: Computations of LS_MSTSP on instances of the TSPLIB – part 2

Name	Time [10^{-2}sec]	Iter.	Approx.	Upper bnd.	α
berlin52:	0.1	46	130.25	736.0	0.18
bier127:	1.3	232	1277.86	6032.0	0.21
ch130:	1.8	203	165.77	340.9	0.49
ch150:	1.2	180	149.6	333.7	0.45
d198:	8.0	625	280.52	2029.9	0.14
d493:	70.7	1671	315.6	1829.9	0.17
d657:	139.8	2284	678.15	2011.0	0.34
eil51:	0.2	82	21.54	31.9	0.68
eil76:	0.5	163	26.68	42.2	0.63
eil101:	1.1	272	34.48	52.2	0.66
fl417:	55.4	1779	350.93	723.3	0.49
fl1400:	1930.4	11435	671.15	1224.9	0.55
fl1577:	2327.5	12249	651.05	1003.2	0.65
fl3795:	32006.2	43728	1222.7	2034.7	0.6
fnl4461:	38264.6	62842	1311.83	2835.2	0.46
kroA100:	0.8	127	891.35	1974.5	0.45
kroA200:	3.1	267	918.45	1996.3	0.46
kroA150:	1.5	196	912.39	2025.5	0.45
kroB100:	0.5	105	755.6	1909.0	0.4
kroB150:	1.7	199	827.04	1915.2	0.43
kroB200:	3.2	239	872.8	1939.1	0.45
kroC100:	1.2	171	887.02	1940.2	0.46
kroD100:	0.5	108	742.01	1880.8	0.39
kroE100:	0.5	109	700.35	1889.2	0.37
lin105:	1.2	302	551.52	1457.8	0.38
p654:	263.4	4040	286.39	2599.8	0.11
pcb442:	90.5	2554	710.04	1415.7	0.5
pcb1173:	859.4	8133	643.09	1074.3	0.6

Table D.3.: Computations of LS_MM2NTSP on instances of the TSPLIB with enumerated initial order – part 1

Name	Time [10^{-2}sec]	Iter.	Approx.	Upper bnd.	α
pcb3038:	13523.1	34271	1038.02	2076.1	0.5
pr76:	0.5	168	2808.01	8400.1	0.33
pr107:	0.9	181	206.65	7650.1	0.03
pr124:	2.0	332	1500.56	4800.4	0.31
pr136:	0.6	127	1817.61	7150.0	0.25
pr144:	3.5	506	2800.19	6550.3	0.43
pr152:	3.3	465	901.98	7150.4	0.13
pr226:	7.1	614	2400.08	7451.5	0.32
pr264:	18.1	1086	405.25	6051.4	0.07
pr299:	12.9	823	1276.51	3365.1	0.38
pr439:	54.2	1542	1356.54	5863.3	0.23
pr1002:	580.1	6553	3204.67	7864.3	0.41
pr2392:	6468.8	19358	2439.63	5167.6	0.47
rat99:	0.8	198	35.69	61.0	0.58
rat195:	6.4	626	68.45	109.2	0.63
rat575:	134.5	3049	177.45	301.7	0.59
rat783:	318.3	4090	236.4	407.2	0.58
rd100:	0.6	104	228.91	481.2	0.48
rd400:	31.9	917	308.95	516.2	0.6
rl1304:	603.7	5301	3878.85	9375.9	0.41
rl1323:	671.4	5255	3953.74	9322.8	0.42
rl1889:	13164.3	7044	4518.52	9472.8	0.48
rl5915:	47402.6	39973	5201.49	9730.3	0.53
rl5934:	38015.4	38678	5128.01	9703.7	0.53
ts225:	7.1	624	3000.04	6000.3	0.5
tsp225:	9.7	816	116.19	252.3	0.46
u159:	4.3	493	811.82	2600.7	0.31
u574:	136.7	3067	678.27	1519.9	0.45
u724:	260.4	4391	735.7	1474.4	0.5
u1060:	775.2	7618	3989.63	8067.2	0.49
u1432:	1960.6	11466	1443.5	2731.3	0.53
u1817:	4589.3	17807	902.46	1632.2	0.55
u2152:	6865.1	21909	992.29	1692.5	0.59
u2319:	7085.3	21049	1634.29	2803.6	0.58
vm1084:	190.3	2725	4060.13	9356.9	0.43
vm1748:	660.4	4860	4368.69	9444.4	0.46

Table D.4.: Computations of LS_MM2NTSP on instances of the TSPLIB with enumerated initial order – part 2

Name	Time [10^{-2}sec]	Iter.	Approx.	Upper bnd.	α
berlin52:	0.2	77	195.92	736.0	0.27
bier127:	1.3	211	1395.52	6032.0	0.23
ch130:	1.9	267	153.67	340.9	0.45
ch150:	2.3	287	162.26	333.7	0.49
d198:	3.6	319	280.19	2029.9	0.14
d493:	23.5	792	294.9	1829.9	0.16
d657:	71.2	1480	625.81	2011.0	0.31
eil51:	0.1	47	22.09	31.9	0.69
eil76:	0.3	83	27.73	42.2	0.66
eil101:	0.6	123	33.3	52.2	0.64
fl417:	34.1	946	361.04	723.3	0.5
fl1400:	401.2	2869	682.32	1224.9	0.56
fl1577:	585.8	3524	639.09	1003.2	0.64
fl3795:	4309.6	10659	1106.56	2034.7	0.54
kroA100:	1.1	201	842.29	1974.5	0.43
kroA200:	4.7	428	805.91	1996.3	0.4
kroA150:	1.5	232	839.12	2025.5	0.41
kroB100:	0.6	141	773.47	1909.0	0.41
kroB150:	1.8	239	839.76	1915.2	0.44
kroB200:	4.6	456	829.69	1939.1	0.43
kroC100:	0.5	134	728.4	1940.2	0.38
kroD100:	0.6	130	743.03	1880.8	0.4
kroE100:	0.6	117	678.17	1889.2	0.36
lin105:	1.1	203	622.35	1457.8	0.43
p654:	138.9	1650	289.52	2599.8	0.11
pcb442:	27.0	1002	700.82	1415.7	0.5
pcb1173:	188.4	2381	594.14	1074.3	0.55

Table D.5.: Computations of LS_MM2NTSP on instances of the TSPLIB with an approximate solution of LS_MSTSP as an initial order – part 1

Name	Time [10^{-2}sec]	Iter.	Approx.	Upper bnd.	α
pcb3038:	4542.7	11343	1056.86	2076.1	0.51
pr76:	0.4	124	2950.11	8400.1	0.35
pr107:	0.6	125	400.13	7650.1	0.05
pr124:	0.9	155	1500.51	4800.4	0.31
pr136:	1.3	191	1817.77	7150.0	0.25
pr144:	1.9	268	2675.24	6550.3	0.41
pr152:	2.3	298	897.72	7150.4	0.13
pr226:	6.2	420	2300.07	7451.5	0.31
pr264:	8.6	444	404.18	6051.4	0.07
pr299:	15.5	727	1275.01	3365.1	0.38
pr439:	29.2	1018	1262.33	5863.3	0.22
pr1002:	332.8	3861	3261.02	7864.3	0.41
pr2392:	2246.9	9019	2492.76	5167.6	0.48
rat99:	0.5	102	37.44	61.0	0.61
rat195:	3.5	300	70.0	109.2	0.64
rat575:	86.0	1433	183.44	301.7	0.61
rat783:	133.2	2027	221.15	407.2	0.54
rd100:	0.7	152	208.97	481.2	0.43
rd400:	24.6	831	291.39	516.2	0.56
rl1304:	472.1	4031	3593.36	9375.9	0.38
rl1323:	571.6	4750	3901.94	9322.8	0.42
rl1889:	1628.7	7362	4474.07	9472.8	0.47
rl5915:	18272.9	19117	4935.24	9730.3	0.51
rl5934:	20749.9	19287	5069.18	9703.7	0.52
ts225:	8.3	605	3000.12	6000.3	0.5
tsp225:	3.6	321	112.74	252.3	0.45
u159:	1.7	204	1009.48	2600.7	0.39
u574:	80.1	1689	699.9	1519.9	0.46
u724:	119.1	1999	724.62	1474.4	0.49
u1060:	280.8	3275	3754.55	8067.2	0.47
u1432:	378.0	3415	1442.78	2731.3	0.53
u1817:	871.4	4620	840.85	1632.2	0.52
u2152:	1472.8	6351	970.95	1692.5	0.57
u2319:	2688.8	8850	1636.16	2803.6	0.58
vm1084:	280.5	3048	4156.63	9356.9	0.44
vm1748:	1341.9	6620	4529.58	9444.4	0.48

Table D.6.: Computations of LS_MM2NTSP on instances of the TSPLIB with an approximate solution of LS_MSTSP as an initial order – part 2

E. Structure of the CLI-file

```
$$HEADERSTART
$$ASCII
$$UNITS/0.001
$$LAYERS/300
$$VERSION/200
$$HEADEREND
$$PARSETSTART //setting of parameters matched to indices
$$POWER/10,180
$$SPEED/10,1600
$$POWER/11,106
$$SPEED/11,800
.
.
.
$$POWER/14,180
$$SPEED/14,800
$$PARSETEND
$$GEOMETRYSTART
$$LAYER/0            //empty layer (with support structure and base)
$$LAYER/30    //empty layer (with support structure and base)
.
.
.
$$LAYER/6000
$$HATCHES/14,1,105052,-4947.5,109948,-4947.5
$$HATCHES/11,1,109948,-4947.5,109948,-4843.35
$$HATCHES/12,1,109948,-4843.35,109635,-4843.35
.
.
.
$$POLYLINE/10,0,5,45,-45,45,-4955,149955,-4955,149955,-45,45,-45
$$LAYER/6030
.
.
.
$$GEOMETRYEND
```

Figure E.1.: Layout of a CLI-file

The whole CLI-file of one sample of the final test contains 599860 lines. Each hatch is indexed in order to match it with the right speed and power of the laser. This is followed by a value which indicates the number of scan vectors defined in that line and by the coordinates of the two endpoints. The list of hatches indicates likewise the scanning order of the hatches. The polyline has as an additional value as second attribute, which indicates the orientation of the line.

F. Average Length of a Random Tour

We found the following proposition by construction.

Proposition 17. *Let $G = (V, E)$ be a complete graph, $n = |V|$ be the number of vertices. Let $\Omega = \{T \in \mathbb{N}_0^n : a_i \in \{0, \dots, n-1\} \wedge T_i \neq T_j$ for $i, j \in \{0, \dots, n-1\}$ with $i \neq j\}$ be the set of TSP-tours, let the σ-algebra $\mathcal{A}$ be the power set of Ω and $p : \Omega \to [0, 1]$, $\omega \mapsto \frac{1}{|\mathcal{A}|}$ be the probability measure. Let $E(T) = \{(i, j) \in E : (i = T_k \wedge j = T_{k+1}$ for $k \in \{0, \dots, n-2\}) \vee (i = T_{n-1} \wedge j = T_0)\}$. Let $d_{T_iT_j}$ be the Euclidean distance between vertex T_i and T_j. Let $L : \mathbb{N}_0^n \to \mathbb{R}$, $T \mapsto d_{T_{n-1}T_0} + \sum_{i=1}^{n-1} d_{T_{i-1}T_i}$ be the length of a TSP tour T. Let the set of all TSP tours be uniformly distributed. Then the expected value for the length across all tours is*

$$\mathbb{E}[L] = \frac{1}{n-1} \sum_{(i,j) \in V^2} d_{ij}. \tag{F.1}$$

Proof. In the following, neither permutation nor symmetries are summarized. The expected value of the tour length is defined as

$$\begin{aligned}
\mathbb{E}[L] =& \frac{1}{n!} \sum_{T:T \in \Omega} L(T) && \text{(F.2)}\\
=& \frac{1}{n!} \sum_{T:T \in \Omega} \sum_{(i,j) \in E(T)} d_{ij} && \text{(F.3)}\\
=& \frac{1}{n!} \sum_{(i,j) \in V^2} \sum_{T:(i,j) \in E(T)} d_{ij} && \text{(F.4)}\\
=& \frac{1}{n!} \sum_{(i,j) \in V^2} \#\{T : (i, j) \in E(T)\} d_{ij} && \text{(F.5)}\\
\overset{(*)}{=}& \frac{1}{n!} \sum_{(i,j) \in V^2} n \cdot (n-2)! \cdot d_{ij} && \text{(F.6)}\\
=& \frac{1}{n-1} \sum_{(i,j) \in V^2} d_{ij}. && \text{(F.7)}
\end{aligned}$$

(*) When we sum up all tours which contain the arc (i, j), there are $(n-2)!$ tours which contain (i, j) as the first edge, and the same number for the kth position $(k = 2, \dots, n)$. The sum of all positions makes $n \cdot (n-2)!$ tours containing the edge (i, j). □

Edge	Rate	Condition
$(0,i)$	$m(n-i)+n(m-i)$	$1 \le i \le m-1$
$(0,i)$	$m(n-i)$	$m \le i \le n-1$
(i,i)	$2(m-i)(n-i)$	$1 \le i \le m-1$
(i,j)	$2\left[(m-i)(n-j)+(m-j)(n-i)\right]$	with $1 \le i < j \le m-1$
(i,j)	$2(m-i)(n-j)$	with $1 \le i < m \le j \le n-1$

Table F.1.: Distances in an $(m \times n)$-Grid (undirected)

For an $(m \times n)$-grid all kinds of possible edges are listed with their rate in table F.1; (i,j)-edges and (j,i)-edges are summarized as an (i,j)-edge with $i \le j$. We distinguish between horizontal or vertical edges, diagonal edges and other edges which could be turned about 90° and those which cannot as i or j is greater than or equal to m. There are $\frac{1}{2}mn(mn-1)$ edges in total, twice the number when taking the direction of an edge into account. With this table the average length of random tours can be computed easily by taking the sum of the edge lengths, each multiplied with its rate. The average length of a random tour in an $(m \times n)$-grid is

$$\begin{aligned}\frac{2}{m \cdot n - 1} \Bigg(& \sum_{i=1}^{m-1} i \cdot (m(n-i)+n(m-i)) + \sum_{i=m}^{n-1} i \cdot m(n-i) \\ & + \sum_{i=1}^{m-1} \sqrt{2i^2} \cdot 2(m-i)(n-i) \\ & + \sum_{i=1}^{m-2} \sum_{j=i+1}^{m-1} \sqrt{i^2+j^2} \cdot 2\left[(m-i)(n-j)+(m-j)(n-i)\right] \\ & + \sum_{i=1}^{m-1} \sum_{j=m}^{n-1} \sqrt{i^2+j^2} \cdot 2(m-i)(n-j) \Bigg).\end{aligned} \tag{F.8}$$

This formula was used to compute the average tour length for Workpiece 4 in CHAMP.

Bibliography

[1] F. Abe, K. Osakada, M. Shiomi, K. Uematsu, and M. Matsumoto. The manufacturing of hard tools from metallic powders by selective laser melting. *Journal of materials processing technology*, 111(1):210–213, 2001.

[2] T. Achterberg. SCIP: Solving constraint integer programs. *Mathematical Programming Computation*, 1(1):1–41, July 2009. accessed on August 23, 2016.

[3] T. Andreae. On the traveling salesman problem restricted to inputs satisfying a relaxed triangle inequality. *Networks*, 38(2):59–67, 2001.

[4] T. Andreae and H.-J. Bandelt. Performance guarantees for approximation algorithms depending on parametrized triangle inequalities. *SIAM Journal on Discrete Mathematics*, 8(1):1–16, 1995.

[5] D. Applegate, W. Cook, and A. Rohe. Chained Lin-Kernighan for large traveling salesman problems. *INFORMS Journal on Computing*, 15(1):82–92, 2003.

[6] D. L. Applegate, R. E. Bixby, V. Chvátal, and W. J. Cook. *The Traveling Salesman Problem - A Computational Study*. Princeton University Press, 2006.

[7] E. M. Arkin, Y.-J. Chiang, J. S. Mitchell, S. S. Skiena, and T.-C. Yang. On the maximum scatter traveling salesperson problem. *SIAM Journal on Computing*, 29(2):515–544, 1999.

[8] S. Arora. Polynomial time approximation schemes for Euclidean traveling salesman and other geometric problems. *Journal of the ACM (JACM)*, 45(5):753–782, 1998.

[9] S. Arora and B. Barak. *Computational complexity: a modern approach*. Cambridge University Press, 2009.

[10] S. Arora, C. Lund, R. Motwani, M. Sudan, and M. Szegedy. Proof verification and the hardness of approximation problems. *Journal of the ACM (JACM)*, 45(3):501–555, 1998.

[11] F. Bechmann, S. Bechmann, B. Günther, I. Hoffmann, H. J. Pesch, and J. Rambau. Verwendungsnachweis für die Oberfrankenstiftung: Wärmesteuerung in der automatischen Modellproduktion (CHAMP – Control of Heat in Automatic Model Production) – Zwischenbericht nach zwei Jahren. 2014.

[12] F. Bechmann, S. Bechmann, B. Günther, I. Hoffmann, H. J. Pesch, and J. Rambau. Verwendungsnachweis für die Oberfrankenstiftung: Wärmesteuerung in der automatischen Modellproduktion (CHAMP – Control of Heat in Automatic Model Production) – Abschlussbericht nach drei Jahren. 2015.

[13] F. Bechmann, S. Bechmann, B. Günther, I. Hoffmann, H. J. Pesch, and J. Rambau. Verwendungsnachweis für die Oberfrankenstiftung: Wärmesteuerung in der automatischen Modellproduktion (CHAMP – Control of Heat in Automatic Model Production) – Technical Report. 2015.

[14] F. Bechmann, S. Bechmann, I. Hoffmann, H. J. Pesch, and J. Rambau. Verwendungsnachweis für die Oberfrankenstiftung: Wärmesteuerung in der automatischen Modellproduktion (CHAMP – Control of Heat in Automatic Model Production) – Zwischenbericht nach einem Jahr. 2013.

[15] F. Bechmann, H. J. Pesch, and J. Rambau. Projektantrag für die Oberfrankenstiftung: Wärmesteuerung in der automatischen Modellproduktion (CHAMP – Control of Heat in Automatic Model Production) – Scientific Details. 2011.

[16] M. A. Bender and C. Chekuri. Performance guarantees for the TSP with a parameterized triangle inequality. *Information Processing Letters*, 73(1):17–21, 2000.

[17] R. G. Bland and D. F. Shallcross. Large travelling salesman problems arising from experiments in x-ray crystallography: a preliminary report on computation. *Operations Research Letters*, 8(3):125–128, 1989.

[18] F. Bock. An algorithm for solving travelling-salesman and related network optimization problems. In *Operations Research*, volume 6, page 897. INST OPERATIONS RESEARCH MANAGEMENT SCIENCES 901 ELKRIDGE LANDING RD, STE 400, LINTHICUM HTS, MD 21090-2909, 1958.

[19] H.-J. Böckenhauer, J. Hromkovič, R. Klasing, S. Seibert, and W. Unger. Towards the notion of stability of approximation for hard optimization tasks and the traveling salesman problem. *Theoretical Computer Science*, 285(1):3–24, 2002.

[20] G. Branner. *Modellierung transienter Effekte in der Struktursimulation von Schichtbauverfahren*, volume 246. Herbert Utz Verlag, 2011.

[21] Brite-EuRam. Common Layer Interface (CLI): Version 2.0. `https://www.forwiss.uni-passau.de/~welisch/papers/cli_format.html`, 1994. received from Concept Laser GmbH on July 17, 2013.

[22] S. L. Campanelli, A. Angelastro, A. D. Ludovico, and N. Contuzzi. *Capabilities and performances of the selective laser melting process*. INTECH Open Access Publisher, 2010.

[23] Y.-J. Chiang. New approximation results for the maximum scatter TSP. *Algorithmica*, 41(4):309–341, 2005.

[24] N. Christofides. Worst-case analysis of a new heuristic for the travelling salesman problem. Technical report, DTIC Document, 1976.

[25] COMSOL. *COMSOL MULTIPHYSICS® MATLAB Interface Guide Version 3.5 a*, 2008.

[26] COMSOL. *COMSOL MULTIPHYSICS® User's Guide Version 3.5 a*, 2008.

[27] Concept Laser GmbH. Concept Laser – Hofmann Innovation Group. `http://concept-laser.de`. accessed on June 15, 2016.

[28] W. Cook. *In pursuit of the traveling salesman: mathematics at the limits of computation*. Princeton University Press, 2012.

[29] T. H. Cormen, C. E. Leiserson, R. L. Rivest, and C. Stein. *Introduction to algorithms second edition*. The MIT Press, 2001.

[30] G. A. Croes. A method for solving traveling-salesman problems. *Operations research*, 6(6):791–812, 1958.

[31] G. Dantzig, R. Fulkerson, and S. Johnson. Solution of a large-scale traveling-salesman problem. *Journal of the operations research society of America*, 2(4):393–410, 1954.

[32] M. De Berg, F. Van Nijnatten, R. Sitters, G. J. Woeginger, and A. Wolff. The traveling salesman problem under squared euclidean distances. *arXiv preprint arXiv:1001.0236*, 2010.

[33] G. A. Dirac. Some theorems on abstract graphs. *Proceedings of the London Mathematical Society*, 3(1):69–81, 1952.

[34] W. Eastman. *Linear programming with pattern constraints [Ph. D. thesis]*. PhD thesis, Cambridge (MA): Department of Economics, Harvard University, 1958.

[35] S. P. Fekete. Simplicity and hardness of the maximum traveling salesman problem under geometric distances. In *SODA*, pages 337–345, 1999.

[36] A. Fischer. *A Polyhedral Study of Quadratic Traveling Salesman Problems*. PhD thesis, TU Chemnitz, 2013. accessed on August 23, 2016.

[37] A. Fischer and C. Helmberg. The symmetric quadratic traveling salesman problem. *Mathematical Programming*, 142(1-2):205–254, 2013.

[38] A. Fischer and P. Hungerländer. The traveling salesman problem on grids with forbidden neighborhoods. 2016.

[39] M. M. Flood. The traveling-salesman problem. *Operations Research*, 4(1):61–75, 1956.

[40] M. R. Garey, D. S. Johnson, and R. E. Tarjan. The planar hamiltonian circuit problem is np-complete. *SIAM Journal on Computing*, 5(4):704–714, 1976.

[41] I. Gibson, D. Rosen, and B. Stucker. *Additive manufacturing technologies: 3D printing, rapid prototyping, and direct digital manufacturing*. Springer, 2014.

[42] M. Grötschel and M. W. Padberg. On the symmetric travelling salesman problem I: Inequalities. *Mathematical Programming*, 16(1):265–280, 1979.

[43] M. Grötschel and M. W. Padberg. On the symmetric travelling salesman problem II: Lifting theorems and facets. *Mathematical Programming*, 16(1):281–302, 1979.

[44] G. Gutin and A. P. Punnen. *The traveling salesman problem and its variations*, volume 12. Springer Science & Business Media, 2006.

[45] K. Helsgaun. An effective implementation of the Lin–Kernighan traveling salesman heuristic. *European Journal of Operational Research*, 126(1):106–130, 2000.

[46] K. Helsgaun. Solving the equality generalized traveling salesman problem using the Lin–Kernighan–Helsgaun Algorithm. *Mathematical Programming Computation*, pages 1–19, 2014.

[47] I. Hoffmann. CHAMP–Control of Heat in Automatic Model Production. Master's thesis, Universität Bayreuth, 2013.

[48] I. Hoffmann, S. Kurz, and J. Rambau. The maximum scatter TSP on a regular grid, 2015.

[49] D. S. Johnson. Local optimization and the traveling salesman problem. In *Automata, languages and programming*, pages 446–461. Springer, 1990.

[50] R. M. Karp. *Reducibility among combinatorial problems*. Springer, 1972.

[51] S. Kirkpatrick, C. D. Gelatt Jr., and M. P. Vecchi. Optimization by simulated annealing. *Science*, 220(4598):671–680, 1983.

[52] B. Korte and J. Vygen. *Combinatorial optimization*. Springer, 2002.

[53] J.-P. Kruth, L. Froyen, J. Van Vaerenbergh, P. Mercelis, M. Rombouts, and B. Lauwers. Selective laser melting of iron-based powder. *Journal of Materials Processing Technology*, 149(1):616–622, 2004.

[54] J.-P. Kruth, P. Mercelis, J. Van Vaerenbergh, L. Froyen, and M. Rombouts. Binding mechanisms in selective laser sintering and selective laser melting. *Rapid prototyping journal*, 11(1):26–36, 2005.

[55] J.-P. Kruth, B. Vandenbroucke, J. Van Vaerenbergh, and P. Mercelis. Benchmarking of different SLS/SLM processes as rapid manufacturing techniques. In *Proceedings of 1st International Conference on Polymers and Moulds Innovations, Gent*, 2005.

[56] S. Lin. Computer solutions of the traveling salesman problem. *The Bell System Technical Journal*, 44(10):2245–2269, 1965.

[57] S. Lin and B. W. Kernighan. An effective heuristic algorithm for the traveling-salesman problem. *Operations research*, 21(2):498–516, 1973.

[58] J. D. Little, K. G. Murty, D. W. Sweeney, and C. Karel. An algorithm for the traveling salesman problem. *Operations research*, 11(6):972–989, 1963.

[59] K.-T. Mak and A. J. Morton. A modified Lin-Kernighan traveling-salesman heuristic. *Operations Research Letters*, 13(3):127–132, 1993.

[60] O. Martin, S. W. Otto, and E. W. Felten. Large-step Markov chains for the traveling salesman problem. *Complex Systems*, 5(3):299–326, 1991.

[61] O. Martin, S. W. Otto, and E. W. Felten. Large-step Markov chains for the TSP incorporating local search heuristics. *Operations Research Letters*, 11(4):219–224, 1992.

[62] J. S. Mitchell. Guillotine subdivisions approximate polygonal subdivisions: A simple polynomial-time approximation scheme for geometric TSP, k-MST, and related problems. *SIAM Journal on Computing*, 28(4):1298–1309, 1999.

[63] G. Morton and A. Land. A Contribution to the "Travelling-Salesman" Problem. *Journal of the Royal Statistical Society. Series B (Methodological)*, pages 185–203, 1955.

[64] A. H. Nickel. *Analysis of thermal stresses in shape deposition manufacturing of metal parts*. PhD thesis, Stanford University, 1999.

[65] C. H. Papadimitriou. The Euclidean travelling salesman problem is NP-complete. *Theoretical Computer Science*, 4(3):237–244, 1977.

[66] C. H. Papadimitriou. *Computational complexity*. Addison-Wesley, 1995.

[67] C. H. Papadimitriou and K. Steiglitz. *Combinatorial optimization: algorithms and complexity*. Courier Corporation, 1982.

[68] R. G. Parker and R. L. Rardin. Guaranteed performance heuristics for the bottleneck travelling salesman problem. *Operations Research Letters*, 2(6):269–272, 1984.

[69] J. Perttunen. On the significance of the initial solution in travelling salesman heuristics. *Journal of the Operational Research Society*, pages 1131–1140, 1994.

[70] H. Pohl, A. Simchi, M. Issa, and H. C. Dias. Thermal stresses in direct metal laser sintering. In *Proceedings of the 12th Solid Freeform Fabrication Symposium, Austin, TX*, 2001.

[71] R. Ramakrishnan, P. Sharma, and A. P. Punnen. An efficient heuristic algorithm for the bottleneck traveling salesman problem. *Opsearch*, 46(3):275–288, 2009.

[72] G. Reinelt. TSPLIB – A traveling salesman problem library. *ORSA journal on computing*, 3(4):376–384, 1991.

[73] G. Reinelt. *The traveling salesman: computational solutions for TSP applications*. Springer-Verlag, 1994.

[74] G. Reinelt. Tsplib95. *Interdisziplinäres Zentrum für Wissenschaftliches Rechnen (IWR), Heidelberg*, 1995.

[75] A. Schrijver. *Theory of linear and integer programming*. John Wiley & Sons, 1998.

[76] A. I. Serdyukov. The maximum-weight traveling salesman problem in finite-dimensional real spaces. In *Operations Research and Discrete Analysis*, pages 233–239. Springer, 1997.

[77] M. Sinirlioglu. Rapid Manufacturing of Dental and Medical Parts via LaserCUSING® Technology using Titanium and CoCr Powder Materials. In *RapidTech 2009: US-TURKEY Workshop on Rapid Technologies*, 2009.

[78] B. Vandenbroucke and J.-P. Kruth. Selective laser melting of biocompatible metals for rapid manufacturing of medical parts. *Rapid Prototyping Journal*, 13(4):196–203, 2007.

[79] J. Vygen. *New approximation algorithms for the TSP*. Citeseer, 2012.

[80] L. A. Wolsey. *Integer programming*, volume 42. Wiley New York, 1998.

[81] L. A. Wolsey and G. L. Nemhauser. *Integer and combinatorial optimization*. John Wiley & Sons, 2014.

[82] M. F. Zaeh and G. Branner. Investigations on residual stresses and deformations in selective laser melting. *Production Engineering*, 4(1):35–45, 2010.

List of Figures

List of Tables

Eidesstattliche Versicherung

Hiermit versichere ich an Eides statt, dass ich die vorliegende Arbeit selbstständig verfasst habe und keine anderen als die von mir angegebenen Quellen und Hilfsmittel verwendet habe.

Weiterhin erkläre ich, dass ich die Hilfe von gewerblichen Promotionsberatern bzw. -vermittlern oder ähnlichen Dienstleistern weder bisher in Anspruch genommen habe, noch künftig in Anspruch nehmen werde.

Zusätzlich erkläre ich hiermit, dass ich keinerlei frühere Promotionsversuche unternommen habe.

. . . .

Ort, Datum Unterschrift